DECLARATION

I declare that *Can Acacia karroo and Boscia albitrunca spp. be used in the Biogeochemical Prospecting for Gold: A Case Study at the Blue Dot Mine, Amalia, Northwest Province, South Africa* is my own work, that is, that it has not been submitted for any degree or examination in any other university, and that all the sources I have used or quoted have been indicated and acknowledged by complete references.

.....

Unathi Mshumi **May 2006**

KEYWORDS

Biogeochemical prospecting

Biogeochemistry

Acacia karroo

Boscia albitrunca

Element absorption

Amalia Greenstone Belt

Blue Dot Mine

ABSTRACT

In areas of transported overburden there is frequently a weak relationship between soil and the underlying mineralized bedrock. Vegetation has the capability to absorb metals from the underlying substrate via its extensive root systems. These metals are translocated to the various organs of the plant such as leaves, twigs bark and roots without negatively impacting on the normal functioning of the plant. The analysis of the vegetation may therefore be used to locate deeply buried mineral targets.

An investigation was undertaken in the Blue Dot Mine area, in Amalia, Northwest province, South Africa, to establish the suitability of *A. karroo* and *B. albitrunca* for biogeochemical prospecting for gold in the area. Geologically, the Blue Dot Mine is situated within the poorly exposed Amalia Greenstone Belt, which comprises of six to ten units of Banded Iron Formation (BIF), which are interlayered with mafic to ultramafic rocks. The BIF units are the main outcropping lithologies in the area. Other rocks found in the area include quartz-chlorite schist, amphibolite-chlorite schist and quartz carbonate schist. Gold mineralization in Abelskop is concentrated within the siliceous BIF unit while the economic gold is concentrated in the jaspilitic BIF unit in the Goudplaats mine, located in the southern part of the northern Amalia Belt.

Leaf samples of *A. karroo* and *B. albitrunca* were collected along traverse lines across the entire area, extending over areas of Au mineralization (Goudplaats and Abelskop) and background where there was no known mineralization. The leaves were ashed and digested in aqua regia and submitted to the laboratory for analysis. A total of 62 elements were determined by ICP-MS (Finigan). Data analysis employed descriptive statistics and multivariate statistical techniques such as factor analysis and cluster analysis in order to determine data distribution, element association patterns and element distribution maps. Based on the factor analysis, four element groups were investigated and these included macronutrients (Ca, Mg, P, S and K), Au and pathfinder elements (As, W, Ag, Hg, Pb, Te, Sb), trace elements (Bi, Se, Ba, Sr) and REEs (La, Ce, Eu). The rare earth elements (REEs) were dealt with separately due to their coherent geochemical behaviour. Geochemical maps were plotted for *A. karroo* only due to the low sampling density of *B. albitrunca* in the study area. Background, threshold and anomalous values were estimated from boxplots.

The results indicate that gold absorption is at its highest in *A. karroo*, compared to *B. albitrunca*. Furthermore these anomalous values are limited to Goudplaats, which is seemingly related to the drainage pattern. Goudplaats is located in a poorly-drained part of the Blue Dot Mine area. Similar levels of absorption of Ag, Hg, P and As occur in both species, with anomalous levels occurring in the mineralized areas of Goudplaats and Abelskop. Tellurium and Sb are more pronounced in the *A. karroo* while W shows a slightly higher average concentration in *B. albitrunca*.

The REEs occur at higher levels in *A. karroo* in comparison to *B. albitrunca*. The high concentration of La and Ce could be the dissolution of less resistant minerals such as apatite during weathering processes. The weathering releases elements such as La, Ce, and Nb and these are taken up into the plant. The geochemical maps of La, Ce and Eu show similar trends such as anomalous values occur mainly in the granite and extending to the adjacent Goudplaats mineralization. The REEs in the vegetation strongly correlate with the mineralization in Goudplaats as expected as the REEs are not widely dispersed during weathering (Middleburg et al., 1988).

On the basis of the results, *A. karroo* and the *B. albitrunca* can be considered for biogeochemical prospecting in the Blue Dot Mine area.

ACKNOWLEDGEMENTS

A number of people have been directly or indirectly in the successful completion this work. I therefore would like to acknowledge the following people:

Special thanks goes to Prof. C. Okujeni for the invaluable supervision and financial support for the duration of this thesis.

I would also like to express my sincere gratitude to my parents Lulama and Theo Mshumi, together with my siblings, Lali, Qiqa and Malu for their love and support throughout my studies.

A special mention also goes out to my partner and friend Mr. N. Simakuhle, thank you for your understanding, love and support.

My thanks also goes out to Prof R. Madsen for statistical consultation, Mr. P. Ackon for assistance in field work and mapping and Mr. W. Baugaard for input and critique. My sincerest gratitude also goes out to Mashudu, Lerato and Mr Z. Madotyeni for helping me with the final touches of this thesis.

Table of Contents

List of Figures

List of Tables

List of Appendices

Chapter 1

1. Introduction

Biogeochemical exploration techniques were initiated by Vernadsky in the 1920s (Beus & Gregorian, 1975) but early pioneering application began independently in Scandinavia, England and the Soviet Union in 1938 and 1939 (Brooks, 1972). In 1938, Russian worker Tkalich made the first biogeochemical discovery of arsenopyrite in Eastern Siberia (Brooks, 1972), where he found that the deposit could be traced by the iron content of the overlying vegetation. At about the same time, Nils Brundin (1939) in Sweden undertook biogeochemical investigations on vanadium and tungsten. Further advances in the biogeochemical prospecting technique were carried out by a number of researchers such as Warren and Delavault (1950) whose work formed the basis of modern concepts of biogeochemistry as an exploration method. In the 1950s and early 1960s, biogeochemical prospecting was widely applied by the U.S. Geological Survey, over numerous known ore deposits (Brooks, 1972).

Biogeochemical prospecting has underlying basic principles that the user needs to take into account. The assumption is made that if there is an enrichment of metals in the ground e.g. a mineral deposit, then there will be enrichment of these metals in the overlying soil (Brooks, 1972). However each plant species has specific nutritional requirements and tolerances to metals, hence during biogeochemical exploration it is important to know which species to sample and more importantly what organ of the plant to sample, so as to best detect hidden mineralization (Dunn & Hall, 1999).

Vegetation, which has deep penetrating root systems can absorb elements from throughout the soil horizons, groundwater, and even underlying bedrock (Raju & Raju, 1999). Arid to semi arid climates commonly have sparse vegetation cover, however many of the species present may be phraetophytes (have deep penetrating roots in excess of 100m) and as a result, will be sampling much greater depths (Hoffmann, 1989, Cohen et

al., 1989). Some of these elements extracted are essential and important for the survival of the plant. The non-essential elements (some of which are toxic to the plant) are stored in the more extreme parts of the plant such as the outer bark, twigs and tree tops. A number of these toxic elements are heavy metals which are of economic value and are moved to the parts of the plants that are easiest to sample (Dunn & Hall, 1999).

Plants growing on soils with high concentration of heavy metals more often than not contain these heavy metals in their tissues (Leavitt et al., 1979). As a result, a number of these plants have been used for biogeochemical prospecting of metals (Lintern et al., 1997; Erdman & Olson, 1985; Brooks, 1972). Element absorption occurs through the root system, by diffusion or cation exchange at the surface of clay minerals (Brooks, 1972). The elements are then translocated to the aerial parts of the plants such as the leaves, bark and shoots. Some plants can accumulate elements in huge quantities without any negative impact on plant physiology. Over ore deposits, plants can accumulate in even greater amounts, so that the plant ash contains more of the element than the substrate (Brooks, 1972). The ability of the plant to reflect the underlying substrate (bedrock, water table or mineralization) is crucial in biogeochemical prospecting.

The ability of a plant to translocate elements from the roots to the aerial parts depends on the depth of its root system. Deep-rooted plants (such as phraetophytes) are useful in biogeochemical prospecting as they penetrate through thick overburden, thus detecting deep- seated deposits (Brooks, 1972). Studies by Erdman & Olson (1985) showed plants phreatophytic plants such as *Prosopis juliflora* were not only useful in the mapping of fault zones but also in reflecting possible mineralization of these faults. Plants in arid and semi-arid environments have deep-rooted systems because they depend on the saturation zone, below the water table for their moisture (Otieno et al., 2005).

Sampling techniques form a very important part of biogeochemical prospecting as a number of precautions need to be taken. Consistency is key when sampling because:

- same species of plant needs to be collected
- same plant organ has to be sampled

- same amount of growth has to be taken
- similar appearance and state health of trees needs to be sampled

Biogeochemical prospecting finds widespread application in areas of minimal outcrop where metal correlation between soil and plant is weak or non-existent, hence the need to sample vegetation. A study carried out at a gold occurrence in Norseman, Western Australia by Smith and Keele (1984) found a lack of correlation between the Au values in the soil and that of the plants growing over the soil. A strong correlation between the Au in plants and the underlying concealed Au mineralization was however found.

Weak plant-soil correlations commonly occur in prospecting terrains, which are overlain by transported overburden (Cohen et al., 1987, Hoffmann, 1989). Semi-arid areas (such as those found in Southern Africa) covered by aeolian and calcrete deposits are therefore renewed challenges to the mining and exploration industry. These terrains pose a serious problem in terms of mineral prospecting, such as interpreting geochemical anomalies in relation to concealed ores. Processes leading to the emplacement of these anomalies and the controls of element dispersion processes are often not fully understood (Okujeni et al., 2005). The use of soil in geochemical prospecting of these regions is therefore fraught with difficulties and may need to be complemented by other geochemical techniques such as biogeochemistry.

Numerous case studies on the application of biogeochemical prospecting have been reported from various parts of the world such as Russia, Australia, USA and Canada. Notable examples from Southern Africa that have been reported include the flora growing over copper mineralization in the Zambian and Sheba Copper Belt (Brooks et al, 1992). Biogeochemical prospecting techniques have not been widely applied in South Africa and there are no known reported studies where the technique has been used successfully.

The study area is located in the town of Amalia, South Africa, in the Kraaipan Greenstone Belt, in a poorly exposed western part of the Archean Kaapvaal Craton. The

poor exposure of rocks in the region has led to a lack of interest to explore this region by the mining and exploration industry. However the discovery of gold mineralization associated with greenstones has brought about renewed interest and this has led to mining companies exploring again in this region. Sporadic mining operations at the Blue Dot Mine area began in the late 1800's, and stopped in November 2001 when the mine was temporarily closed down. The Ph.D dissertation done by Kiefer (2004), gives a comprehensive summary of mining operations and ownership of the mine from the time of discovery until its final closure. A number of other researchers, Van Eeden et al., (1963), Vearncombe (1986), Johnson, (1995) have published studies on the study area.

The Blue Dot Mine area is mainly covered by transported aeolian sands. The main lithologies include Banded Iron Formation (BIF), mafic metavolcanic rocks and various schists (Vearncombe, 1986) which were metamorphosed under greenschist-facies conditions. Gold mineralization in the Blue Dot Mine area is confined to the BIF units. The lack of good outcrops in the study area brought about the need to evaluate other geochemical prospecting techniques like biogeochemical prospecting. Soil and regolith geochemistry investigations (Kiefer, 2004, Ackon, 2001) have been undertaken in the area, with limited success. A need arose to evaluate biogeochemistry as an alternative or complementary technique for geochemical exploration in the Blue Dot Mine area.

The Blue Dot Mine area is characterized by semi-arid to arid conditions and this is reflected in its natural vegetation. The area is mainly covered in by vast stretches of desert grasses with an uneven dispersion of trees and shrubs. *Acacia karroo* is the most widespread occurring throughout the study area with *Boscia albitrunca* being the next most abundant tree. The principal aim of this study is to ascertain the suitability of *A. karroo* and *B. albitrunca* for the biogeochemical prospecting of gold in the study area. The basis for choosing *A. karroo* and *B. albitrunca* for sampling is due to their abundance (Brooks, 1972) and their extensive root systems (both are phraetophytes). In order to determine the suitability of these tree species, great emphasis will be placed on their element absorption patterns with respect to elements such as gold and its pathfinder elements, rare earth elements (REEs) and macronutrients. The second objective of the

work is to determine the relationship between the element absorption patterns and their controlling processes e.g. bedrock, mineralization, plant physiology and drainage.

1.1 Location

The study area is located in the gold mining and prospecting ground held by the Blue Dot mine. The area is situated 28km southwest of the town Schweizer Reneke and 10km southeast of the town Amalia (Fig 1.1) in the Northwest Province, South Africa. The Blue Dot mine extends over three farms namely, Goudplaats 96HO, Abelskop 75HO and Bothmasrust 76HO and covers an area of 22 square kilometres.

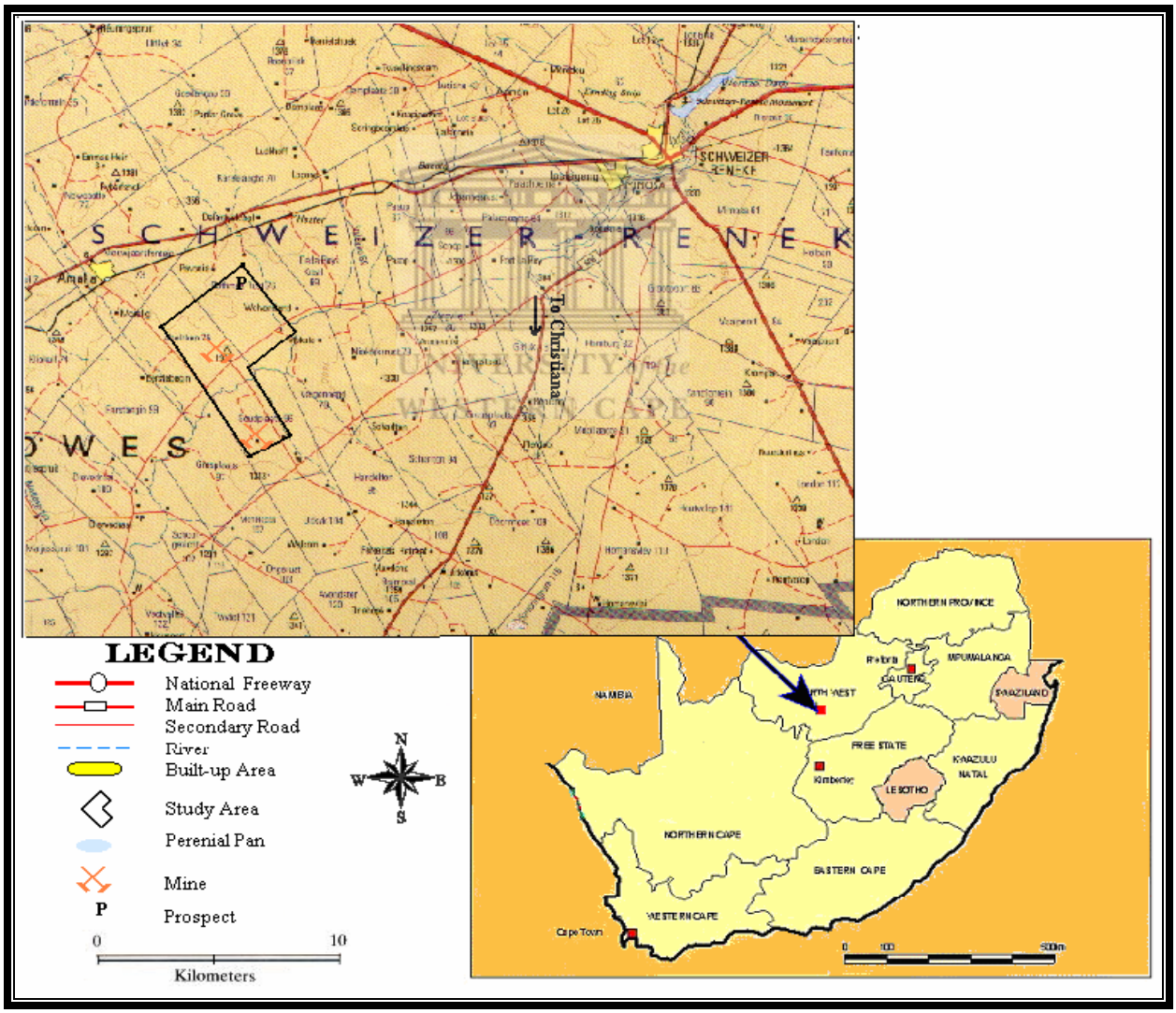

Fig 1.1 Location of the study area

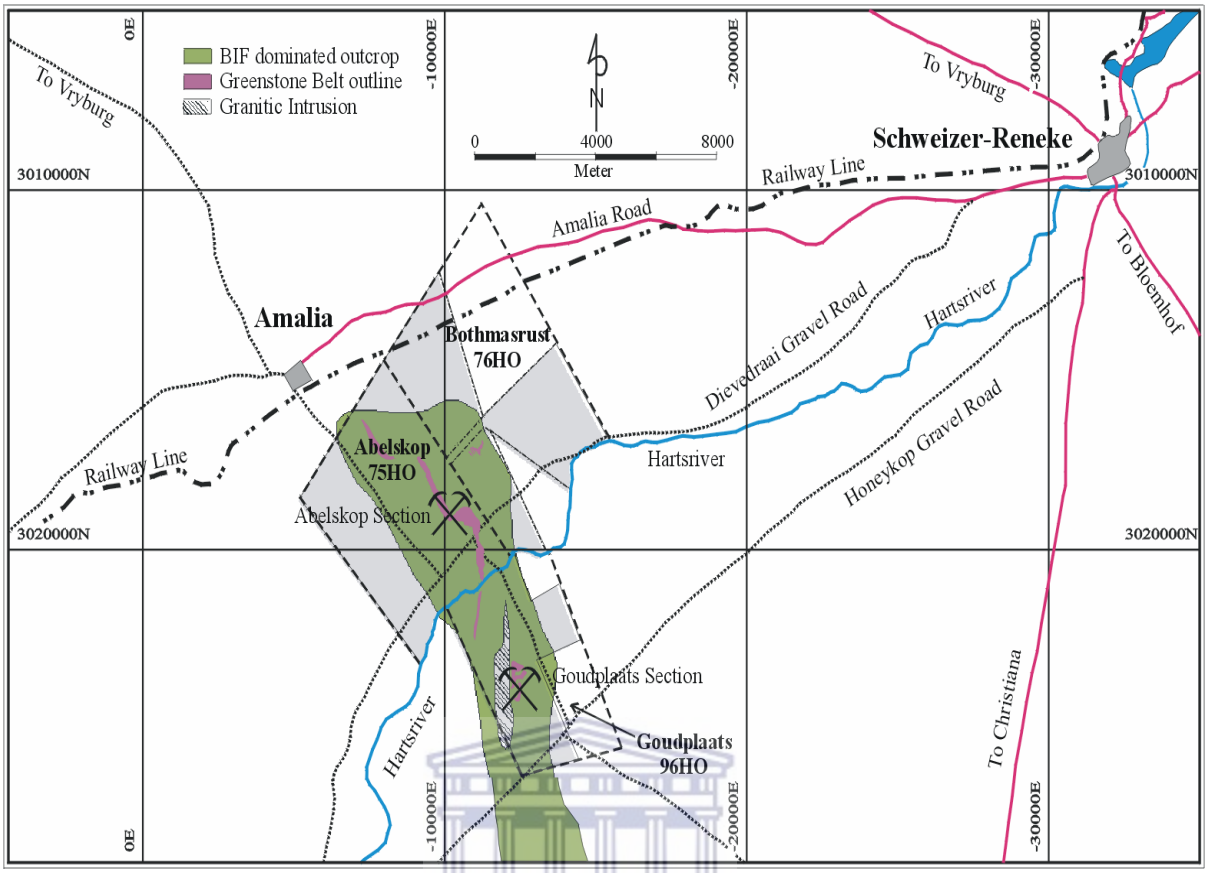

Fig 1.2 Location of Blue Dot Mine (modified after Kiefer, 2004)

The area is mostly covered by transported Kalahari sands with poorly exposed greenstones and banded iron formation (BIF), which is similar to geological environments found in Australia, North America and Zimbabwe. This aeolian cover has a thickness of up to 5m within the study area (Ackon, 2001) and is estimated to reach 60m towards the north of the Amalia Greenstone Belt.

1.2 Climate

The area is situated in the central region of the Northwest Province of South Africa hence it is dominated by typically semi-arid climate. On average the area receives annual rainfall around 444mm p.a. with the dominant rainfall season during midsummer (peaking in January). Thunderstorms with a ground flash density of about 5-6 flashes/km^2/yr occur during summer. Sporadic hailstorms occur during summer (1-3p.a).

Windy months occur between August and November with a predominantly northerly wind direction. The area is characterized by hot summers and cold winters. Mean annual temperatures range between 9°C and 27°C with July being the coldest month during winter.

1.3 Vegetation

Given the semi arid conditions in the area, the vegetation comprises plants that are adapted to these conditions. The area is mainly covered by vast stretches of desert grasses with an uneven dispersion of trees and shrubs belonging to the acacia family. A thick impenetrable cluster of acacia trees is found around the Abelskop mineralization. The vegetation in the area consists of two main trees viz *Acacia karroo* and *Boscia albitrunca* and less abundant shrubs and trees such as *Acacia tortilis*, *Acacia Caffra, Acacia hebeclada, Lycium hirstum* and *Grewia flava.* The most dominant grasses found in the area include *Eragrostis lehmannia*, *Schmidtia kalahariensis* and *Stiptagrostis uniplumis*.

1.4 Drainage

The Harts River is the main river occurring in the study area, with its source in the northeast of Vryburg. It forms the main boundary between Abelskop and Goudplaats, where it runs along the eastern and western parts of Goudplaats farm and extends into the Abelskop valley (Fig1.1) (Kiefer, 2004). The Harts River is an ephemeral since it flows mainly during the rainy season in November till April, where it usually overflows its shallow banks and is dry for the rest of the year. Due to the low relief and extensive cover of superficial deposits, the runoff throughout the year is small and hence few tributaries join the Harts River (Kiefer, 2004).

Chapter 2

2. GEOLOGY

2.1 Regional Geology

The Kraaipan Greenstone Belt and Amalia Greenstone Belt occur in the western part of the Kaapvaal Craton. These belts are separated by the overlying Ventersdorp Supergroup (Fig 2.1) and are lithostratigraphically grouped as the Kraaipan Group (Visser, 1989). The rocks belonging to the Archean Kraaipan Group are found in the northern part of the Cape Province, between Vryburg and Mafikeng, where they crop out in three narrow belts viz in the area around Stella, Kraaipan and Amalia (Visser, 1989) (Fig 2.1). Regionally, the Blue Dot Mine area is situated within the southern limb of the Kraaipan Group. The Kraaipan Group is poorly exposed and deeply weathered or covered by windblown Kalahari sands especially in the north. The only distinct outcrops are the more resistant, banded iron formation (BIF), which are visible as long parallel ridges (Jones & Anhaeusser, 1991). The lack of outcrops has made it very difficult to establish an acceptable regional stratigraphy (Jones & Anhaeusser, 1991).

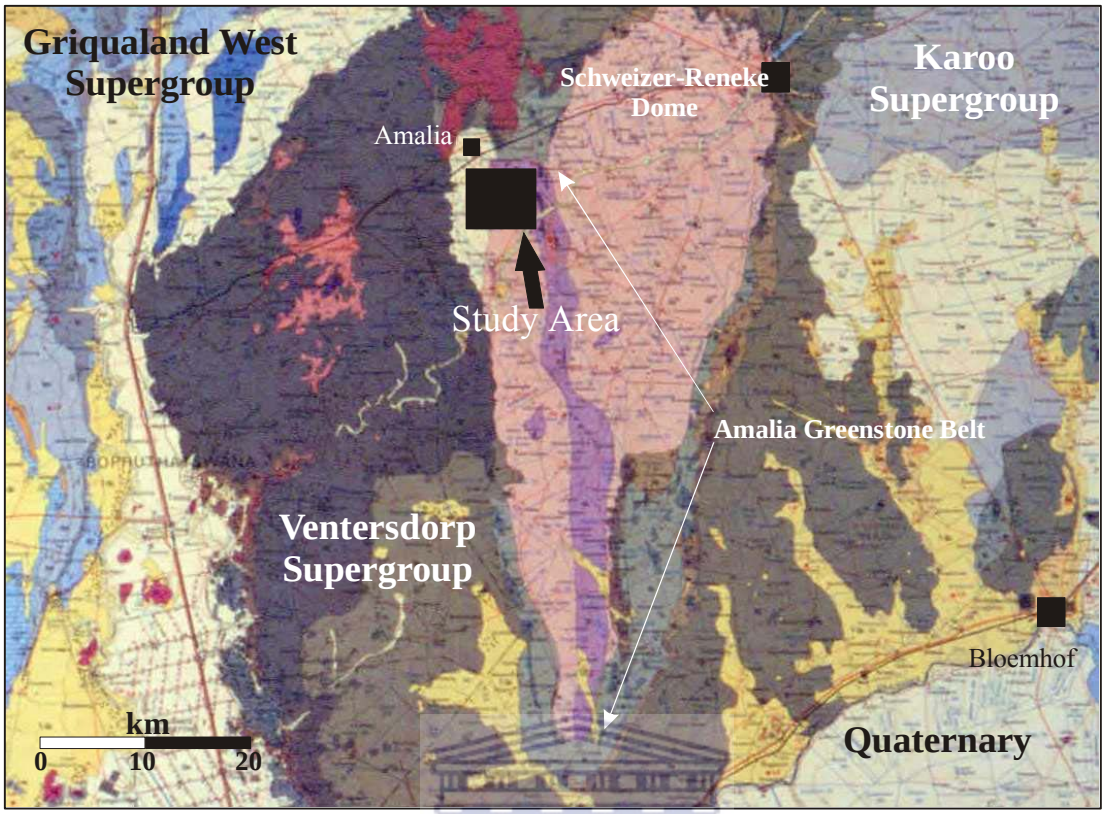

Fig 2.1 Regional Geology of the study area enclosing Amalia Greenstone Belt (From geological map of Christiana)

The volcanic rocks of the Kraaipan Group consist mainly of metamorphosed volcano-sedimentary rocks. These rocks now consist mainly of altered massive and schistose amphibolites and amphibole-chlorite-epidote schists (Poujol et al., 2002). Banded iron formations (magnetite quartzites, banded ferruginous cherts, jaspilites, and iron formation breccias) are the main Archean rocks types exposed throughout the Amalia-Kraaipan region (Anhaeusser & Walraven, 1999). Other rocks types encountered include serpentinites carbonate rocks, agglomerates, accretionary lapilli tuffs, conglomerates grits, shales and phyllitic metasediments (Jones & Anhaeusser, 1994, Van Eeden et al., 1963).

Three varieties of granitoids have been identified by researchers (SACS, 1980; Zimmerman & Anhaeusser, 1991). Anhaeusser & Walraven (1999) further confirmed the subdivision of these granites sing their petrological, geochemical and isotopic characteristics. These granitoid rocks include:

i. foliated leucogneisses and migmatites containing remnants of Kraaipan amphibolites BIF similar to those found in the south east of Kraaipan
ii. fine to medium grained grey or pink homogenous or in places weakly foliated, massive granitoids as well as cross-cutting dykes and veins similar to those encountered in the Schweizer-Reneke Dome
iii. course grained to pegmatitic, homogenous, pink granite

All the above varieties contain xenoliths of Kraaipan rocks and appear younger.

The Ghaap Group (belonging to the Transvaal Supergroup) occurs to the west of Blue Dot Mine area and overlies the Ventersdorp Supergroup. This group comprises of dolomite and black reef quartzite. The entire stratigraphic succession is stratigraphically exposed in the Vryburg area. A carbonate series consisting of dolomite limestone, chert with intercalated quartzite, shale and flagstones make up the Ghaap Plateau, which dips towards the west at an angle 2^0 to 7^0 along the escarpment (Van Eden et al., 1963).

The Carboniferous Dwyka Group and the Permian Ecca Group, belonging to the Karoo Supergroup occur to the northeast of the study area. The rocks of this group consist of shales, tillite, mudstone and boulder shales.

2.2 Amalia Greenstone Belt

The Amalia greenstone Belt is one of the four, narrow linear and roughly north-south trending belts of the Kraaipan Group, which forms part of the Swaziland Supergroup (Visser, 1989). The belt occupies a narrow 4km strip of country, extending for a distance of 55km and is characterized by generally poor exposure and has ill-defined boundaries (Jones & Anhaeusser, 1993). According to Zimmerman & Anhaeusser, (1991) the Amalia Greenstone Belt is considered to be Archean in age (3250Ma) but younger than the Barberton Greestone Belt (Jones & Anhaeusser, 1993).

The rocks of the Amalia Greenstone Belt consist mainly of steeply dipping massive and schistose mafic metavolcanic rocks (altered tholleiitic basalts) together with intercalated BIFs (six to ten units). The BIF consists of fine layers of alternating hematite/magnetite and microcrystalline chert, which display intense folding and boudinaging. This deformation is indicative of a high strain environment. A fine-grained grey-green quartz chlorite schist is also dominant, together with outcrops of greywacke, slate, carbonate rocks and felsic intrusives (Jones & Anhaeusser, 1993).

Gold mineralization is found in the highly deformed siliceous BIF units (Kiefer, 2004). According to Hunt (1996), the structure and mineralization of the Amalia Greenstone Belt seem to be influenced by the surrounding granite bodies. These granite bodies are of adamellitic or granodioritic to tonalitic composition. Due to multi-episodic deformation and pervasive chloritic, silicic and carbonate alteration, the primary mineralogy and texture of the Kraaipan Group has been obscured (Hunt, 1996). The contact between the granites and the Amalia Greenstone Belt are inferred because of their poor exposure (Jones & Anhaeusser, 1991).

.

2.3 Blue Dot Mine Area

Blue Dot Mine area covers a total area of about 22km^2 (Fig 2.2), comprising three mineralized sections viz: Abelskop, Bothmansrust and Goudplaats. The main rock type found in the Blue Dot Mine is oxide facies BIF, which hosts the gold mineralization at some places. The BIF is intercalated with carbonate altered schist of tholeiitic composition and thin ultramafic rocks (Kiefer, 2004). Abelskop section is situated within a large scale S-shaped feature comprising of the largest continuous BIF succession. BIF outcrops consist of two lithologic units, the central BIF, which is more cherty with thinner bands of hematite-magnetite and the ferruginous distal BIF, which is reddish brown in colour (Kiefer, 2004).

In the area around Goudplaats farm, a poorly exposed granitic body cuts across the greenstone succession to the west of the mine. This granitic body trends in a northeasterly direction towards Bothmasrust (Kiefer, 2004) and is pinkish-grey in colour, equigrannular in appearance and similar to the adamellites in Schweizer-Reneke (Johnson, 1995). These granites crop out in the area north of the Harts River. The BIF succession in Goudplaats has undergone more complex deformation compared to that of Abelskop section. The BIF is rich in carbonate especially near the mineralized areas.

The Bothmasrust section is located approximately 2.5km northwest of the main Diewedraai/Schweizer-Reneke gravel road (Fig 2.2). This section is characterized by extremely intense deformation, hence the highly brecciated nature of the BIFs, compared to Abelskop and Goudplaats. The section comprises discontinuous lithologies such as oxide facies BIF, metamorphosed mafic lavas, quartz-rich schists, brecciated horizons and outcrop accretionary lapilli. For the purpose of this investigation, Bothmasrust section has not been covered.

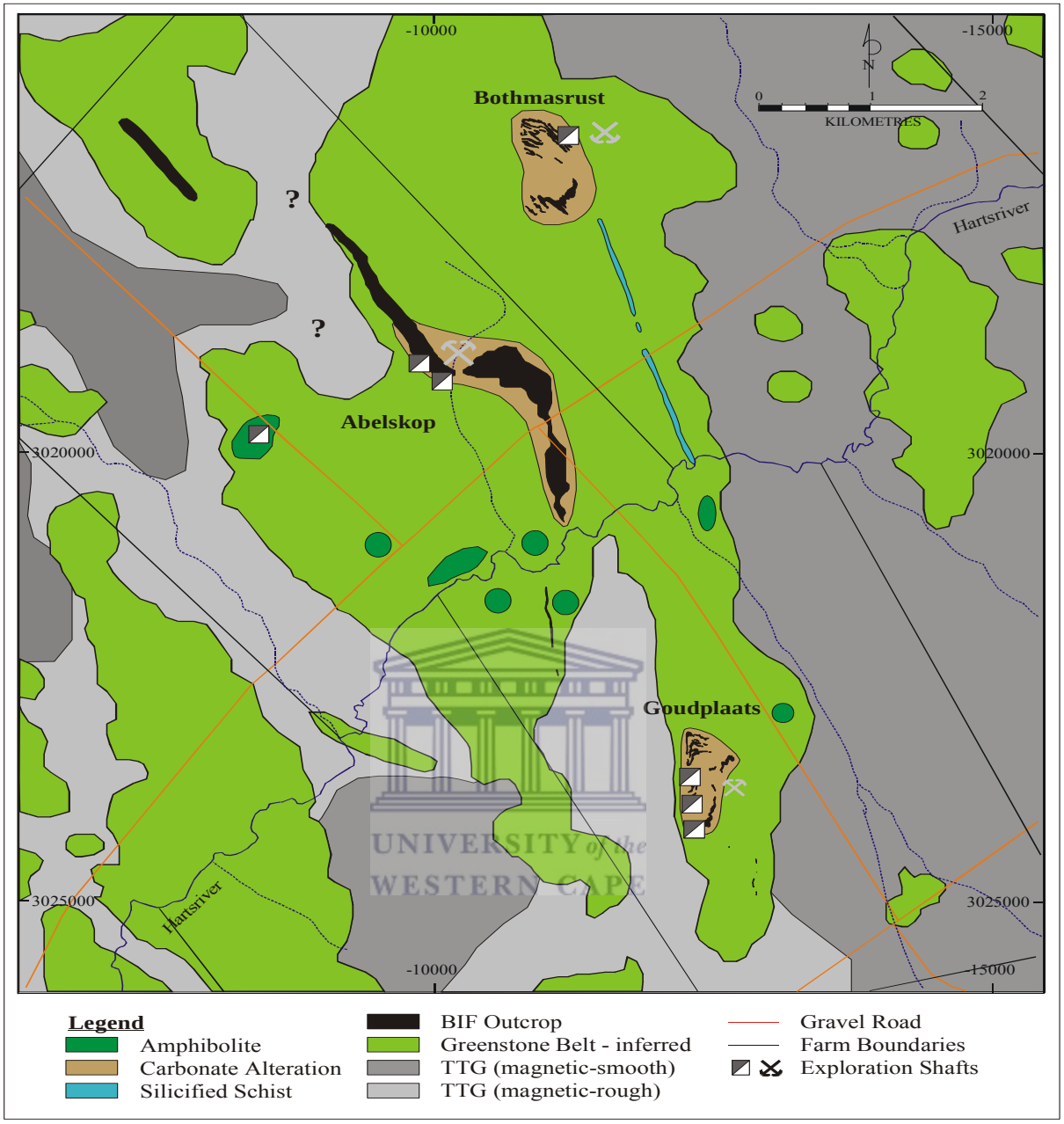

Fig. 2.2 Geological Map of Blue Dot Mine (from Kiefer, 2004)

2.3.1 Mineralization

Gold mineralization is controlled by a siliceous, jaspilitic BIF, which has a rheological difference in relation to the surrounding schists (Kiefer, 2004). The BIF units underwent intense deformation which caused structural thickening in the form of folding and boudinaging. Gold is found in the form of quartz veins, stringers and irregular masses

emplaced in brecciated zones in the banded ironstone and often also occurs as replacement of oxide bands by sulphides and sulphide disseminations in quartz veins. These veins are often oblique and parallel to the BIF body are filled with either quartz and/or carbonate (Johnson, 1995). Field observations and underground mapping showed a direct relation between the fold axial plunge direction and the vein direction. This implies that strongly deformed BIF will be most likely mineralized compared to undeformed BIF. This trend was often observed in Goudplaats and Abelskop during mining (Kiefer, 2004).

2.3.2 Ore Mineralogy

The ore mineralogy consists of pyrite with traces of chalcopyrite, pyrrhotite and gold suggesting subgreenschist and upper greenschist facies conditions during mineralization. Gangue minerals include quartz and various carbonates. High grade ore is characterized by massive inclusions of pyrite at the contact between the hematite and the cherts. Magnetites occur as scattered patches within the matrix of the cherts. In some places quartz-chlorite schist is altered to quartz-chlorite-carbonate schist. The degree of alteration and mineralization is determined by the amount carbonates present (Kiefer, 2004). Carbonate alteration results in increase in quartz and iron carbonate and a decrease in chlorite and Fe-micas.

2.3.3 Bedrock Geochemistry

The influence of bedrock on the overlying vegetation needs to be established by this investigation. Bedrock geochemistry of the main rock types found in the Blue Dot Mine area is therefore important.

Due to the lack of fresh, unweathered outcrops, the lithological description of the different rock types in the northern part of the Amalia Greenstone belt was never carried out. Kiefer, (2004) is the only author to have carried out an extensive geochemical

characterization of the rocks in the Blue Dot Mine area. Most of the information came from surface and underground diamond drill cores and from outcrop areas in Bothmasrust North and Bothmasrust South the Amalia Gold Mine. Some unweathered material was also obtained from underground operations in Abelskop and Goudplaats.

The major rock type that an outcrop is the BIF units, which are surrounded by carbonate altered and silicified metavolcanic rocks consisting of quartz chlorite and carbonate. Away from the mineralized areas, the most common rock type is amphibolite, which is only exposed in exploration trenches and in open pits of diamond workings. Abelskop and Goudplaats contain numerous BIF layers that are partly surrounded by fuchsitic quartz-carbonate-chlorite schist, a variety of quartz-carbonate rocks and rarely talc-chlorite-carbonate schist.

2.3.3.1 Banded iron formation (BIF)

The best BIF outcrops occur in the Goudplaats, Abelskop and Bothmasrust (North and South), with the longest continuous strike occurring in Abelskop extending over a length of 4000m. Two types of BIF were identified namely, iron-rich BIF and siliceous BIF. These BIFs have varying amounts of chert and hematite-magnetite. Siliceous BIF is of great economic importance as it the only economic gold carrier in all of the Amalia gold deposits. This strongly magnetic unit is carbonate altered in some places and is enveloped by silicified schist and iron-rich BIF. Siliceous BIF occurs in central Bothmasrust and in Abelskop and Goudplaats.

The iron-rich BIF is the most common rock type in the Amalia Belt and is well developed in Abelskop section. These iron-rich BIF units are depleted in all trace elements except Rb. The BIFs from Abelskop are characterized by low TiO_2, Al_2O_3, MgO, K_2O, Na_2O, Y, Zr, Nb, Zn, V and Co content. There is an inverse relationship between Fe_2O_3 and SiO_2 where high SiO_2 coincides with low Fe_2O_3. SiO_2 varies over a wide range from 32.38wt% to 93.26wt% for the main mineralized BIF and 27.52wt% to 78.74% for the unmineralized BIF. Fe_2O_3 ranges from 3.8wt% to 41.42% in the mineralized BIF and

2.24wt% to 43.35wt% in unmineralized BIF. On average the mineralized BIF has a higher SiO_2 and lower Fe_2O_3 values compared to the unmineralized BIF.

With the exception of the siliceous BIF wherein the gold occurs, the rest of the BIF units in Goudplaats belong to the iron-rich variety. The BIF samples from Goudplaats are divided into black iron-rich BIF and jaspilitic BIF that is partly mineralized. Both BIF units are characterized by high Fe_2O_3, P_2O_5 and Rb content and low MgO, CaO, TiO_2 and Al_2O_3 content. The mineralized jaspilitic BIF is characterized by a wide SiO_2 range (29wt% to 56wt%) an elevated LOI and high As concentrations. The wide SiO_2 range is due to pervasive carbonate alteration that affected the jaspilitic BIF particularly. The iron-rich BIF is characterized by a higher Fe content of up to 56wt% has strong depletion of trace elements except Rb. The SiO_2 content is consequently lower when compared to the mineralized jaspilitic BIF.

2.3.3.2 Amphibolites

Since no amphibolites outcrops occur in the northern Amalia terrane, Kiefer (2004) used samples from the diamond exploration and mining pits that occur along the Harts river. The amphibolites to the west of Goudplaats and Abelskop can be divided into Fe and Mg tholeiites and komatiitic basalts. SiO_2 ranges from 46wt% to 56wt% and Fe_2O_3 ranges from 9wt% to 17wt%. MgO varies from 4wt% to 15wt% while Al_2O_3 varies from 11wt% to 15wt%. Their overall composition is similar to the Archean tholeiites.

2.3.3.3 Granitoids

The granitoids in the Amalia belt are mainly covered by sands of the Kalahari group and are mainly exposed along the river courses. These granitoids can be geochemically classified to include tonalities, trondhjemites and granodiorites (TTG) and granites. The Amalia gneisses have a narrow compositional range 66.28wt% to 75.34wt% for SiO_2 and are relatively depleted in ferromagnesian minerals (Fe_2O_3 + MgO + $TiO_2 \leq$ 5wt%) but rich in Al_2O_3 (>15wt%). Due to the high Al_2O_3, the Amalia gneisses can be classified as

high Al_2O_3 trondhjemites (TTG). These rocks are also characterized by high Na_2O (3.98wt% to 7.49wt%) content relative to K_2O (1.07wt% to 3.31wt%). The tonalities and trondhjemites have high content of Ba and Sr (average 540ppm) and unusually high concentrations of Ni (average 384ppm) and Cr (average 104ppm). Transition elements such as Zn, V and Cr tend to decrease with increasing SiO_2 concentration.

2.3.4 Regolith and Regolith Studies

The Blue Dot Mine area has a generally flat relief with very little outcrops except for BIF units that form long parallel ridges that are clearly visible on aerial photos, eg at Abelskop and Goudplaats. These low-lying BIF outcrops, which form the most prominent topographic features, occur as discontinuous north-south to NW trending ridges. These ridges are partially obscured by brick-red aeolian sand and/ or associated rubble or scree of BIF and greenstone fragments (Ackon 2001). Regolith cover is of varying thickness; up to 5m between parallel ridges comprising of BIF, with increased thickness to more than 10m towards the broad valley and drainage systems.

The regolith in the entire area comprises of three recognizable horizons. These horizons from bottom to top include 1) in situ regolith comprising of weathered basement rocks; 2) a colluvium and valley-filled sediment sequence, calcified or carbonate-impregnated pebbly to coarse/medium-grained sands at the base, followed by reworked friable/laminated calcrete and sands and 3) an unconformable horizon of fine-medium grained ferruginized aeolian sand.

The weathered basement comprises of assorted weathering products of the parent rock. These weathered products include saprolite, bleached or partly hematized parent rock, dirty brown to yellowish intensely decomposed parent rock and hematite nodules siliceous and gossanous fragments derived from weathering of sulphides in mineralized intercepts.

Colluvium and valley-filled sediments comprise of a lower pebbly zone composed of rock fragments. This pebbly zone grades into a pebbly to coarse and into a grey to light

brown medium grained sands that are intensely calcified. The calcrete seems to have been precipitated from groundwater (Ackon, 2001). The valley-filled sediments contain imprints of earlier mottling or laterization, such as relics of ferruginized sands and mottled quartz in association with gossanous fragments. Major constituents that have been identified by XRD include quartz, microcline, albite and accessory Fe-oxide (Ackon, 2001). The upper zone consists of a reworked friable and laminated pedogenic calcrete zone. In places, the calcrete occurs as hardpan calcrete, which contain siliceous concretions and coalesced carbonate nodules in a matrix of friable fine-grained and intensely mottled calcrete sand. Calcite and quartz are the major constituents with Fe-oxide granules, feldspars and dolomite being subdued.

Ferruginised aeolian sand unconformably overlies the colluvium and valley-filled sediments together with fresh and weathered basement rocks. The aeolian sand is deep red in colour at the bottom and yellow with reddish tint or dark brown at the top. The different colours at the top may be due to the varying presence of humus, Fe-oxides and other components in the sand. Two major constituents are found in the sand and these include: 1) partially decomposed and /or aggregated mottled quartz and Fe-Mn granules possibly derived from underlying ferricrete and calcrete horizon and 2) glassy to vitreous angular quartz of aeolian provenance whose relative contents decrease from up to 70% at the top to about 60% at the bottom of the horizon.

Petrographic studies conducted by Ackon (2001), reveal coarse-grained soils in upland areas accompanied by a high degree of mottling, suggesting a high degree of interaction between bedrock and the overlying soils. Therefore the regolith found at the ridges of Abelskop and Goudplaats may be classified as relict and erosional. Using the same criteria, the flat-lying areas with thick aeolian cover and colluvium greater than 3m can be grouped under depositional environment. The depositional areas can be classified into shallow and deep depositional areas with over 5m cover.

Regolith cover at the Blue Dot Mine area varies in thickness from skeletal soil cover to in elevated areas mostly along ridges of BIF. Regolith thickens to more than 10m towards

the broad valley and drainage system. Regolith of less than 1m thickness occurs in the northern section of Goudplaats and around Abelskop hill. The regolith in this area consists of medium-fine grained and contains higher mottled quartz and iron oxide content at the base. Most of the area is overlain by aeolian sand greater than 3m that shows medium-grained reddish-brown coloration with low mottled quartz content. Colluvium and valley-filled sediment sequence is mainly found along the drainage and paleochannels of the Harts river. The regolith cover in these areas is dark-grey to whitish, compact and more clayey (Ackon, 2001).

P. Ackon (2001) and Okujeni et al., (2005) investigated the distribution patterns of major and trace elements in various horizons in the regolith profiles around the Blue Dot Mine. Colluvial regolith shows a decrease from bottom to top of major elements such as Al_2O_3, K_2O, TiO_2 and Na_2O while CaO, MgO, H_2O and LOI show enrichment in the middle of the profile, coinciding with calcrete. CaO and SiO_2 exhibit an antagonistic relationship, which may be due to the removal of SiO_2 during the introduction of calcrete. High concentrations of CaO in the calcrete are accompanied by high contents of Au, Zn and Pb, while Bi and Cu show opposite trends.

The aeolian sand regolith consists mainly of SiO_2, Fe_2O_3, Al_2O_3, K_2O, TiO_2 H_2O and LOI and together they constitute 97% of the bulk sample. Gold content is closely associated with Fe_2O_3 since the Au decreases with decreasing Fe_2O_3 content. Hence it is concluded that Fe-Mn oxides control dispersion of Au.

Kiefer, (2004) gives an outline of the history of the Blue Dot mine and the soil sampling that has taken place since the mine's inception through to its closure. Prospecting in Goudplaats and Abelskop began in 1976 and this came about as a result of failed attempts in the areas around Blue Dot Mine. Due to the lack of outcrops in the area, a soil sampling/gossan search was conducted so as to locate Cu-Zn massive sulphide deposits. This was done in the hope that Au would be reflected by base anomalies. A total of 1383 soil samples were collected between December 1976, and January 1977. However the results were disappointing as neither base nor Au gold anomalies were detected. Soil

sampling was resumed again in 1987 whereby 2341 samples were analysed for gold. Percussion drilling at 9277m took place in five key areas. Based on these drilling results, two steeply plunging zones of mineralization of varying grade and thickness were identified in Abelskop. This investigation led to mining in Goudplaats, Abelskop and Bothmasrust but this only continued till beginning of 1998, when technical problems were encountered leading to the auctioning of the mine. Mining activities started again in 1999. In September 1999, a total of 278 soil samples from the top and bottom profiles were collected by Ackon (2001). One of the main objectives of the work was to do regolith mapping in the area and therefore determining element dispersion within the regolith framework. The outcome of the research was a success in areas characterized by skeletal regolith cover (<3m). In areas of thick regolith cover the results were inconclusive. The need therefore arose to utilize biogeochemistry.

Chapter 3

3. Methodology

3.1 Field Methods

The field work was conducted during summer in November/December 2004. Prior to this an extensive desktop study was carried out into the vegetation types, climate and geology of the area. Vegetation mapping was carried out with the aid of a compass and topographical maps of the area.

3.2 Vegetation Mapping and Sampling

A rectilinear asymmetrical grid sampling pattern was used and the profiles were laid perpendicular to the strike of the ore bodies. The main aim of the sample collection is to determine the multi-element signatures of the common species. Plant collection of the species in the survey area was carried out mainly for chemical analysis. The study area is sparsely vegetated, with vast stretches of land covered by grass. There is an abundance of shrubs belonging mainly to the acacia family. The area comprises mainly of two plant species namely *Acacia karroo* and *Boscia albitrunca,* which were collected for the analysis.

The plants were sampled at 500m intervals along E-W profiles (Fig 3.1), roughly perpendicular to the strike of the ore body. The intervals were reduced to 250m at the vicinity of Goudplaats and Abelskop mineralizations. Ground distances were determined by tape measure and the direction with the aid of a compass. At each sample point, leaves from the plants were collected using a pair of cutting shears. The leaves were subsequently placed in pre-marked plastic bags and were air-dried for the duration of the fieldwork, so as to prevent decay. Approximately 50g of leaves were collected from each plant. The samples were marked in accordance to their relative grid position on the

geological map. A total of 101 samples were collected from both species depending on their availability at each sample point.

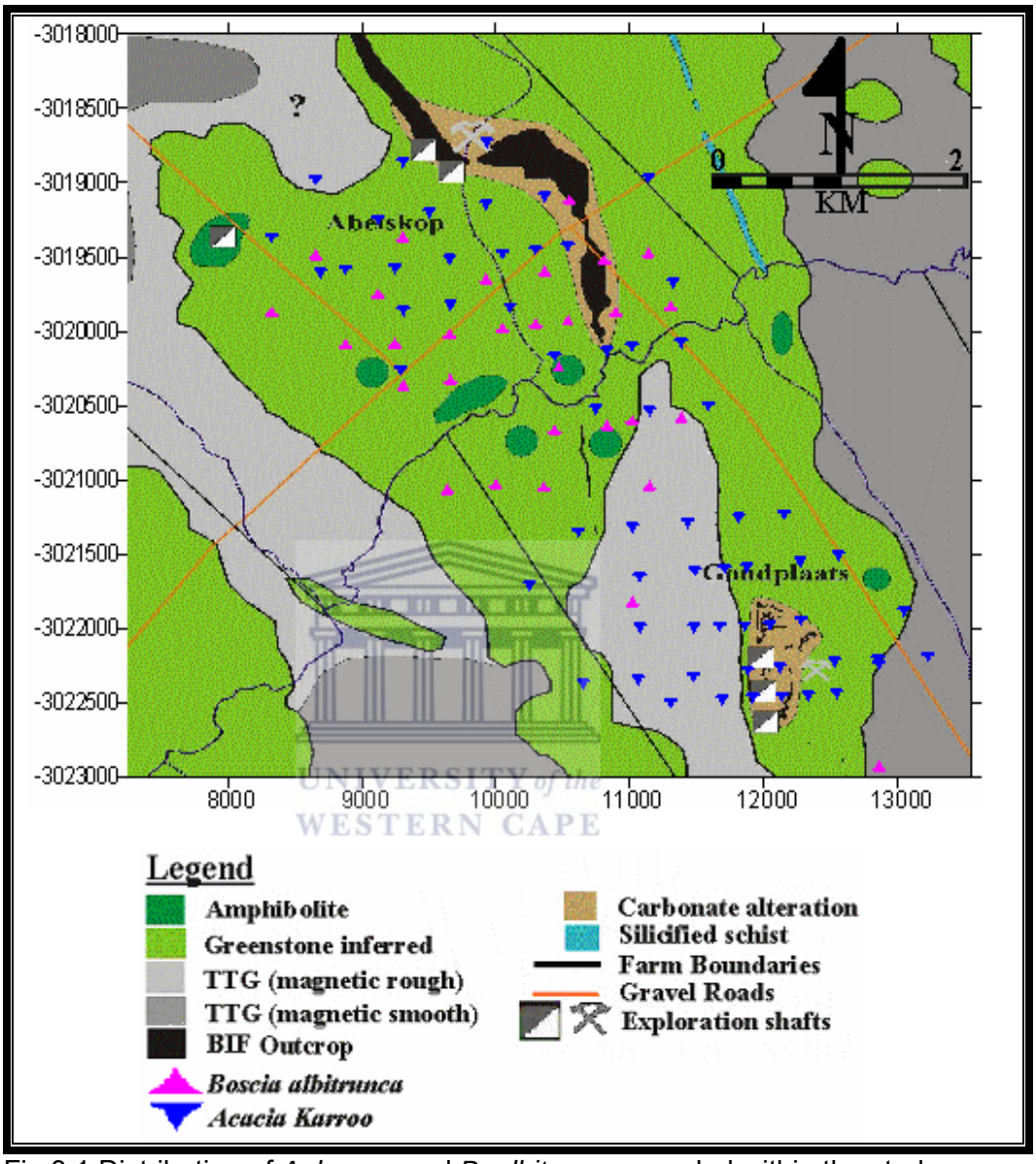

Fig 3.1 Distribution of *A. karroo* and *B. albitrunca* sampled within the study area

3.3 Sample Preparation

The samples were taken to the laboratory for preparation. Washing of the leaves was omitted because sampling took place during the rainy season, thus minimizing the effects of dust contamination. After removal of woody material, the leaves were dried in an oven at 110°C for about two hours. They were subsequently ashed in a muffle furnace at 450°C for a maximum of six hours. This was done in accordance with previous work where it was found that the optimum temperature for the ashing of plant material has been found to be 450˚C. At temperatures higher than this, vaporization may occur while at temperatures lower than this, ashing is incomplete (Zhihui, 1987). A total of 110 samples were ashed and ash weight varied from 0.16g to 2.0g.

3.4 Laboratory Analysis

A mass of 0.5g was taken from each sample except where the ash yield was less. In this case the all the ash was used. The samples were digested in aqua regia solution and taken to dryness in a sand bath. The residues were then taken up in 2M HNO_3. The samples however did not dissolve complete and were stirred overnight on a shaker. The remaining undissolved material was filtered and the filtrate was stored in vials for further analysis.

Chemical analysis of the samples was performed using a Finigan ICP-MS at the AERLS Laboratories in Johannesburg, South Africa. A total of 62 elements were measured. The raw analytical data have been presented in appendix 1. Vegetation analyses throughout this work are quoted on ash weight basis unless otherwise stated.

3.5 Data Evaluation

Statistical evaluation of analytical data was carried out with the aid of statistical software, SAS and STATG. The data obtained from the analysis was subjected to descriptive statistics, factor and cluster analysis. Summary statistics are presented in tables 4.1 and 4.2 and element boxplots have been presented in figures 4.1 to 4.8. The raw analytical data for and histograms are presented in appendices 1, 2 and 3 respectively.

Factor analysis and cluster analysis were performed on the data to minimize and detect trends in the data. Results of cluster analysis are presented in the form of a dendrograms (Figs 4.9 to 4.16) and the results of factor analysis are presented in tables 4.3-4.6 and appendix 4. Background and anomalous values (tables 4.7 and 4.8) were separated using boxplots.

The REEs were treated separately from the other trace elements, because of their unique coherent nature. These elements were plotted using PetroPlot to determine their distribution patterns in relation to bedrock, drainage and mineralization. These graphs are presented in figures 4.15 to 4.26.

Single element geochemical maps (Figs 4.27 to 4.30) were plotted to determine the spatial distribution of elements in the study area in relation to mineralization, bedrock and drainage. These maps were plotted with SURFER 7.0 software. A total of 62 elements were measured however not all the elements have been used. Four element groupings (macronutrients, gold and pathfinder elements, REEs and trace elements) were identified based on the results of factor analysis.

Chapter 4

4. Results

4.1 Patterns of element distribution in study area

In order to appraise patterns of element distribution in the Blue Dot Mine area, statistical evaluation of the analytically data needs to be considered first. Statistical summary of the elements obtained from the chemical analysis of *A. karroo* and *B. albitrunca* are presented in tables 4.1 and 4.2. Cluster and factor analysis were used to determine element groupings and correlations. As indicated earlier in chapter 3.5, four element groups will be considered in this study. These groups include, macronutrients (Ca, Mg, S, P, K), gold and pathfinder elements (As, Hg, Pb, Sb, Te, W and Ag), trace elements (Se, Sr,) and REEs (La, Ce and Eu).

4.1.1 Descriptive Statistics

The data statistical summaries for *A. karroo* and *B. albitrunca* have been tabulated in tables 4.1(a&b) and 4.2(a&b) and these tables include the means, medians, standard deviations, maximums and minimums. Boxplots (Figs 4.1-4.8) and frequency histograms (appendix 3) were used to describe the variability frequency distribution of the elements and to detect the occurrence of any outliers.

	Element	Min	Max	Mean	Median	Std Dev	Plants	Angiosperms
	Mg	2.4	7.9	4.118	4.08	1.24	0.2	0.32
	P	0.74	8.58	2.005	1.69	1.30	0.2	0.23
Macro	S	0.19	5.94	0.9654	0.7	0.86	0.3	0.34
nutrients	Ca	10.9	39.6	23.14	22.8	5.86	1	1.8
(%)	K	3.31	20	6.19	5.83	2.34	1.9	1.4
	B	143.0	748.7	410.0	382.8	175.3	0.2	0.085
Micro	Al	1118.2	9806.0	3383.7	2710.6	1821.3	0.5	<34
nutrients	V	2.8	20.1	7.8	6.6	3.8	0.05	NA
(%)	Mn	212.3	2416.4	630.1	550.7	382.4	0.2	≤24
	Fe	1314.0	9687.1	3956.0	3652.4	1837.6	0.04	0.0055
	Co	0.85	9.68	2.09	1.69	1.39	0.008	0.021
	Ni	15.2	146.8	49.4	48.7	22.6	0.04	NA
	Cu	16.5	204.0	56.2	45.0	33.7	0.008	NA
	Zn	92.1	604.0	246.3	222.5	108.4	0.03	NA
	La	1.01	59.17	4.93	3.00	7.55	0.008	NA
	Ce	1.72	12.61	4.93	4.38	2.25	0.02	NA
	Pr	0.18	10.20	0.87	0.57	1.29	0.004	NA
	Nd	0.59	37.68	3.05	2.00	4.78	0.02	<0.0015
REEs	Sm	0.13	7.38	0.58	0.37	0.93	0.003	NA
(ppm)	Eu	0.10	2.82	0.47	0.39	0.39	4.32	50
	Gd	0.13	9.16	0.62	0.38	1.15	80	550
	Tb	0.02	1.23	0.10	0.06	0.16	0.5	1.6
	Dy	0.09	4.59	0.38	0.26	0.58	200	630
	Ho	0.02	0.92	0.07	0.05	0.12	150	140
	Er	0.04	2.04	0.18	0.13	0.26	0.2	0.48
	Tm	0.01	0.24	0.02	0.02	0.03	1.5	2.7
	Yb	0.04	1.25	0.14	0.11	0.16	10	14
	Lu	0.01	0.18	0.02	0.02	0.02	50	160
	Li	1.65	21.49	6.94	5.79	3.86	0.2	0.1
	Be	0.04	0.75	0.12	0.10	0.10	0.001	<0.1
Trace	Rb	9.36	98.6	31.0	26.1	18.0	50	NA
elements	Sr	298.9	2372.5	1166.4	1120.8	488.8	50	26
(ppm)	Y	0.52	33.23	2.40	1.51	4.20	0.2	<0.6
	Zr	0.06	6.84	0.45	0.17	0.94	0.1	0.64
	Nb	0.07	0.83	0.25	0.23	0.13	0.05	0.3
	Pd	0.01	0.34	0.03	0.02	0.04	0.001	NA
	Ag	0.06	0.80	0.17	0.14	0.11	0.2	0.06
	Cd	0.02	0.56	0.08	0.06	0.08	0.05	0.64
	In	0.00	0.75	0.11	0.08	0.10	0.001	NA

Table 4.1a Statistical summary of elements in *A. karroo* (all elements in ppm except Au =ppb; macronutrients in %)

* Plant data obtained from Hall & Dunn (1999)

⁕ Angiosperm data obtained from Bowen (1964)

	Element	Min	Max	Mean	Median	Std Dev	Plants	Angiosperms
	Sn	0.15	1.46	0.36	0.29	0.23	0.2	<0.3
	Sb	0.00	0.42	0.16	0.15	0.07	0.1	0.06
	Te	0.05	0.18	0.10	0.10	0.03	0.05	NA
	Cs	0.15	227.5	7.10	1.05	29.25	0.2	0.2
	Ba	81.14	2948.3	917.4	769.4	616.9	40	14
	Hf	0.00	0.19	0.02	0.01	0.03	0.05	NA
Trace	Ta	0.001	0.013	0.003	0.002	0.002	0.001	NA
elements	W	0.20	1.69	0.41	0.37	0.22	0.2	0.07
(ppm)	Au	1.00	74.00	9.15	7.00	10.70	0.001	<0.00045
	Hg	0.03	20.32	0.89	0.21	2.71	0.1	0.015
	Tl	0.01	0.04	0.02	0.02	0.01	0.05	NA
	Pb	4.15	28.09	9.56	8.14	4.68	1	NA
	Bi	0.01	0.06	0.02	0.02	0.01	0.01	0.06
	Th	0.24	1.90	0.62	0.55	0.27	0.005	NA
	U	0.05	0.40	0.14	0.13	0.06	0.01	0.038
	Na	486.6	3470.3	1075.6	946.4	500.1	150	12000
	Sc	0.30	2.45	0.87	0.72	0.46	0.02	0.008
	Ti	39.9	407.2	118.8	97.1	64.0	5	1
	Cr	23.2	145.2	48.7	42.7	21.7	1.5	0.23
	Ga	0.71	29.46	4.41	2.91	4.48	0.1	0.05
	Ge	0.01	0.04	0.02	0.02	0.01	0.01	NA
	As	0.32	3.20	1.05	0.88	0.62	0.1	0.2
	Se	0.42	14.65	2.46	1.82	1.80	0.02	0.2

Table 4.1b Statistical summary of elements in A. karroo (all elements in ppm except Au =ppb; macronutrients in %) NA = not avaliable

* Plant data obtained from Hall & Dunn (1999)

⁑ Angiosperm data obtained from Bowen (1964)

	Element	Min	Max	Mean	Median	Std Dev
Macro nutrients %	Mg	0.67	5.47	3.12	3.11	1.27
	P	0.71	3.68	1.87	1.92	0.70
	S	0.26	2.29	1.01	0.96	0.56
	Ca	3.55	28.1	15	15.85	6.58
	K	4.91	17.9	8.39	7.47	3.55
Micro nutrients ppm	B	72.0	1052.0	406.0	347.1	270.3
	Al	891.1	10166.8	3481.9	3100.6	1879.3
	V	2.45	21.79	8.24	7.11	4.06
	Mn	217.1	2417.5	879.5	594.4	600.8
	Fe	1009.8	8375.2	3903.9	3872.3	1577.9
	Co	1.04	4.93	2.83	2.88	1.21
	Ni	31.0	227.2	75.7	70.7	41.4
	Cu	31.7	486.9	178.5	188.5	117.9
	Zn	141.2	637.1	331.7	335.4	125.7
REEs ppm	La	1.73	10.24	4.21	3.39	2.32
	Ce	2.58	11.29	5.66	5.21	2.40
	Pr	0.34	2.50	0.79	0.66	0.50
	Nd	1.11	9.72	2.70	2.14	1.91
	Sm	0.20	2.06	0.53	0.41	0.40
	Eu	0.06	0.86	0.27	0.20	0.22
	Gd	0.19	1.93	0.53	0.39	0.39
	Tb	0.03	0.39	0.09	0.07	0.07
	Dy	0.12	1.68	0.37	0.28	0.32
	Ho	0.02	0.34	0.07	0.06	0.06
	Er	0.06	0.78	0.18	0.14	0.15
	Tm	0.01	0.10	0.03	0.02	0.02
	Yb	0.04	0.48	0.14	0.12	0.09
	Lu	0.01	0.07	0.02	0.02	0.01
Trace elements ppm	Li	1.58	17.15	5.58	4.00	3.92
	Be	0.04	0.35	0.13	0.12	0.08
	Rb	9.06	63.9	31.5	25.2	18.6
	Sr	111.3	2322.5	627.8	485.7	460.5
	Y	0.68	10.56	2.19	1.79	2.04
	Zr	0.08	2.25	0.62	0.36	0.62
	Nb	0.11	1.00	0.35	0.28	0.21
	Pd	0.01	0.10	0.04	0.04	0.03

Table 4.2a Statistical summary of elements in *B. albitrunca* (all elements in ppm except Au =ppb; macronutrients in %)

	Element	Min	Max	Mean	Median	Std Dev
Trace Elements ppm	Ag	0.10	0.55	0.17	0.15	0.10
	In	0.03	0.38	0.13	0.12	0.09
	Sn	0.22	0.52	0.34	0.31	0.09
	Sb	0.10	0.24	0.14	0.13	0.04
	Te	0.03	0.14	0.07	0.07	0.02
	Cs	0.22	5.40	1.91	1.35	1.62
	Ba	33.9	1743.5	357.0	153.2	457.3
	Hf	0.01	0.06	0.02	0.01	0.02
	Ta	0.002	0.005	0.003	0.002	0.001
	W	0.23	1.39	0.60	0.54	0.29
	Au	3.00	10.00	5.36	5.00	1.68
	Hg	0.14	3.63	1.34	1.27	0.95
	Tl	0.00	0.03	0.01	0.01	0.01
	Pb	5.68	22.06	12.12	12.02	4.99
	Bi	0.01	0.30	0.04	0.02	0.06
	Th	0.40	1.34	0.66	0.60	0.23
	U	0.06	0.20	0.13	0.12	0.04
	Na	438.0	2737.0	948.8	809.0	493.1
	Sc	0.24	2.35	0.91	0.87	0.45
	Ti	52.0	257.0	144.0	139.6	56.4
	Cr	31.0	103.8	59.0	54.0	20.5
	Ga	0.31	8.94	1.94	1.26	1.96
	Ge	0.01	0.04	0.02	0.03	0.01
	As	0.42	3.34	1.15	1.10	0.70
	Se	1.43	4.79	2.79	3.05	0.94

Table 4.2b Statistical summary of elements in *B. albitrunca* (all elements in ppm except Au =ppb; macronutrients in %)

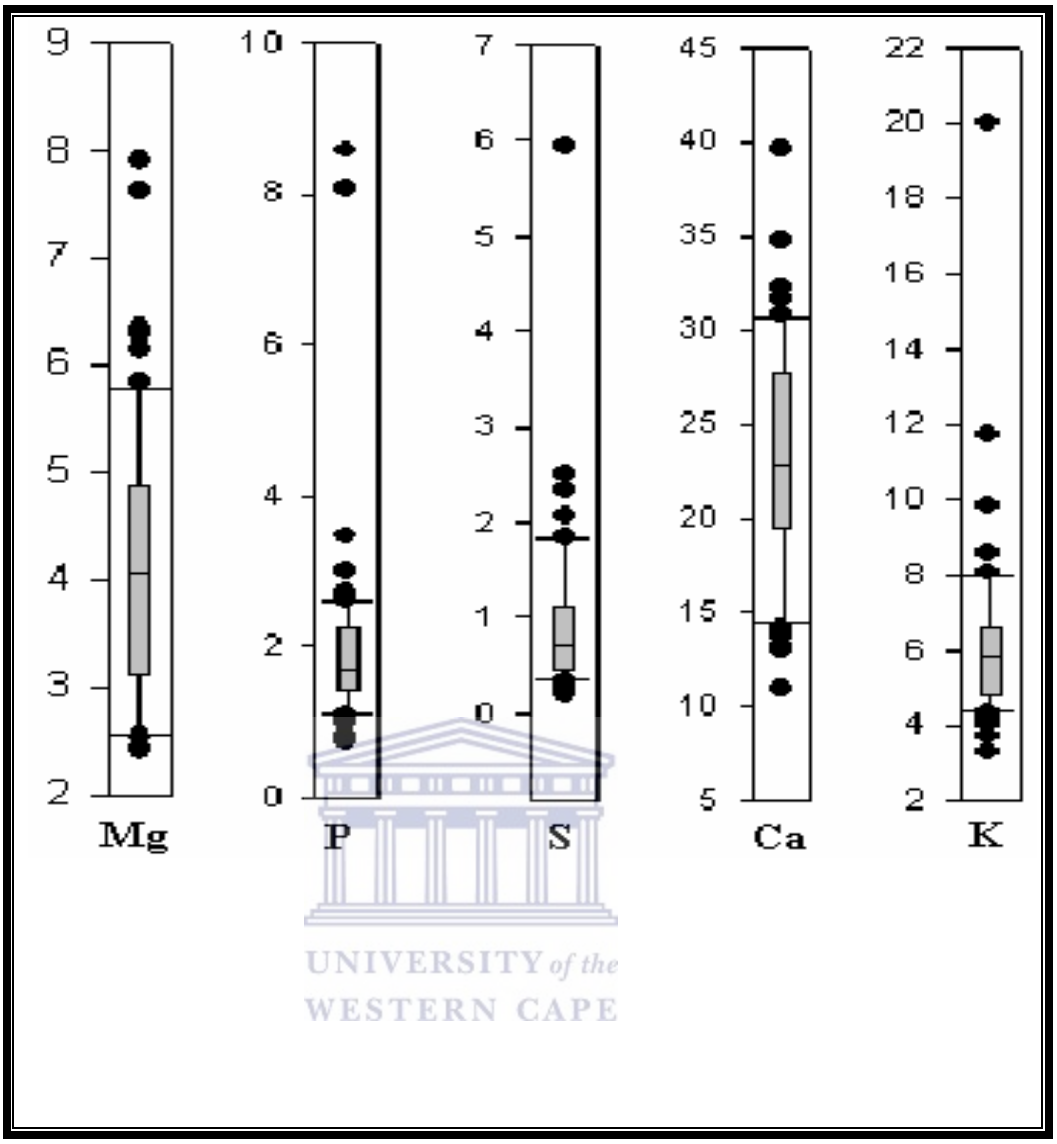

Fig 4.1 Boxplots for macronutrients in *A. karroo*

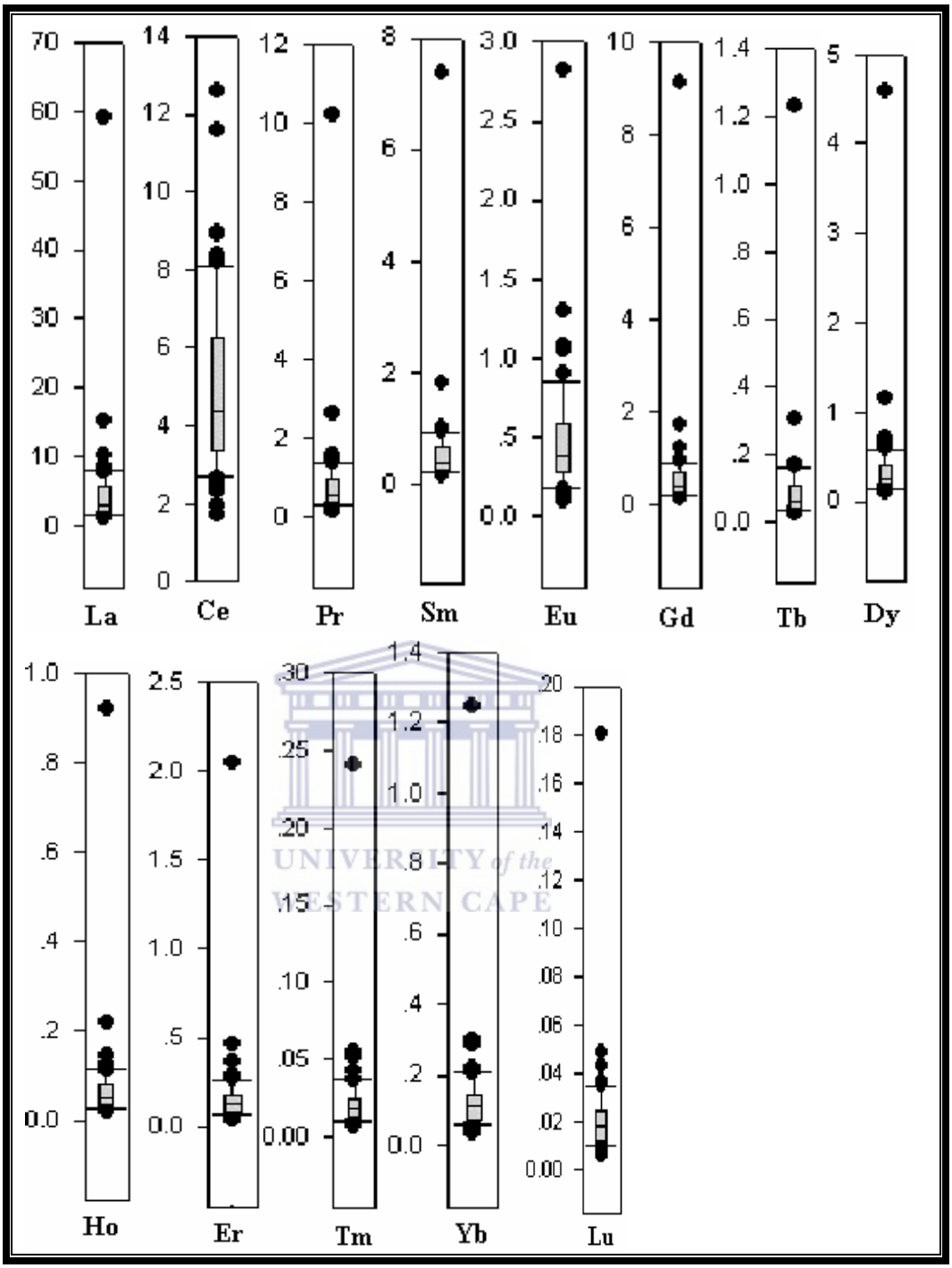

Fig 4.2 Boxplots for REEs in A. karroo (all elements in ppm)

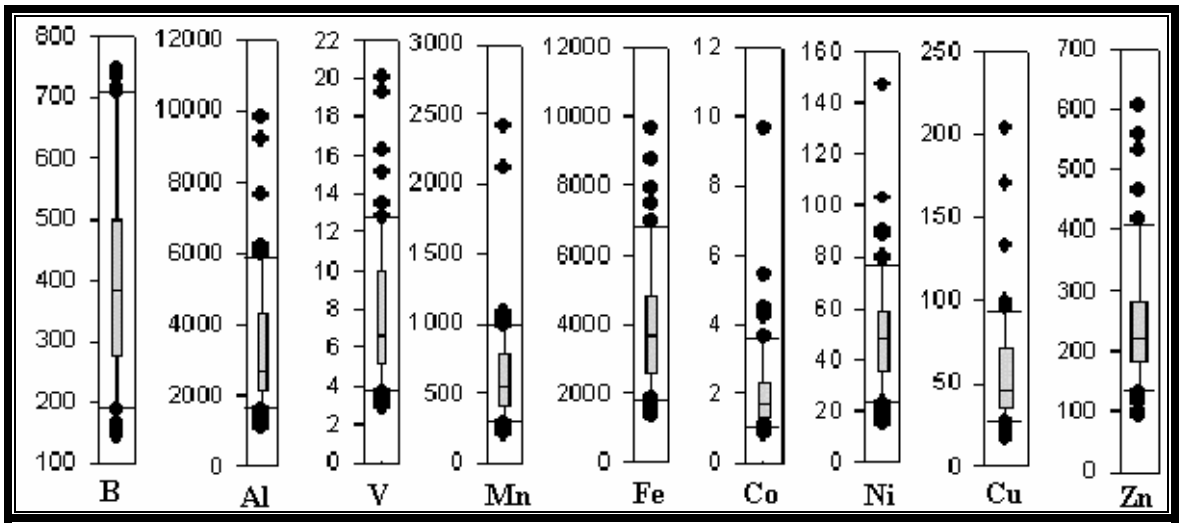

Fig 4.3 Boxplots of the micronutrients in *A. karroo* (all elements in ppm)

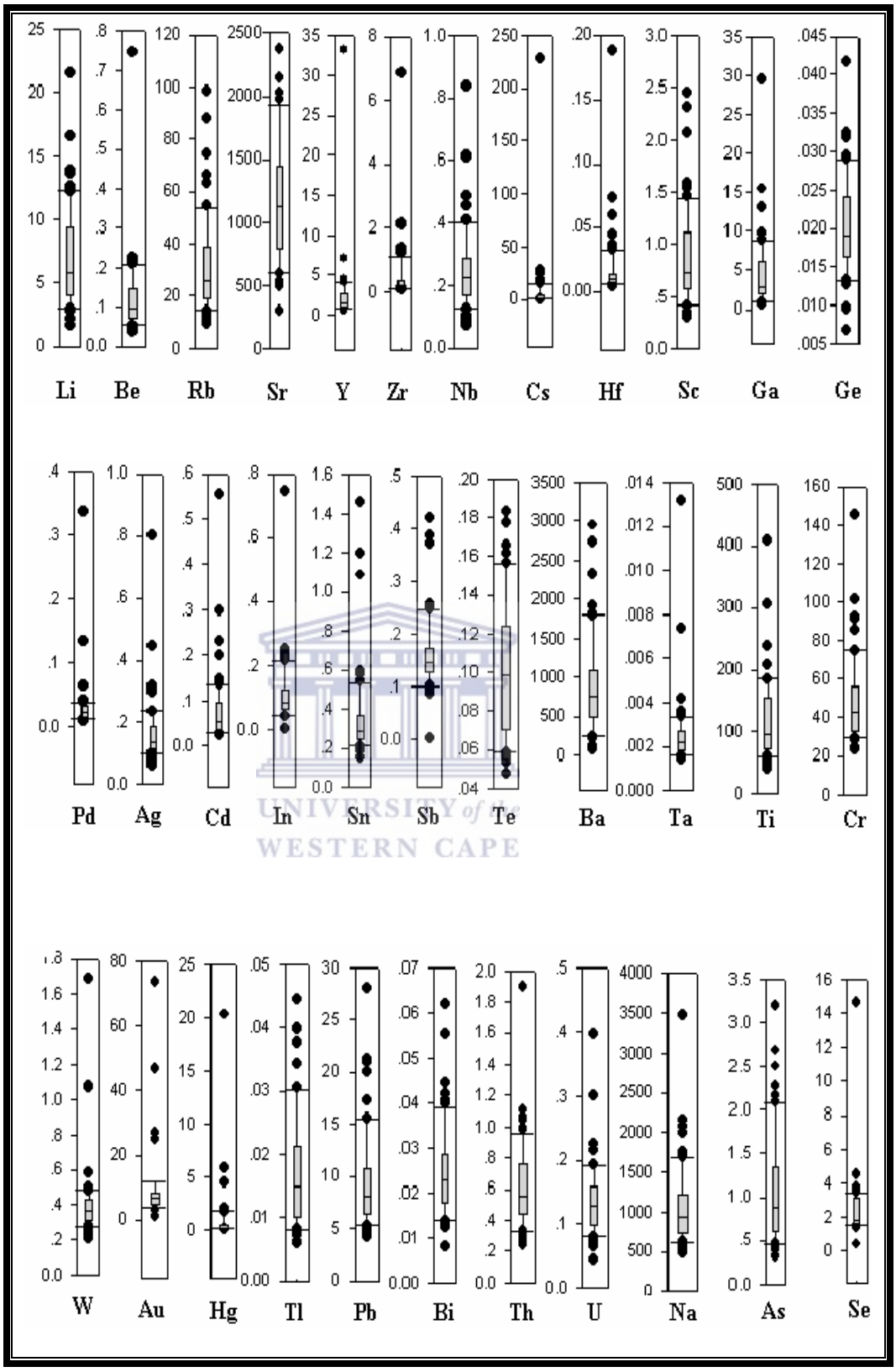

Fig 4.4 Boxplots of the trace elements in *A. karroo* (all elements in ppm except Au in ppb)

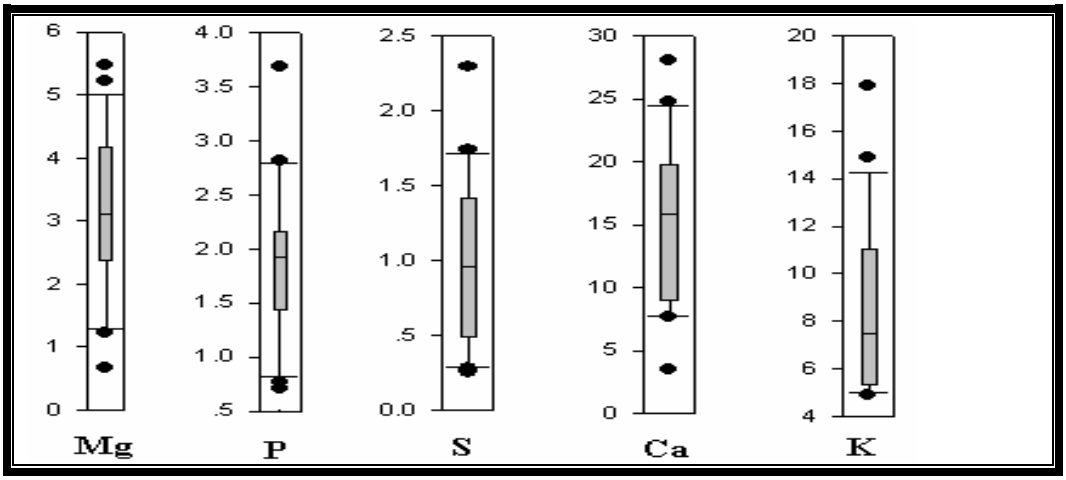

Fig 4.5 Boxplots of macronutrients in B. albitrunca (all elements in ppm except Au in ppb, macronutrients in %)

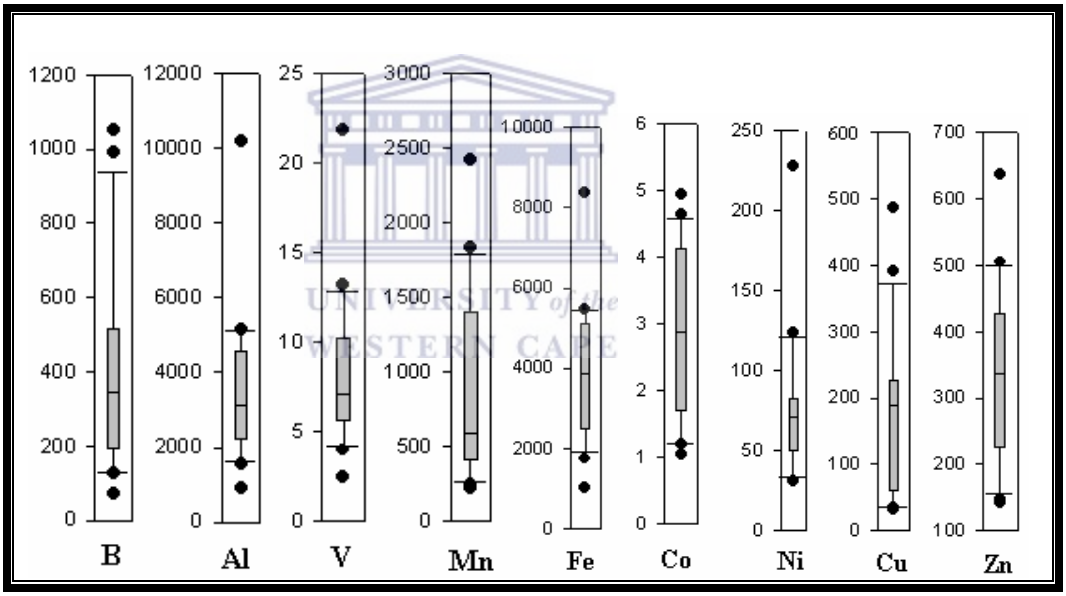

Fig 4.6 Boxplots of micronutrients in B. albitrunca (all elements in ppm except Au in ppb, macronutrients in %)

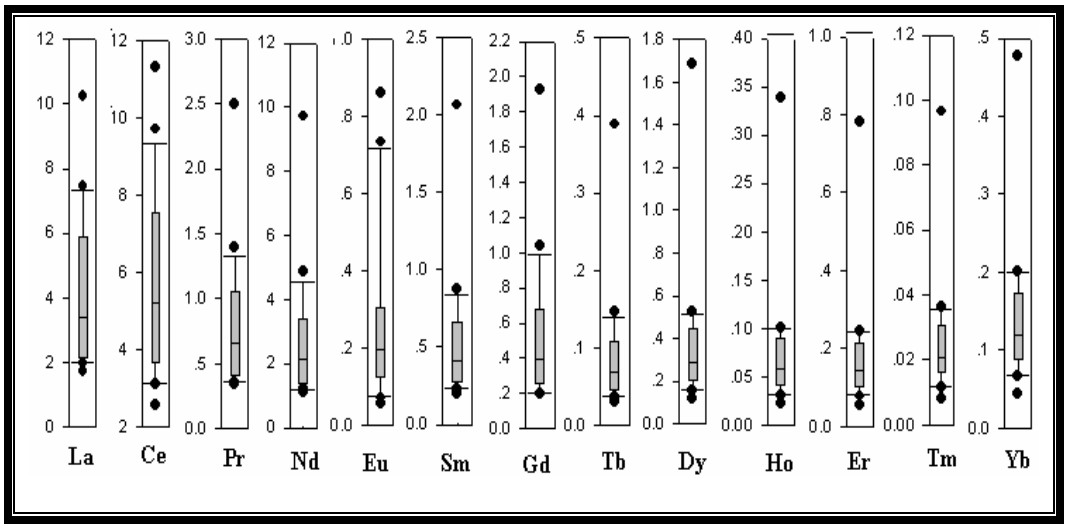

Fig 4.7 Boxplots of REEs in B. albitrunca (all elements in ppm except Au in ppb, macronutrients %)

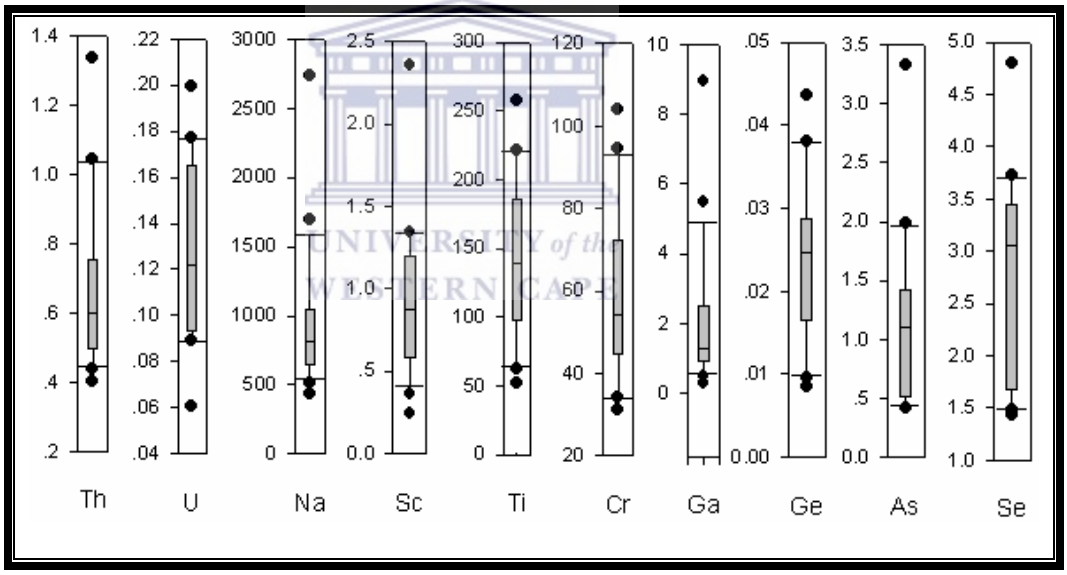

Fig 4.8a Boxplots of trace elements in B. albitrunca (all elements in ppm except Au in ppb, macronutrients in %)

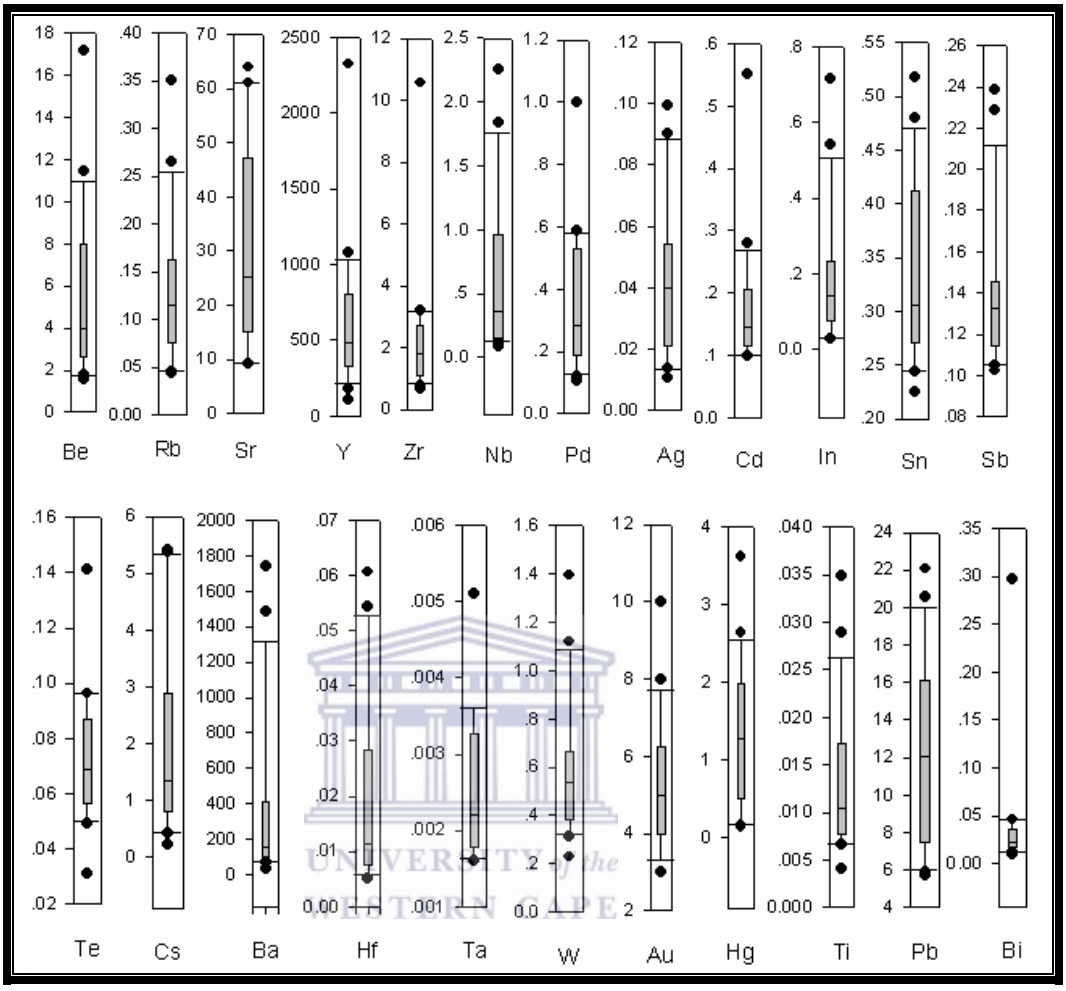

Fig 4.8b Boxplots of trace elements in B. albitrunca (all elements in ppm except Au in ppb, macronutrients in %)

4.1.1.1 Macronutrients

Calcium

Calcium content in *A. karroo* varies between 10.9 to 39.6% with an average value of 23.1% (~2.3% dry wt) and a median value of 22.8% (2.28% dry wt). Lower Ca contents and therefore level uptake occurs in *B. albitrunca* (3.5-28.1%) with an average value of 15.0% (1.5 dry wt). The average Ca content in *A karroo* and *B. albitrunca* compare favourably with available literature reported in dry wt (table 1) eg. 1% dry wt as an average content for plants (Hall and Dunn, 1999), 1.8% dry wt for angiosperms (Bowen, 1964). Ca is taken up by plants in the form of bivalent Ca and plays an important structural role in plants because of its capacity for coordination, by which it provides stable but reversible intermolecular linkages, predominantly in the cell walls at the plasma membrane (Marschner, 1995). Calcium can hyperaccumulate by as much as 10% dry wt in mature leaves without symptoms of toxicity being displayed (Marschner, 1995). The Ca content in the investigated species is well within the 'normal' range.

The boxplots for calcium indicate slightly greater variability for *B. albitrunca* compared to *A. karroo.* The data for *A. karroo* is nearly symmetrical with an outlier whilst *B. albitrunca* is negatively skewed with no outliers. This is further shown by the histograms of the two plants.

Calcium is one of the most common nutrient elements in nature that is taken up by the roots as divalent ions through facilitated passive diffusion (Greger, 2004). At the cells, the Ca concentration is confined to the cell walls and cell compartments so as not to interfere with P at the cytoplasm. Calcium readily forms complexes with phosphates and hence may affect metabolism (Greger, 2004).

Phosphorus

Very similar levels of P absorption occur in the two investigated plants with average values of 2.01% (0.2% dry wt) for *A karroo* and 1.87% (0.187% dry wt) for *B.*

albitrunca. The median values of 1.69% (0.169 dry wt) and 1.92% (0.192% dry wt) respectively are also similar and also compare favourably with values reported for plants (0.2% dry wt) and slightly higher for angiosperms (3.2% dry wt).

This macronutrient has more or less equal distribution between the two plants though it slightly higher in *A. karroo.* The boxplot of both species show great variability and *B. albitrunca* has an outlier. The *B. albitrunca* data is negatively skewed and the *A .karroo* is positively skewed.

Magnesium

The average Mg content in *A karroo* and *B. albitrunca* is 4.12% (0.412% dry wt) and 3.12% (0.312% dry wt) respectively. Both values compare well with literature values for angiosperms (0.32% dry wt) (Bowen, 1964) and plants (0.2% dry wt) (Hall & Dunn, 1999). *A karroo* has a median value of 4.08% (0.408% dry wt) with Mg content ranging from 2.4% (0.24% dry wt) to 7.90% (0.79% dry wt) while *B. albitrunca* has a median value of 3.11% (0.311% dry wt) and ranging from 0.67% (0.067% dry wt) to 5.47% (0.547% dry wt). There is great variability in both plant species but lesser values for *B. albitrunca*. *A. karroo* data is negatively skewed and has outliers. *B. albitrunca* has symmetrical data and no outliers.

Magnesium is found in ionic form in the cell due to its involvement in electro-potential regulation and osmotic adjustments. It is also important in photosynthesis and carbon fixation. The binding strength of the hydrated Mg^{2+} is rather low at the exchange sights in the cell wall, hence other cations such as Ca^{2+} and K^{+} compete effectively with Mg^{2+} (Marschner, 1995). Uptake into the roots takes place by passive diffusion.

Potassium

Potassium content in *A. karroo* varies from 3.31% to 20% with an average value of 6.19% (0.62% dry wt) and a median value of 5.83% (0.58% dry wt). Potassium content is slightly higher in *B. albitrunca*, averaging at 8.39% (0.84% dry wt) and a median value

of 7.47% (0.75% dry wt). These values are lower when compared to the reported literature values for both angiosperms (1.4% dry wt) (Bowen, 1964) and plants (1.90% dry wt). The boxplot of the two plants show slightly lower values for *A. karroo,* and much greater variability for *B. albitrunca*. Histograms of the two plants show a number of outliers for *A. karroo* and a single outlier for *B. albitrunca.*

Potassium mostly occurs as a free cation and is important for the maintenance of electro-chemical potentials of plant cells. Due to its high mobility in plants, the uptake of K is highly selective and closely coupled to metabolic activity (Marschner, 1995). Depending on the external K concentration, its uptake depends on low and high affinity carriers (biphasic) (Marschner, 1995). Potassium is not metabolized and forms weak complexes in which it is easily exchangeable especially with hydrated Rb^+. The radius of hydrated Rb^+ is similar to that of hydrated K^+ hence the binding site at the plasma membrane is unable to distinguish between the two cations (Greger, 2004). Sodium and caesium also often substitute potassium.

Sulphur

A. karroo has a S content that varies from 0.19% to 5.94% and that of *B. albitrunca* varies from 0.26% to 2.29%. *B. albitrunca* has a higher average S content of 1.01ppm (0.101ppm dry wt) compared to *A. karroo* which averages at 0.97% (0.097% dry wt). The average content in both species is much lower compared to the literature values in angiosperms (0.34ppm dry wt) and plants (0.30ppm dry wt).

The boxplots of the two plants indicate a wide distribution of the data with outliers in each plant however *A. karroo* has lower values compared to *B. albitrunca* and the histograms of the two species show that the data is positively skewed.

4.1.1.2 Gold and Pathfinder Elements

Gold

The average gold content in *A. karroo* is 9.15ppb (0.92ppb dry wt) with a median value of 7ppb (0.7ppb dry wt). The gold content is lower in *B. albitrunca*, averaging at 5.36ppb (0.54ppb dry wt) with a median value of 5ppb (0.5ppb dry wt) that is similar to *A. karroo*. The average Au content in *A. karroo* compares favourably with literature plant values (0.001ppm dry wt) (Hall & Dunn, 1999). However this is not the case with respect to values of angiosperms as the reported value is very much smaller (<0.00045ppm dry wt) when compared to the average content of the two species. Outliers and no variability characterize the data in both plants. *B. albitrunca* has a single outlier, which is note depicted in its histogram.

Gold in soils is found in mobile complexes such as Au $(CN)_2^{2-}$, AuI_2^-, $AuBr_4^-$ and is transported as organometallic complexes or chelates. Upon entry into the plant, Au is easily translocated to the top of the plant. Root excudates of cyanogenic plants are able to dissolve gold hence such plants are known to hyperaccumulate Au by up to 1ppm dry wt (Greger, 2004).

Arsenic

Arsenic in *A. karroo* has an average value of 1.05ppm (0.101ppm dry wt) with a median value of 0.88ppm (0.088ppm dry wt). In *B. albitrunca* the average As content is 1.15ppm (0.115ppm dry wt) with a median value of 1.10ppm (0.11ppm dry wt). The reported As values for plants, 0.1ppm dry wt compares favourably with the two plants whereas the value for the angiosperms is slightly higher at 0.2ppm dry wt. The variability is more or less the same in both plant species and both data are skewed, *A. karroo* is positively skewed and *B. albitrunca* negatively skewed. *B. albitrunca* has a single outlier and *A. karroo* has three outliers. The above is also reflected in the histograms of the two plants.
Arsenic is absorbed in the plant as arsenate as a result of bacterial oxidation of arsenites. Arsenate and phosphate are taken up passively by water flow due to the linear

relationship between uptake and soil concentration (Greger, 2004). Thus high arsenate levels in the soil can be countered by the introduction of phosphates. High concentrations of As are normally encountered in the roots and old leaves.

Silver

The levels of Ag absorption are identical in both plants with average values of 0.17ppm (0.017ppm dry wt) and median values of 0.14ppm (0.014ppm dry wt) for both *A. karroo* and *B. albitrunca*. These values are lower than the reported values for angiosperms (0.06ppm dry wt) and even lower for plant values (0.2ppm dry wt) (Hall & Dunn 1999). Both species display similar trends in terms of variability and positively skew data. *A. karroo* has more outliers compared to *B. albitrunca.* The histograms are in agreement with the boxplots of the two plants.

Silver is easily released during weathering and then precipitated in alkaline reduction potential and S enriched solutions, forming a variety of anions and cations (Greger, 2004). Silver complexes are however immobile above pH4. Plant uptake of Ag differs between time of the year, with increased uptake during spring and decreased uptake during autumn.

Mercury

A higher average Hg content of 1.34ppm (0.13ppm dry wt) with a median value of 1.27ppm (0.127ppm dry wt) was detected for *B. albitrunca* while *A. karroo* averages at 0.89ppm (0.088ppm dry wt) with a median value of 0.21ppm (0.021ppm dry wt). The values for *B. albitrunca* compare favourably with the literature values for plants (0.1ppm dry wt) (Hall & Dunn, 1999) and *A. karroo* compares with the values for angiosperms (0.015ppm dry wt) (Bowen, 1964).

B. albitrunca has greater variability and positively skewed data. *A. karroo* has extreme outliers, which are not clearly visible in the histograms.

Mercury exists in five forms i.e. Hg^{2+}, Hg^{+}, Hg^{0}, $HgCH^{3+}$ and $Hg(CH_3)^{2+}$. Plant uptake occurs via the roots in both organic and organic methyl mercury. Since Hg also occurs in the gaseous form it can be accumulated in the leaves (Greger, 2004). The translocation of root to shoot and vice versa is very poor.

Lead

The total Pb content in *A. karroo* is 9.56ppm (0.96ppm dry wt) with a median value of 8.14ppm (0.81ppm dry wt). The Pb content in *B. albitrunca* is higher at 12.1ppm with a median value of 12ppm. There is greater variability displayed by *B. albitrunca* compare to *A. karroo*. Both data are slightly positively skewed and *A. karroo* has outliers and extreme outliers. The histogram for *B. albitrunca* indicates the presence of outliers but these are not visible on the boxplots. The uptake of Pb into the plants takes place passively, via the root hairs and accumulated in the cell walls. Very little of the absorbed Pb makes it to the shoot (Greger, 2004).

Antimony

Antimony contents in *A. karroo* vary between 0.03ppm to 0.42ppm with an average value of 0.16ppm (0.016ppm dry wt) and a median value of 0.15ppm (0.015ppm dry wt). Lower Sb contents and therefore uptake occurs in *B. albitrunca* (0.10- 0.24ppm) with an average of 0.14ppm (0.014ppm dry wt) and a median value of 0.13ppm (0.013ppm dry wt). In comparison with literature values the above values are less (0.06ppm dry wt) for angiosperms and (0.1ppm dry wt) for plants.

A. karroo has greater variability compared to *B. albitrunca.* Both data have outliers and extreme outliers, which are reflected on their respective histograms. The association of Sb with Fe hydroxides indicates a relatively high mobility in the environment. The uptake of Sb in the plants occurs at its most soluble form.

Tellurium

Tellurium content in *A. karroo* varies between 0.05 to 0.18ppm with an average value of 0.1ppm (0.01ppm dry wt) and a median value of 0.1ppm (0.01ppm dry wt). Lower Te contents and therefore uptake occurs in *B. albitrunca* (0.03 to 0.14ppm) with an average of 0.07ppm (0.007ppm dry wt) and a median value of 0.07ppm (0.007ppm dry wt). The above values are much lower than the average plant values, 0.05ppm dry wt (Hall & Dunn, 1999). The values for angiosperms were not available for comparisons.

A. karroo shows a greater variability compared to *B. albitrunca* with regards to their respective boxplots. *B. albitrunca* has a positively skewed boxplot with some outliers whereas *A. karroo* has a more or less symmetric boxplot with no outliers. This trend is shown in the histograms of the two plants.

Tungsten

B. albitrunca has a higher W average 0.60ppm (0.06ppm dry wt) and median (0.54ppm, 0.054ppm dry wt) tungsten value, when compared to *A. karroo*. *A. karroo* has an average W content of 0.41ppm (0.041ppm dry wt) and a median value of 0.37ppm (0.037ppm dry wt). The value for angiosperms, 0.07ppm dry wt compare favourably with *A. karroo* and *B. albitrunca* values. The boxplots show greater variability for *B. albitrunca* and lesser variability for *A. karroo* and outliers for both plants. The geochemical behaviour of W resembles that of Mo even in the case of plants where it is taken up in the anionic form, WO_4^{2-}. Values below 1ppm dry wt W seem to be more common in plants.

4.1.1.3 Trace Elements

Selenium

Average Se content is 2.46ppm (0.25ppm dry wt) for *A .karroo* and 2.79ppm (0.28ppm dry wt) for *B. albitrunca* with median values of 1.82ppm (0.182ppm dry wt) and 3.05ppm (0.31ppm dry wt) respectively. The Se content in both plants compares well with that of

angiosperms, 0.2ppm dry wt (Bowen, 1964). There is very little variability in *B. albitrunca* and the data also has negative outliers. *A .karroo* has a boxplot that is very positively skewed with an extreme outlier. The histogram for *B. albitrunca* does not show the outliers, which are visible in the boxplots. Selenium has common features with sulphur as it can exist in the Se^{2-} (selenide), Se^{4-} (selenite) and Se^{6-} (selenate) oxidation states. However the plants have a strong preference for selenate compared to selenite (Marschner, 1998). Due to the similarities between S and Se, the uptake of selenate is strongly decreased by the presence of sulphates as the two compete for uptake sites. *A .karroo* and *B. albitrunca* show a slight Se enrichment

Strontium

Strontium in *A .karroo* has an average value of 1166.4ppm (116.6ppm dry wt) with a median value of 1120.8ppm (112.1ppm dry wt) while *B. albitrunca* has an average Sr content of 627.8ppm (62.8ppm dry wt) with a median value of 485.7ppm (48.6ppm dry wt). *B. albitrunca* compares favourably with literature for Sr content in plants (50ppm dry wt) (Hall & Dunn, 1999). The Sr content is significantly high in *A .karroo* and does not compare with neither the plant values nor the angiosperm values (26ppm dry wt) (Bowen 1964).

The Sr is highly variable in *A. karroo* and the data is near symmetrical. *B. albitrunca* has positively skewed data with a single extreme outlier as depicted in its histogram. Strontium is often closely associated with Ca and sometimes Mg and occurs as Sr^{2+}. It is easily mobilized during weathering and is incorporated in clay minerals and fixed in organic matter (Greger, 2004). Thus the availability of Sr is dependent on soil pH and organic content of soil. Strontium is very mobile in acidic and anaerobic soils. The root uptake of Sr in soils is related to the mechanisms of both mass flow and exchange diffusion. The availability of Sr may however be affected by Na, Ca, K and Mg (Greger, 2004).

4.1.1.4 Rare Earth Elements

Lanthanum

The average La content in *A. karroo* is 4.93ppm (0.49ppm dry wt) with a median value of 3ppm (0.3ppm dry wt). *B. albitrunca* has slightly lower average of 4.21ppm (0.42ppm dry wt) and a higher median value of 3.39ppm (0.34ppm dry wt). The values compare favourably with the plant content 0.2ppm dry wt (Hall & Dunn, 1999). Both species display same amount of variability with *A. karroo* positively skewed with outliers. *B. albitrunca* is symmetrical with no outliers.

Cerium

The Ce content in *A. karroo* varies from 1.72 to 12.6ppm with an average value of 4.93ppm (0.49ppm dry wt) and that of *B. albitrunca* varies from 2.58 to 11.3ppm with average value of 5.66ppm (0.57ppm dry wt). Cerium values for plants (0.5ppm dry wt) are in agreement with the investigated plants. Both species show same amount of variability in the boxplots. *B. albitrunca* is positively skewed with outliers while *A. karroo* is negatively skewed with outliers.

Europium

Europium content in *A. karroo* is 0.47ppm (0.047ppm dry wt) with a median value of 0.39ppm (0.039ppm dry wt) and *B. albitrunca* has an average content of 0.27ppm (0.027ppm dry wt) with a median value of 0.20ppm (0.020ppm dry wt). The content in the two plants is higher than the average content reported for plants, 0.008ppm dry wt (Hall & Dunn, 1999). The variability in the boxplots is less equal with some outliers present.

4.1.2 Factor Analysis

Element associations are important in mineral exploration and geologists tend to look for these associations in rocks and soils during prospecting. Element associations found in rocks and soils may also be prevalent in plants. However the behaviour of these element associations in rocks and soil is different in plants (Hall & Dunn, 1999). This difference is due to a number of factors: plants have certain physiological requirements; seasonal variations in plant chemistry i.e. some associations occur at a certain time (season) of the year and not in another; plants have different requirements and/or tolerances for certain elements.

Because of the above factors, it is therefore necessary to treat biogeochemical data sets differently from those of soil and rocks (Hall & Dunn, 1999). Furthermore, classic element associations such as Sb, As and Au can be found but associations (such as Cs and Br) that have never been seen in any other sample media can occur (Hall & Dunn, 1999). The key to locating underlying or hidden ores is to look at spatial relationships among the elements by recognizing patterns. There are a number of multivariate techniques such as factor analysis that can be used to establish element associations.

Factor analysis (FA) is a well-known statistical technique, which offers a powerful tool to study the interrelationship among variables. The principal aim of factor analysis is to explain the variation in a multivariate data set by a few "factors" as possible and to detect hidden multivariate structures (Reimann et al., 2002). The term factor as used by psychologists, is equivalent to "controlling processes" in geochemistry. The statistical analysis of the data, correlation, cluster and factor analysis and interpretation of obtained results for every data set were performed using SAS software. A brief summary of the underlying principles of FA is given below.

The main applications of FA technique are to reduce the number of variables and to detect structure in the relationships between variables that is to classify variables. Therefore FA is a data reduction or structure detection method. What factor analysis does

is to take thousand or millions of measurements and qualitative observations and resolves them into distinct patterns of occurrence.

The percentage of common variance figures indicate how whatever regularity exists in the data is divided among the factor patterns. The percent of total variance figures, measure how much of the data variation is involved in a pattern; the percent of common variance figures measure how much of the variation accounted for by all the patterns is involved in each pattern.

The most often employed techniques of factor analysis centroid and principal axis are applied to a matrix of correlation coefficients among all the variables. The correlation matrix has the following features:

The coefficients of correlation express the degree of linear relationship between the row and column variables of the matrix. The closer to zero the coefficient, the less the relationship; the closer to one, the greater the relationship.

To interpret the coefficient, square it and multiply by 100. This will give the percent variation in common for the data on the two variables.

The correlation coefficient between two variables is the cosine of the angle between the variables as vectors plotted on the coordinate axes.

The principal diagonal of the correlation matrix usually contains the correlation of a variable within itself, which is always 1.0. Often, however, when the correlation matrix is to be factored (using the common factor analysis model), the principal diagonal will contain communality estimates instead. These measure the variation of a variable in common with all the others together.

The eigenvalues equal the sum of the column of squared loadings for each factor. They measure the amount of variation accounted for by a pattern. Dividing the eigenvalues either by the number of variables or by the sum of h^2 values and multiplying by 100 determines the percent of either total or common variance, respectively.

4.1.3 Results of factor analysis

Due to the large differences in concentration ranges of the different elements, the elements were divided into macronutrients, trace elements, rare earth elements (REE) and micronutrients. The initial step in the FA is the computation of a correlation matrix, whose results are presented in appendix 4. This step is followed by extraction of statistically significant principal components from the correlation matrix. The factor analysis extracted 2 factors for the macronutrients, 1 factor for the REE, 2 factors for the micronutrients and 9 factors for the trace elements. The factor extraction matrix was done with the minimum acceptable eigenvalue > 1. The eigenvalues and factor scores are given in tables 4.3-4.4 respectively.

4.1.3.1 Macronutrients

In the macronutrients, only two eigenvalues >1(table 4.3) were detected hence only two factors (table 4.6) account for 70% of the total variability in the data. It is therefore reasonable to assume that the five variables (Mg, P, S, Ca, K) are well represented by these two factors.

Factor 1 accounts for 40.9% of the variance, with high factor loadings for Ca and Mg. This factor, shows highest scores for Ca and Mg, which is indicative of ultramafics rocks. The ultramafic rocks that are found in the Blue Dot Mine are Fe and Mg tholeiites and komatiitic basalts and these are enriched in Ca and Mg (Kiefer, 2004).

Factor 2 comprises 29% of the variance and has high factor loadings for P, S and K. Factor 2 which groups K, S, and P, the lesser abundant elements in the study area. These elements especially S are associated with mineralization. Gold mineralization in the study area is associated with pyrite and chalcopyrite.

	Eigenvalue	Difference	Proportion	Cumulative
1	2.04568021	0.58521308	0.4091	0.4091
2	1.46046713	0.73459238	0.2921	0.7012
3	0.72587475	0.19003336	0.1452	0.8464
4	0.53584139	0.30370488	0.1072	0.9536
5	0.23213651		0.0464	1.0000

Table 4.3 Eigenvalues for Macronutrients

4.1.3.2 Trace elements

The trace elements, which have the most numerous of variables, has nine eigenvalues above 1 (table 4.4) and hence nine factors, which account for 78% of the variability.

- Factor 1 groups In, Se, Be, Pd, Hg, As, Ag, W, Sn, and Cd, with variance of 26%. Most of the pathfinder elements with the exception on In and Be are grouped under factor 1.
- Factor 2 has high factor loadings for Th, Sc, Ti, Tl, U and Sb, with a 12% variance. The trace elements grouped under factor 2 are mainly immobile elements with the exception of Sb.
- Factor 3 groups Sr, Ba, Ga and Te together at a variance of 11%. Factor 3 groups Sr, Ba, Ge and Te together, a clear indication of feldspars. Feldspars are major constituents of granites.
- Factor 4 explains 7% of the variance and groups Zr, Hf and Cr together. Zr, Hf and Cr make up factor 4, which is also a group of immobile elements and are resistant to weathering. Zr and Hf are elements that are often geochemically associated due to their similarities.
- Factor 5 has high factor loadings for Li, Nb, Na and Pb and accounts for 6% of the variance and this is indicative lithology.
- Factor 6 represents 5% of the variance and groups Y and Ta together. Y and Ta constitute factor 6 and the two are immobile elements. The two elements are found mainly in granitic rocks. Ta is normally associated with alkaline rocks such as granites.
- Ge and Bi are grouped under factor 7 with a variance of 4%. Factor 7 consists of Ge and Bi, which are indicative of mineralization
- Factor 8 also has a 4% and groups Cs, and Rb together. Cs and Rb belong to factor 8 and these two elements are major constituents of feldspars, which are in turn found in granites.

The last factor, factor 9 comprises only one element, Au and explains 3% of the variance. Gold is indicative of mineralization.

	Eigenvalue	Difference	Proportion	Cumulative
1	8.97323956	4.76533909	0.2639	0.2639
2	4.20790046	0.37178840	0.1238	0.3877
3	3.83611206	1.52340674	0.1128	0.5005
4	2.31270533	0.15860451	0.0680	0.5685
5	2.15410081	0.51073171	0.0634	0.6319
6	1.64336910	0.30397864	0.0483	0.6802
7	1.33939046	0.14726005	0.0394	0.7196
8	1.19213041	0.12144901	0.0351	0.7547
9	1.07068140	0.12608634	0.0315	0.7862
10	0.94459505	0.06761645	0.0278	0.8139
11	0.87697860	0.04297233	0.0258	0.8397
12	0.83400627	0.13778755	0.0245	0.8643
13	0.69621872	0.16438687	0.0205	0.8847
14	0.53183185	0.01696741	0.0156	0.9004
15	0.51486444	0.06059564	0.0151	0.9155
16	0.45426880	0.07507666	0.0134	0.9289
17	0.37919214	0.05432865	0.0112	0.9400
18	0.32486349	0.03618244	0.0096	0.9496
19	0.28868105	0.03579220	0.0085	0.9581
20	0.25288885	0.03468169	0.0074	0.9655
21	0.21820716	0.03571306	0.0064	0.9719
22	0.18249410	0.02068952	0.0054	0.9773
23	0.16180459	0.01054121	0.0048	0.9821
24	0.15126338	0.05459541	0.0044	0.9865
25	0.09666797	0.00775314	0.0028	0.9894
26	0.08891483	0.02105448	0.0026	0.9920
27	0.06786035	0.00373962	0.0020	0.9940
28	0.06412073	0.00916215	0.0019	0.9959
29	0.05495858	0.02027882	0.0016	0.9975
30	0.03467976	0.01097635	0.0010	0.9985
31	0.02370341	0.01137978	0.0007	0.9992
32	0.01232363	0.00234746	0.0004	0.9996
33	0.00997616	0.00496967	0.0003	0.9999
34	0.00500650		0.0001	1.0000

Table 4.4 Eigenvalues for Trace elements

4.1.3.3 Rare Earth Elements

The REE correlation matrix shows a very high degree of correlation with one another, having only one eigenvalue greater than 1 (table 4.5), hence this group is adequately represented by one factor. This single factor accounts for more than 90% of the total variability in the data.

	Eigenvalue	Difference	Proportion	Cumulative
1	12.6685422	11.7641236	0.9049	0.9049
2	0.9044185	0.5767647	0.0646	0.9695
3	0.3276538	0.2527391	0.0234	0.9929
4	0.0749147	0.0589224	0.0054	0.9983
5	0.0159923	0.0116095	0.0011	0.9994
6	0.0043828	0.0022281	0.0003	0.9997
7	0.0021547	0.0011877	0.0002	0.9999
8	0.0009669	0.0005452	0.0001	0.9999
9	0.0004217	0.0001056	0.0000	1.0000
10	0.0003161	0.0002060	0.0000	1.0000
11	0.0001101	0.0000494	0.0000	1.0000
12	0.0000607	0.0000164	0.0000	1.0000
13	0.0000443	0.0000232	0.0000	1.0000
14	0.0000211		0.0000	1.0000

Table 4.5 Eigenvalues for REEs

Macronutrients

	Factor1	Factor2
Ca	0.87844	0.02173
Mg	0.88495	0.40480
P	0.37859	0.78167
S	0.13705	0.72825
K	-0.43159	0.60930

Micronutrients

	Factor 1	Factor 2
V	0.97011	0.25640
Al	0.95931	0.30986
Fe	0.93826	0.33690
Mn	0.20919	0.87329
Zn	0.27904	0.75875
Ni	0.13216	0.69269
B	0.20710	0.64212
Cu	0.42061	0.67738
Co	0.59485	0.69776

Rare Earth Elements

	Factor1	Factor2	Factor3	Factor4	Factor5	Factor6	Factor7	Factor8	Factor9
In	0.89599	0.17581	-0.14909	0.06841	0.17941	-0.00982	0.18051	0.01559	-0.02842
Se	0.91622	0.16256	-0.17279	0.14674	0.23293	0.14833	0.00553	0.10992	-0.00289
Be	0.91396	0.38408	-0.04559	0.11480	0.26938	0.05072	0.12379	-0.01906	0.02453
Pd	0.91347	0.22993	-0.18036	0.53102	0.42743	0.09878	-0.26081	-0.04034	-0.00819
Hg	0.85546	0.27936	-0.16688	0.21866	0.37862	0.07470	-0.39024	-0.07470	-0.04569
As	0.62231	0.25111	-0.08116	-0.08776	-0.02016	-0.08108	0.44280	-0.11856	0.02817
Ag	0.66573	0.42395	-0.00791	0.34778	0.29898	0.03686	-0.47072	-0.05508	0.35728
W	0.65395	0.15404	-0.24032	0.61739	0.52745	-0.02310	-0.25391	-0.03135	-0.08833
Sn	0.6877	0.46595	0.08002	0.63671	0.55206	0.00415	-0.45462	-0.00995	-0.01335
Cd	0.56979	0.15068	-0.44393	0.41590	0.33965	0.11263	-0.09800	-0.20805	-0.00417
Th	0.21460	0.88309	-0.03612	-0.04268	0.05734	0.10897	0.15754	-0.16636	0.03656
Sc	0.13338	0.87033	-0.02710	0.05835	0.24082	0.07284	0.17576	-0.19919	0.13261
Ti	0.23930	0.84883	-0.06777	0.14840	0.45869	0.09805	0.12925	-0.25481	0.04430
Tl	0.21001	0.68298	0.05491	0.04929	-0.09105	0.40051	-0.03414	0.32862	0.11337
U	0.22555	0.73615	0.24536	-0.00054	0.21513	0.05712	-0.02784	-0.19390	-0.04510
Sb	0.43219	0.55008	0.10170	0.15936	0.27986	0.00418	-0.34838	-0.02102	-0.17367
Sr	-0.11354	0.02616	0.88818	0.08976	0.08278	0.11806	-0.13434	0.05288	0.03313
Ba	-0.16861	-0.07744	0.86538	0.03555	0.15188	0.08730	-0.11268	0.05118	0.00461
Ga	-0.10128	0.09947	0.77416	0.02947	0.22021	0.02544	-0.13613	-0.09439	0.01467
Te	0.11378	0.30022	0.69175	0.29389	0.24284	0.02161	-0.48103	0.03001	-0.00860
Zr	0.18926	0.05490	0.03439	0.96149	0.31012	-0.00977	-0.21480	-0.04213	0.01630
Hf	0.12961	0.04981	0.12779	0.93571	0.26120	0.17714	-0.23583	-0.02378	-0.00432
Cr	0.65777	0.58959	-0.20662	0.56654	0.51196	0.01969	-0.04416	-0.18023	0.04678
Li	0.13805	0.22996	0.42701	0.08747	0.71167	-0.06653	-0.10834	-0.05952	0.07097
Nb	0.21147	0.12268	-0.02651	0.54168	0.71308	0.13849	0.04302	-0.01803	0.10598
Na	0.46911	0.30819	0.43004	0.33566	0.78596	0.08642	-0.26808	0.04537	0.04686
Pb	0.51839	0.45990	-0.09670	0.11328	0.59598	0.00841	-0.18882	-0.20237	-0.24103
Y	-0.04551	0.12556	0.09287	0.03399	-0.03740	0.95740	-0.01192	0.10524	-0.00475
Ta	0.31608	0.27920	0.08895	0.20181	0.18791	0.93852	-0.13276	0.14218	0.02517
Ge	0.11847	0.36902	-0.15453	-0.04553	0.10178	-0.00285	0.74815	-0.04249	-0.01263
Bi	0.27379	0.34109	-0.07805	0.14068	0.25112	0.08042	0.34506	-0.03546	-0.11844
Cs	-0.02988	-0.10179	-0.01660	-0.05969	-0.14599	0.00407	0.00536	0.84766	0.02961
Rb	-0.06109	-0.28837	0.00525	-0.05357	-0.04458	0.22259	0.08316	0.82258	-0.05277
Au	0.04876	0.06130	0.02676	0.03881	0.08396	-0.00948	-0.09528	-0.01978	0.91117

4.1.4 Cluster Analysis

A variety of techniques exist to quantify complex patterns of correlations between variables in large multi-element geochemical datasets and to establish association between samples (Clare & Cohen, 2001). According to Cheng & Yang (1996), defining common groups (clusters) that relate to regional scale geological processes requires the fundamental task of isolation of anomalous samples from the rest of the geochemical analysis.

Cluster Analysis (CA) is a classification method that is used to arrange a set of cases into clusters. The aim is to establish a set of clusters such that cases within a cluster are more similar to each other than they are to cases in other clusters. It may reveal associations and structure in data, which, though not previously evident, nevertheless are sensible and useful once found. Data may be thought of as points in a space where the axes correspond to the variables. Cluster analysis divides the space into regions characteristic of groups that it finds in the data.

Cluster Analysis can also be used for outlier detection where outliers may emerge as singletons or as small clusters far removed from the others. To do outlier detection at the same time as clustering the main body of the data, use enough clusters to represent both the main body of the data and the outliers.

Inter-object similarity is measured by distance between pairs of objects. Often used, is Euclidean distance, the length of the hypotenuse of a right triangle formed between the points. Usually when standardization of the data is needed, the statistical distance is preferred. Standardization of the data is needed if the range or scale of one variable is much larger or different from the range of the others. This distance also compensates for intercorrelation among the variables.

Hierarchical cluster analysis is a statistical method for finding relatively homogeneous clusters of cases based on measured characteristics. It starts with each case in a separate

cluster and then combines the clusters sequentially, reducing the number of clusters at each step until only one cluster is left. A dendrogram is a way to represent the results of hierarchical clustering. Hierarchical clustering follows one of two approaches: Agglomerative methods start with each observation as a cluster and with each step combine observations to form clusters until there is only one large cluster. Divisive methods begin with one large cluster and proceed to split into smaller clusters items that are most dissimilar.

The purpose of using cluster analysis is to organize the large data into groups thus facilitating potentially meaningful pattern recognition. These patterns are then related to geological processes such as mineralization, drainage and geology. The various element groups (macronutrients, micronutrients, trace and REEs) were dealt with individually for each plant species so as to compare the two plants. A map showing all sample points and sample numbers is presented in appendix 5. A total of 8 dendrograms for *A. karroo* and *B. albitrunca* were constructed using SAS (Fig 4.9-4.16).

4.1.5 Results of Cluster Analysis

4.1.5.1 Macronutrients

The dendrogram for macronutrients in *A. karroo* (Fig 4.9) has a total of four clusters (A1-A4) that are closely related. Group A1 comprises samples from areas underlain by greenstones related to greenstone lithology and the other cannot be attributed to any particular geological process. Group A2 contains mainly samples from mineralized areas in the vicinity of Goudplaats mine. The remaining two groups A3 and A4 are both associated with mineralization, however A3 can also be associated with greenstone lithology. Sample 11.1, located at the mineralized area seems isolated without any association to other clusters.

Three clusters that are closely related can be found in the dendrogram of the macronutrients for *B albitrunca*. Group A5 (Fig 4.10) consists of samples that are located

in and around the Harts river. Groups A6 has a mixture of samples found in well drained and mineralized areas and A7 has those from mineralized areas only. A number of samples do not form any clusters and these are mainly from the mineralized areas.

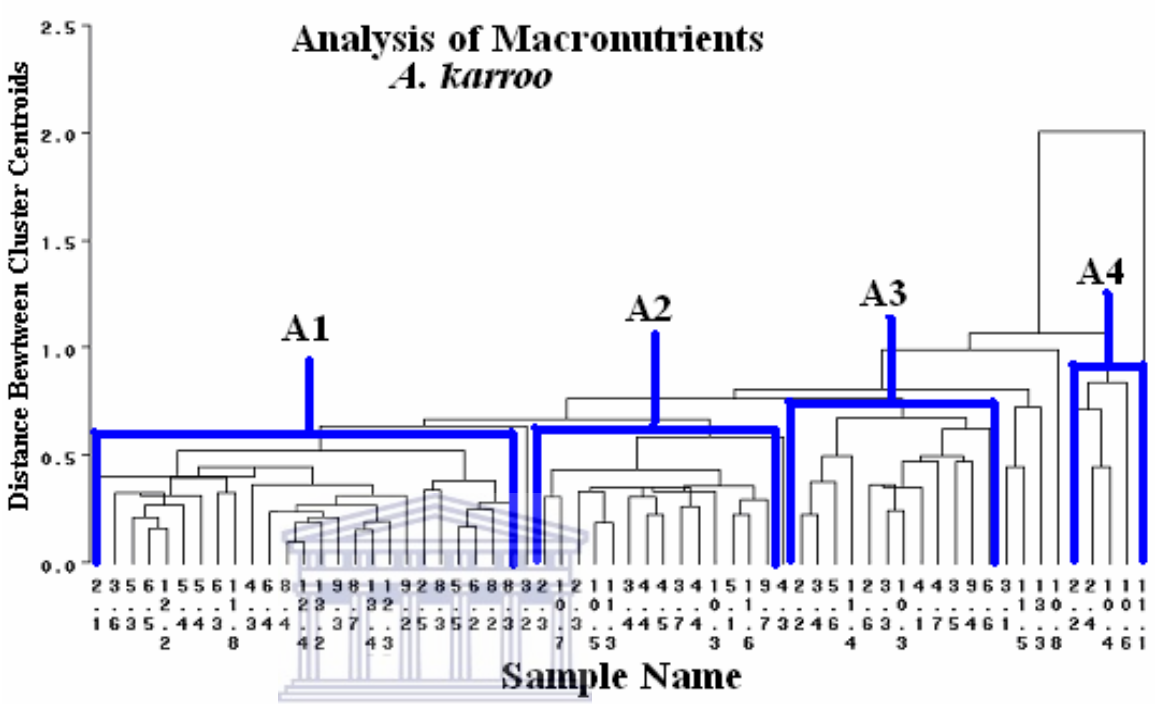

Fig 4.9 Dendrogram for macronutrients in *A. karroo*

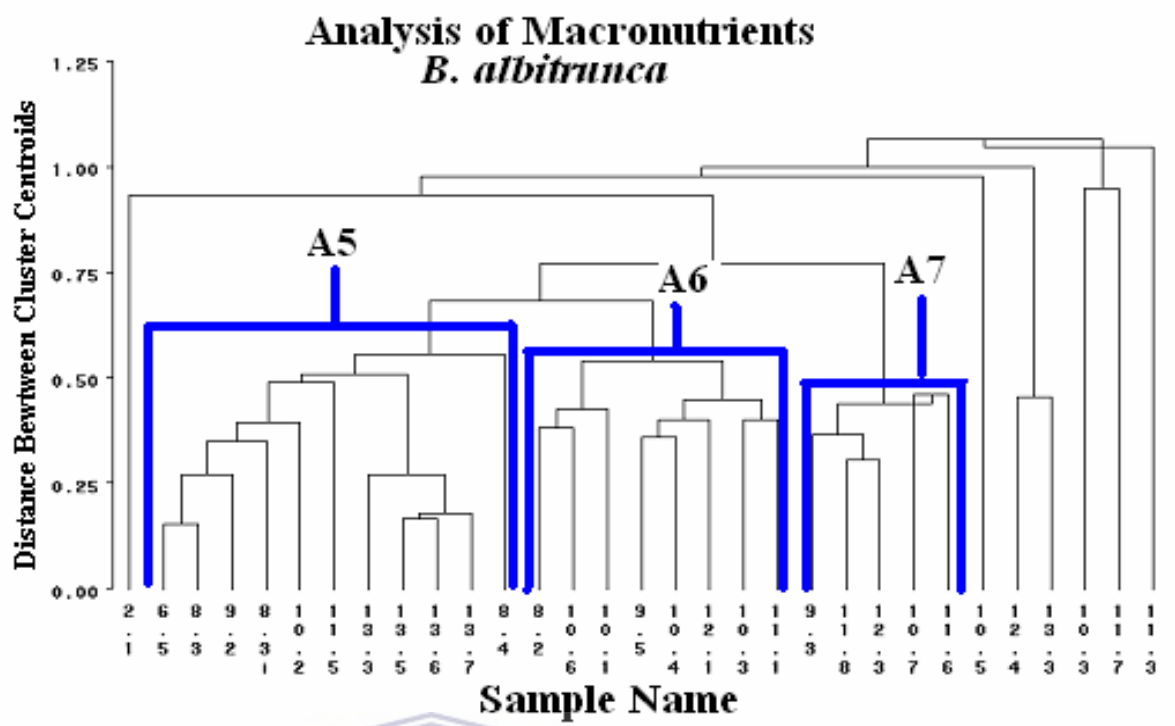

Fig 4.10 Dendrogram for macronutrients in *B. albitrunca*

4.1.5.2 Micronutrients

The dendrogram for micronutrients in *A. karroo* reveals a rather complex relationship between the various sample points with no significant pattern that can be associated with the various geological processes (Fig4.11).

The dendrogram for micronutrients in *B. albitrunca* shows three different clusters, B1, B2 and B3 (Fig4.12). Samples from B1 are come from well-drained and mineralized area whereas those from B2 only come from areas that are well drained. Group B3 contains samples from areas covered by greenstones and from mineralized areas.

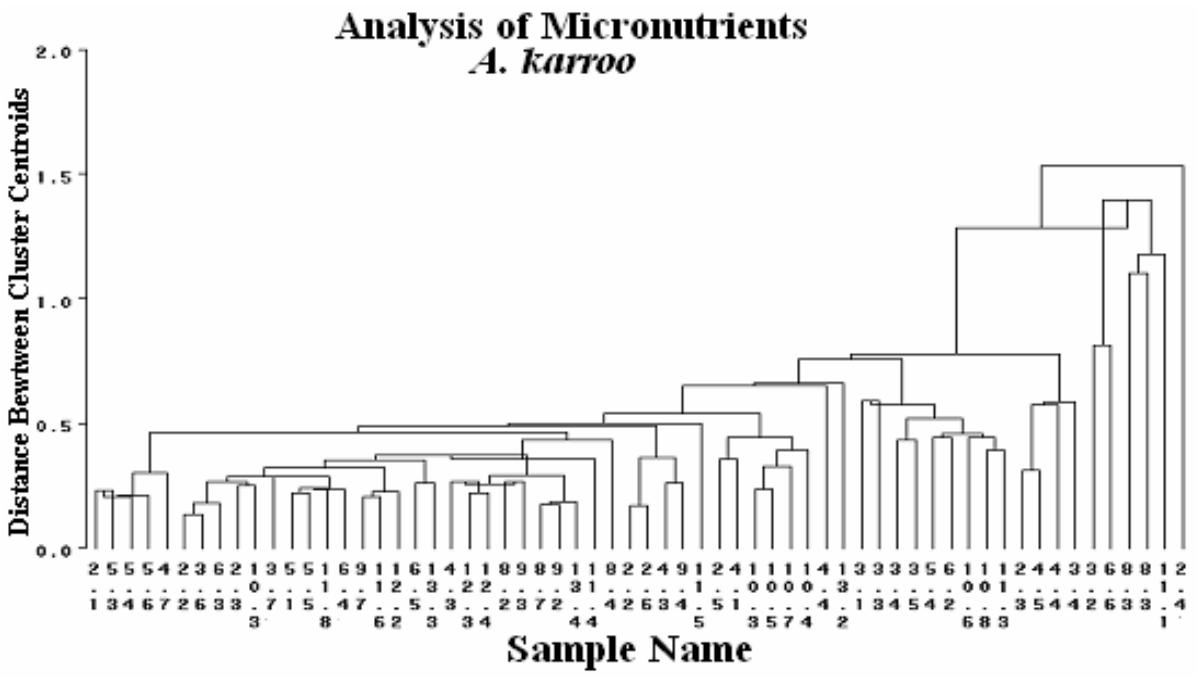

Fig 4.11 Dendrogram for micronutrients in *A. karroo*

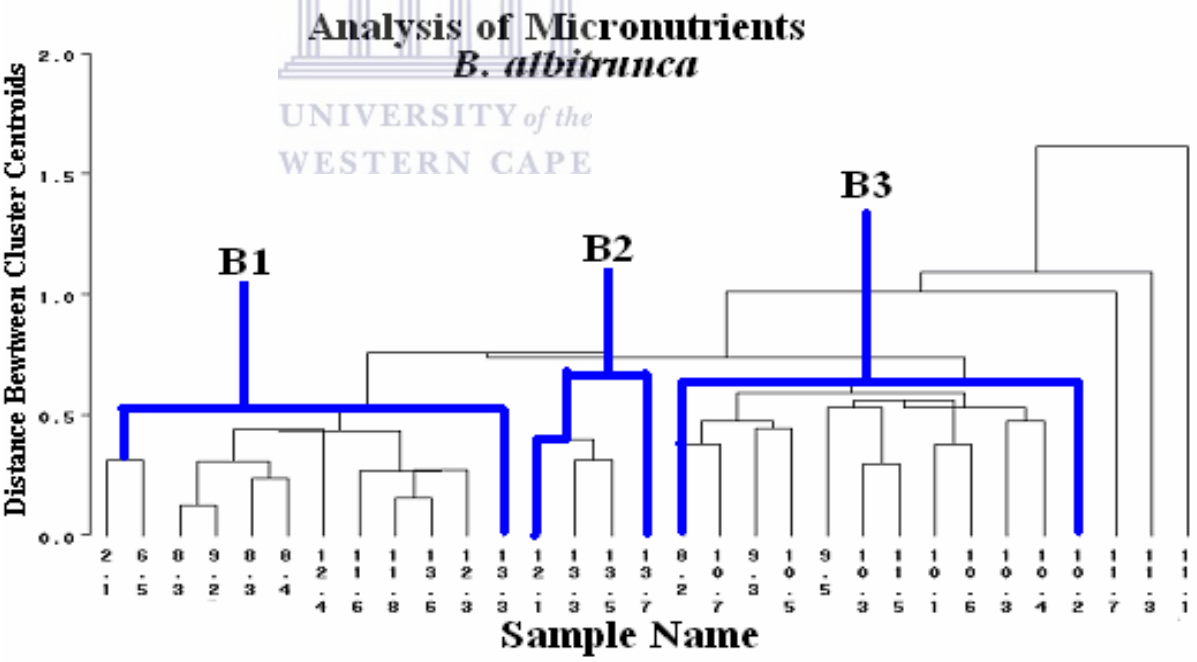

Fig 4.12 Dendrogram for micronutrients in *B. albitrunca*

4.1.5.3 Trace Elements

The dendrogram for the trace elements in *A. karroo* also shows a complex interrelationship between the various samples. One group, C1 (Fig4.13) is identified with samples mainly from mineralized Goudplaats area. Once again sample point 11.1 is isolated from other clusters just as in the macronutrients described above.

The trace element dendrogram for *B. albitrunca*, which contains a mixture of samples from areas with mineralization and well drained areas has just one significant group, C2 (Fig4.14). Nearly half of these samples represent mineralization.

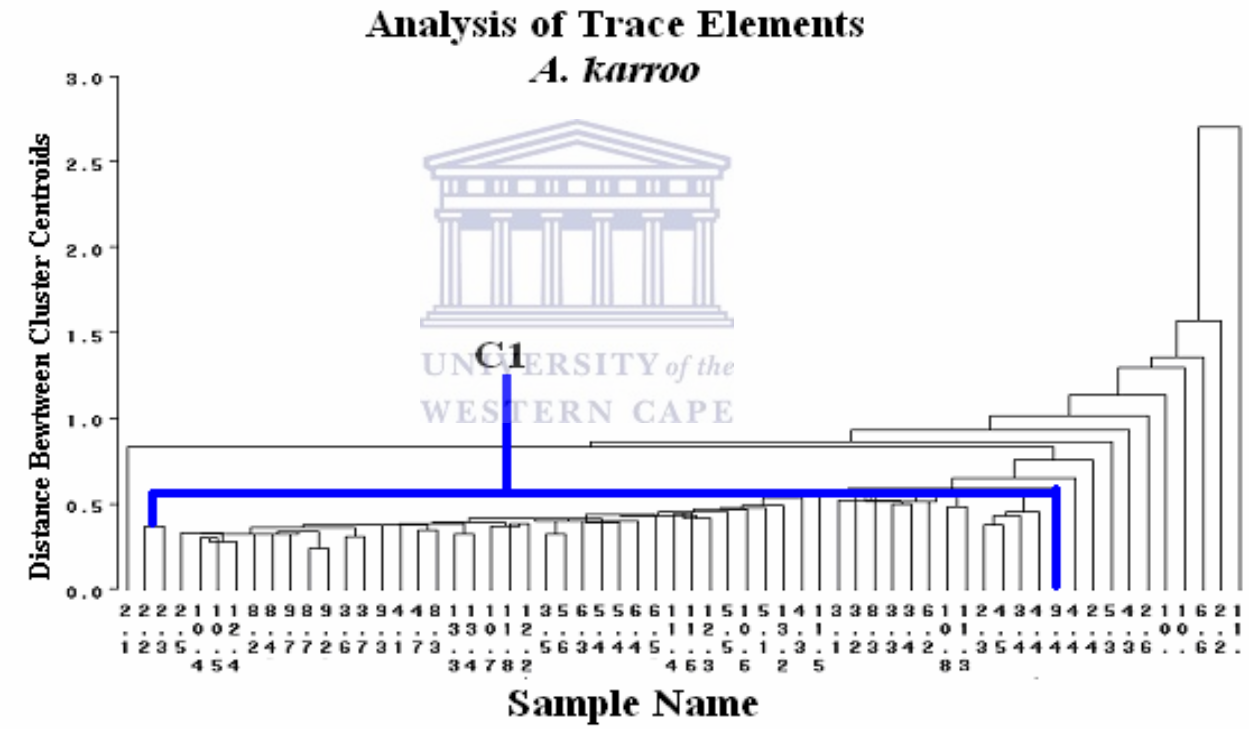

Fig 4.13 Dendrogram for trace elements in *A. karroo*

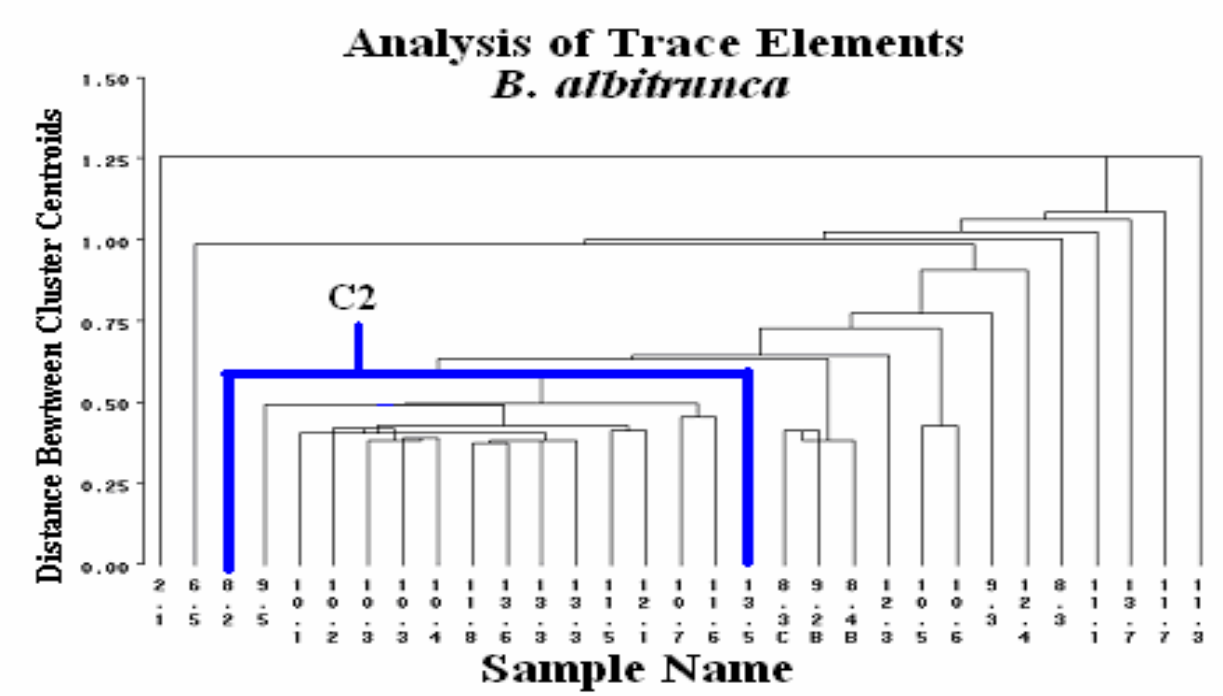

Fig 4.14 Dendrogram for trace elements in *B. albitrunca*

4.1.5.4 REEs

Two clusters are identified for the REEs, D1 and D2. Group D1 does not reveal any significant trend or pattern whereas group D2 (Fig4.15) contains mainly samples occurring within the granite rocks and mineralized areas.

Two groups, D3 and D4 (Fig 4.16) are identified for this element grouping in *B. albitrunca*. D3 contains mainly samples from mineralized parts while D4 consists of samples near the Harts River. Sample 8.3i does not correspond with the other clusters. This sample is located at the river near the mineralized area of Abelskop.

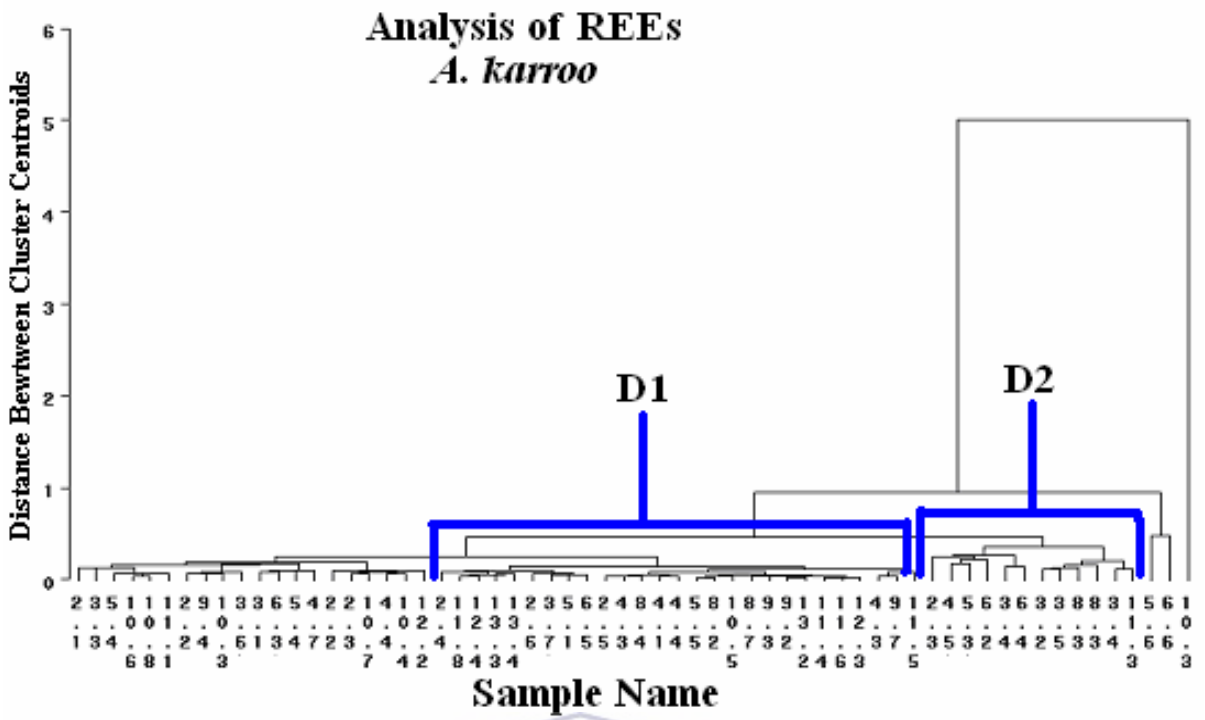

Fig 4.15 Dendrogram for REEs in *A karroo*

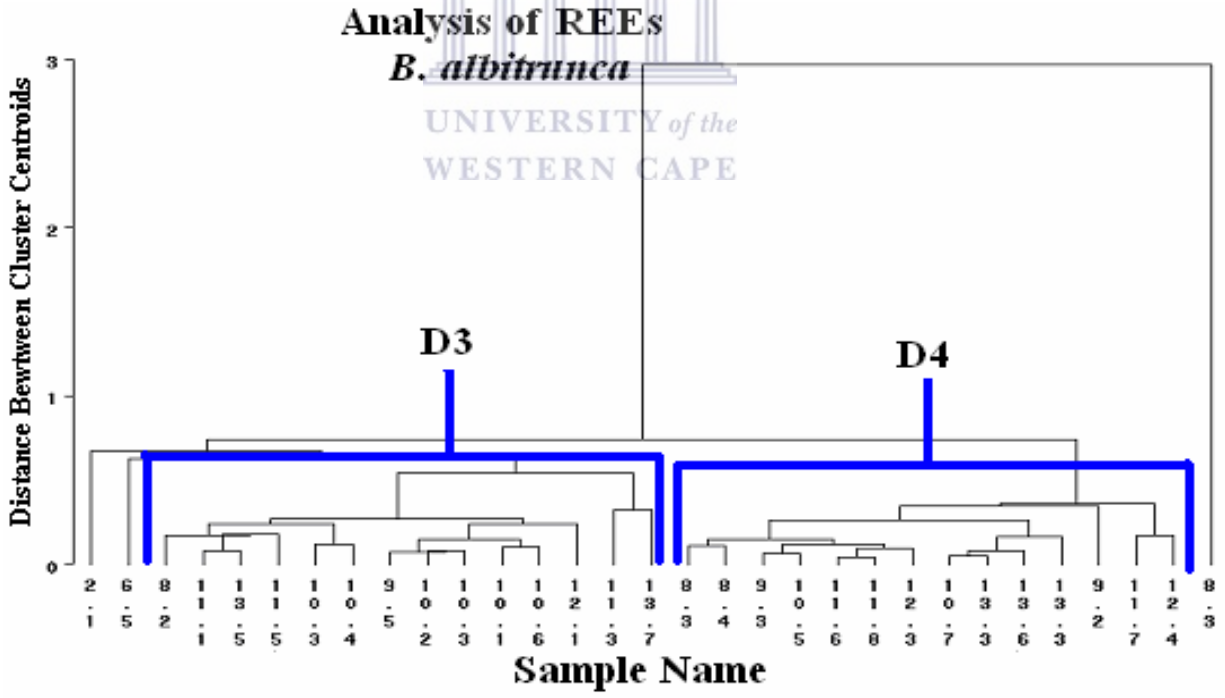

Fig 4.16 Dendrogram for REEs in *B. albitrunca*

4.2 Rare Earth Elements

4.2.1 Chemistry and Geochemistry of the Rare Earths

The REE are becoming more and more technologically significant due to their unique coherent chemical behaviour. These elements comprise a total of 14 elements from atomic number 57 (La) to 71 (Lu) and have similar chemical and physical properties. The most stable oxidation state for REEs is trivalent and because of this, REEs are adsorbed strongly on rock surfaces or bound on to organic substances such as humic acid, which results in their low availability to plants from soil (Ozaki & Enomoto, 2001). Ce, however forms a stable +4 species, which is a very strong oxidizing agent and Eu exhibits +2 oxidation under reducing conditions. Eu^{2+} and Yb^{2+} are the most stable divalent REEs.

Rare earth elements have an average crustal abundances of 0.015%, which matches that of Cu, Pb and Zn but is higher than Co, Sn, Hg and Ag (Hu et al., 2004). The REEs, especially the light REEs (La, Ce, Pr, Nd, Sm and Eu) are classified as incompatible elements because of their large radii and high charge (White, 1997). The heavy REEs (Gd, Tb, Dy, Ho, Er, Tm, Yb, Lu), have sufficiently smaller radii and hence are accommodated in many common minerals such as garnet, where the Al^{3+} is substituted.

Rare earth elements are best expressed by plotting them on rare earth plots or diagrams, where the log of their relative abundances are plotted as a function of their atomic numbers (White, 2003). These relative abundances are calculated by dividing each REE concentration by a set of normalizing values obtained from chondritic meteorites (White, 1997). Relative abundances are used because the even numbered elements are greater than the neighbouring odd-numbered element (Oddo-Harkins Rule). In addition, abundances generally decrease with increasing atomic number, thus producing a plot with a saw-tooth pattern of decreasing abundances (White, 1997). A number of chondritic values are available in literature and there is no general rule on which set to use. Popular methods of normalizing REE data include the use of Cl chondrite (McDonough & Sun, 1995), mid-ocean ridge basalt (MORB) and shale normalized chondrites.

4.2.2 REE in Plants

The content of REEs in plants was previously detected using INAA but this technique was only able to detect 8 REEs (La, Ce, Nd, Eu, Tb, Yb, Lu) (Xu et al., 2003). However in recent years, with the advancement of high resolution ICP-MS, all 14 REEs including Y and Sc have been detected in biological and environmental samples.

REEs have mostly been analyzed in geological samples and in mineral waters (Raju & Raju, 1999) but very little literature is available on their distribution in plants. REEs are taken up by the plant through the roots and concentrations decrease in the order of roots>leaves>seeds (Liang et al., 2001). Concentrations of REE in vascular plants is usually quite low. A number of studies have been reported on plant REE concentrations in the scientific literature, however these concentrations vary greatly hence it is difficult to determine whether the concentrations are actually present or it is due to dust contamination (Tyler, 2004).

Some typical REE concentrations of various vegetation types from a study conducted by Markett and Li, (1991) are presented in Table 4.7. The values they obtained are generally low especially in commercially grown cabbage. There are however plants such as ferns that can be regarded as REE hyperaccumulators. In a study conducted by Ozaki, et al., 2001, a total of 96 fern species were considered. In at least nine of these species, huge anomalous amounts of La (10-40µg/g) and Ce (3-30µg/g) were found. This was a huge amount compared to other species. Mosses and lichens were also characterized as accumulators by Market and Deli (1991), since they accumulated huge amounts of REEs compared to vascular plants in other forest species. Lichens and mosses from Arctic Canada had comparatively lower concentrations than those from the continental crust (Chirianzelli et al., 2001).

REEs	Forest plants, Germany (ranges)	Grass leaves (Agrostis capillaries)	Cabbage mean	Cabbage max.	Moss carpets south Sweden (ranges)
Y	0.15-0.25	0.03	0.0032	0.010	0.120-0.134
La	0.15-0.25	0.110	0.014	0.114	0.248-0.285
Ce	0.25-0.55	0.150	0.028	0.081	0.466-0.519
Pr	0.03-0.06	0.017	0.0017	0.010	0.053-0.059
Nd	0.10-0.25	0.091	0.0054	0.033	0.373-0.431
Sm	0.02-0.040	0.11	0.0006	0.0054	0.035-0.037
Eu	0.005-0.015	0.026	-	0.020	0.0093-0.0106
Gd	0.025-0.050	0.010	0.0017	0.015	0.036-0.039
Tb	0.005-0.015	0.0011	0.0002	0.0010	0.0048-0.0052
Dy	0.025-0.050	0.0051	0.0007	0.0075	0.0235-0.0253
Ho	0.005-0.015	0.0010	0.00014	0.0015	0.0045-0.0049
Er	0.015-0.030	0.0031	0.0003	0.0032	0.0127-0.0139
Tl	0.0025-0.005	0.0029	0.00006	0.0004	0.0016-0.0019
Yb	0.015-0.030	0.0019	0.0002	0.0016	0.0107-0.0120
Lu	0.0025-0.005	0.0003	0.0001	0.0005	0.0015-0.0017

Table 4.7 REE concentrations in above-ground biomass of plants, µg g−1 dry weight (Tyler, 2004).

4.2.3 Distribution Patterns of REEs in A. karroo and B. albitrunca

Rare earth plots were made for *A. karroo* and *B. albitrunca* in order to determine the distribution patterns and relate this distribution to mineralization, lithology, geology or mineralization. The REE distribution patterns of *A. karroo* and *B albitrunca* are presented in Figs 4.16 to 4.21. The REE concentrations of the two plants are standardized with contents of REE in Cl chondrites (McDonough & Sun, 1995). To further describe the distribution patterns, a table of $(La/Yb)_N$ has been drawn up.

	Granite	CS	Greenstone	Drained	Poorly-drained	Mineralized	non-mineralized
A. karroo	**21.4**	**27.5**	**19.9**	**17.8**	**25.8**	**28.6**	**18.2**
B. albitrunca	**24.3**	**18.7**	**16.3**	**19.9**	**21.8**	**17.9**	**21.8**

Table 4.8 Average $(La/Yb)_N$ for *A. karroo* and *B. albitrunca*
CS- carbonate schist

4.2.3.1 Lithological Control on REE Distribution

The Blue Dot Mine area comprises of three main rock types i.e. greenstones, granites and carbonate schist. The BIF unit, which hosts the gold mineralization, is found within the carbonate schist.

Greenstones

The distribution pattern of REE contents in *A. karroo* in the areas covered by greenstones show a negative slope (Fig 4.17a) and a very strong positive Eu anomaly. The average $(La/Yb)_N$ ratio is 19.9 while ∑LREE/∑HREE is 10.91 (table 4.8) which is indicative of very high enrichment in LREEs (La-Eu) and depletion of HREEs (Gd-Lu).

The distribution pattern in *B albitrunca* has some similarities to A. *karroo* above. The REE plot for *B albitrunca* also has a negative slope (Fig 4.17b) but less steeper slope ($(La/Yb)_N$ ratio is 16.31) than *A karroo*. Furthermore, enrichment of LREEs in *B albitrunca* is more or less the same as in *A. karroo*, with a ∑LREE/∑HREE of 10.20. The Eu anomaly is however not as pronounced as in *A karroo*.

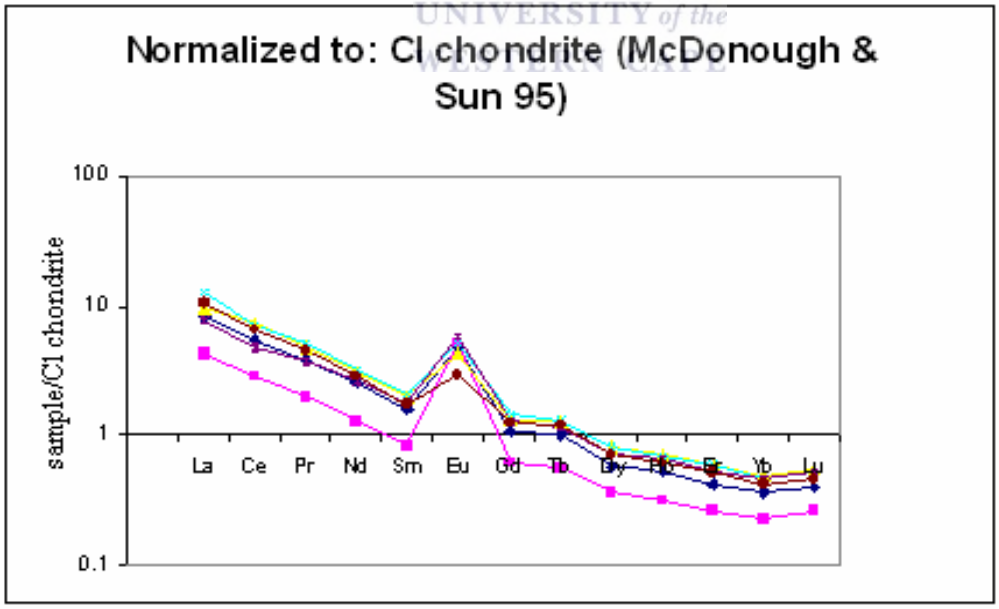

Fig 4.17a REE Distribution in A. karroo found in greenstone

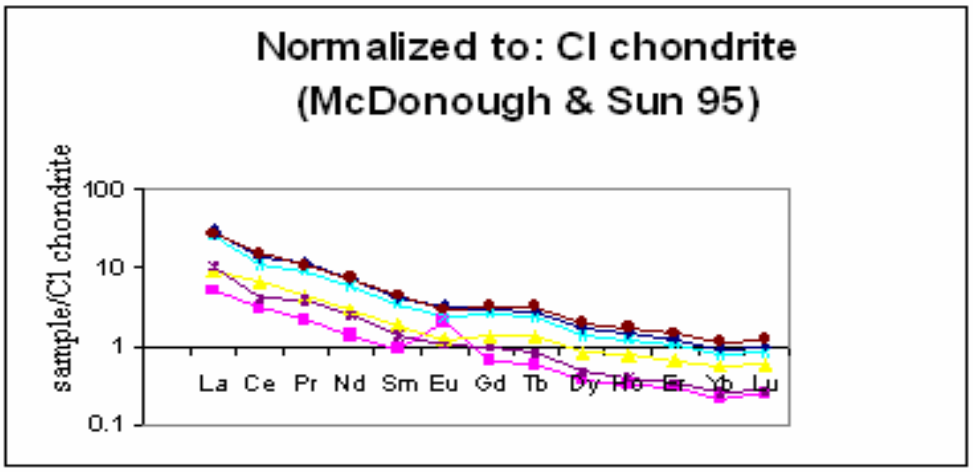

Fig 4.17b REE Distribution in *B albitrunca* found in greenstone

Carbonate schists

The curve showing the distribution pattern in *A karroo* (Fig 4.18a), has a large Eu anomaly together with large $(La/Yb)_N$ ratio of 27.50, which is indicative of a very steep slope and a very high enrichment of LREE in relation to HREE. The prominent feature of this plot is the large Ce anomaly. The pattern displayed by the carbonate schist is similar to granite.

Compared to *A. karroo*, the distribution pattern in *B albitrunca* (Fig 4.18b) has a gentle slope, with a significantly lower $(La/Yb)_N$ ratio of 18.73. The ∑LREE/∑HREE ratio (8.18) is similar. The Eu anomaly for this plant is insignificant.

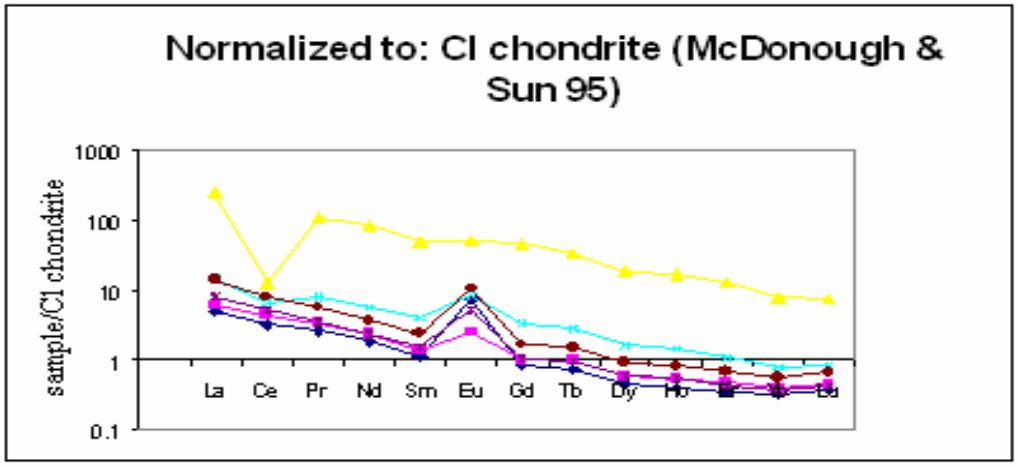

Fig 4.18a REE Distribution in *A. karroo* found in carbonate schist

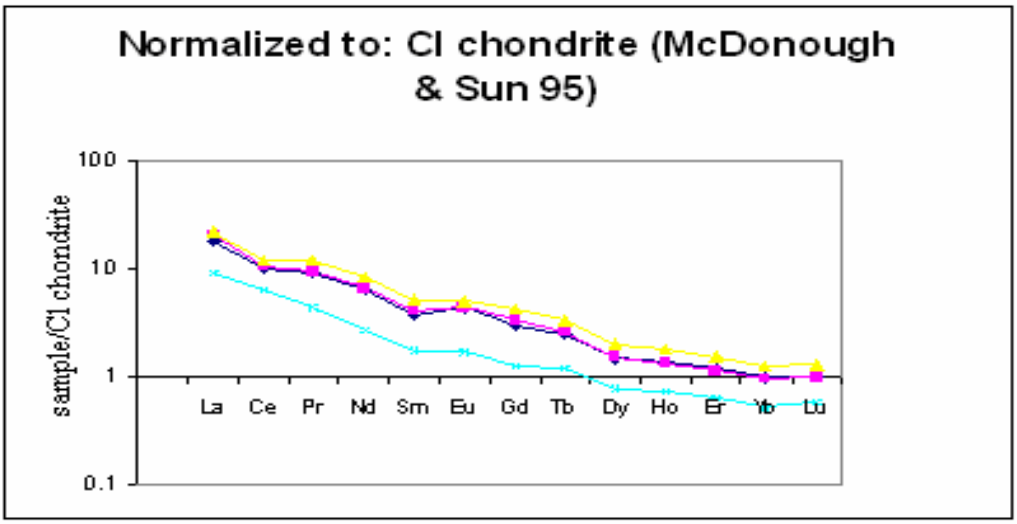

Fig 4.18b REE Distribution in *B albitrunca* found in carbonate schist

Granites

The distribution pattern of REE content in *A karroo* (Fig 4.19a) has a $(La/Yb)_N$ of 21.41 and a ∑LREE/∑HREE ratio of 10.74. The Eu anomaly is prominent.

The distribution pattern in *B. albitrunca* is similar to *A karroo* with a $(La/Yb)_N$ of 24.33 and a ∑LREE/∑HREE ratio of 10.8 (Fig4.19b). Both plants exhibit similar REE patterns with high enrichment of LREEs.

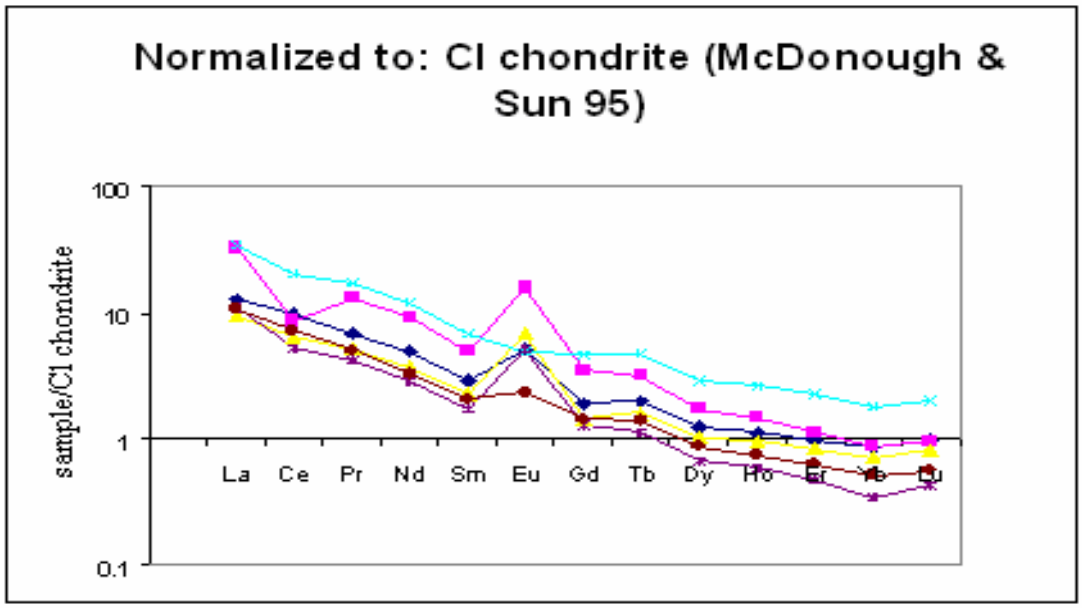

Fig 4.19a REE Distribution in *A. karroo* found in granite

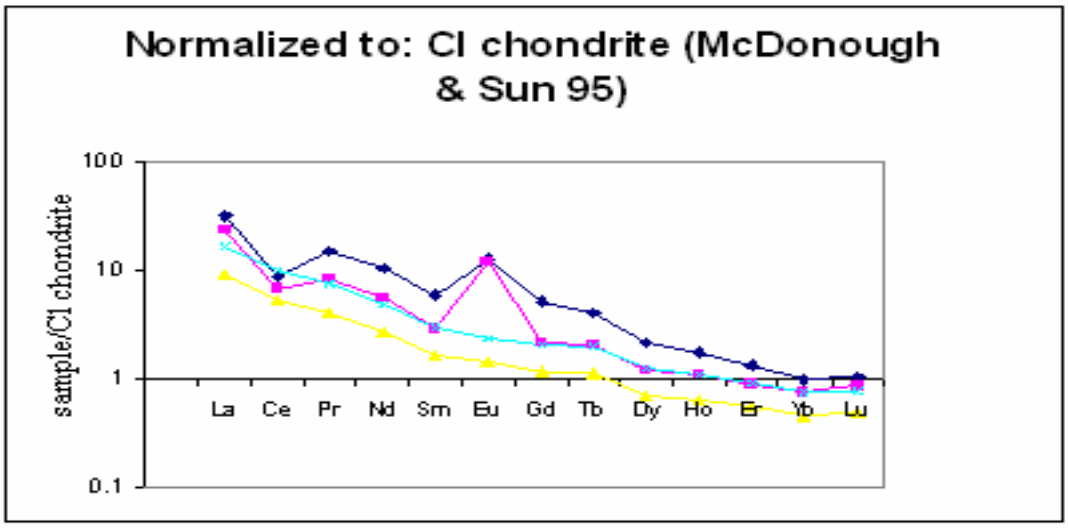

Fig 4.19b REE Distribution in *B albitrunca* found in granite

4.2.3.2 REE Distribution in Well-drained Areas

The study area is drained by the Harts River, which enters the Blue Dot Mine area in the north and eastern parts of the Goudplaats farm. The river runs along the east and western parts of Goudplaats and extends into the Abelskop Valley. The distribution pattern of REE content in *A karroo* along the drainage of the Harts river is characterized by a gentle slope and a $(La/Yb)_N$ ratio of 17.77 (Fig 4.20a). A ratio of 10.7 describes the higher content of LREE compared to HREE. A positive Eu anomaly is also present.

The distribution pattern in *B. albitrunca* shows a slightly higher ($(La/Yb)_N$ is 19.9) than *A karroo*. There is not much difference in ∑LREE/∑HREE ratio (9.50) when comparing the two plants (Fig 4.20b). The Eu anomaly is not significant.

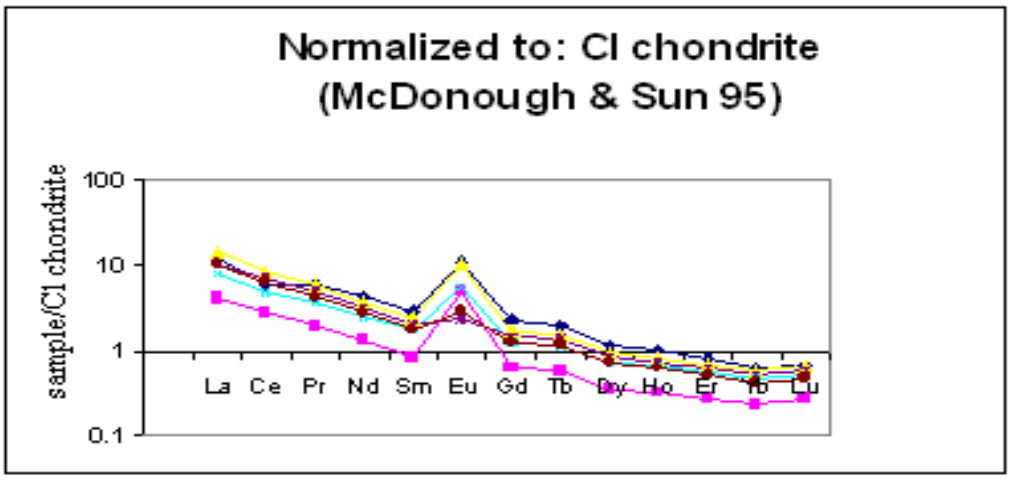

Fig 4.20a REE Distribution in *A. karroo* found along drainage pattern

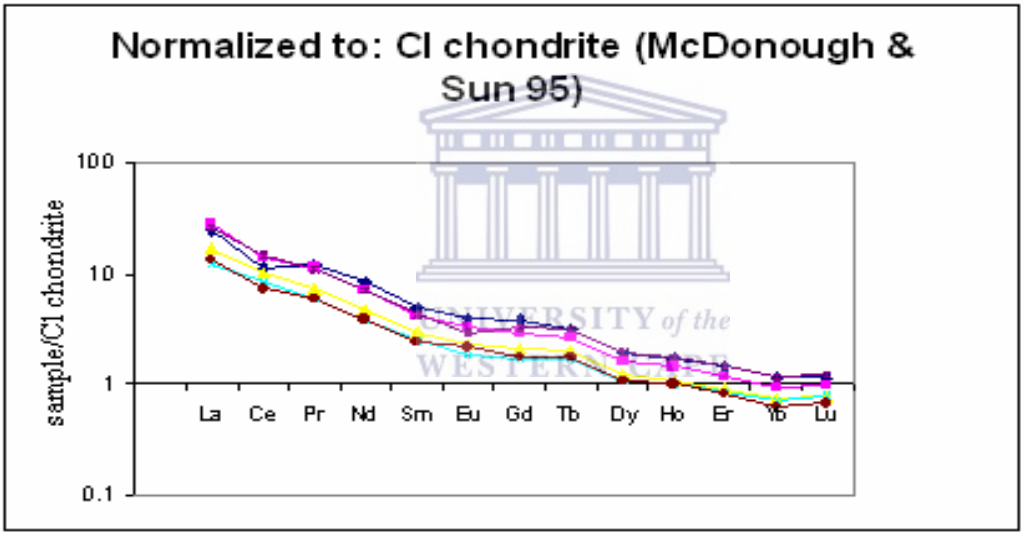

Fig 4.20b REE Distribution in *B albitrunca* found along drainage pattern

4.2.3.3 REE Distribution over Mineralized Areas

In mineralized areas, the REE distribution pattern in *A. karroo* is similar to the REE distribution in carbonate schist, with similar parameters such as $(La/Yb)_N$ ratio (28.59) and ∑LREE/∑HREE ratio (8.34). This is because the BIF wherein the gold mineralization occurs is located within the carbonate schist. The plot (Fig 4.21a) is characterized by a strong negative Ce anomaly and a positive Eu anomaly.

The plot (Fig 4.21b) for *B. albitrunca* is characterized by a much smaller ($(La/Yb)_N$ ratio is 17.9) when compared to *A karroo*.

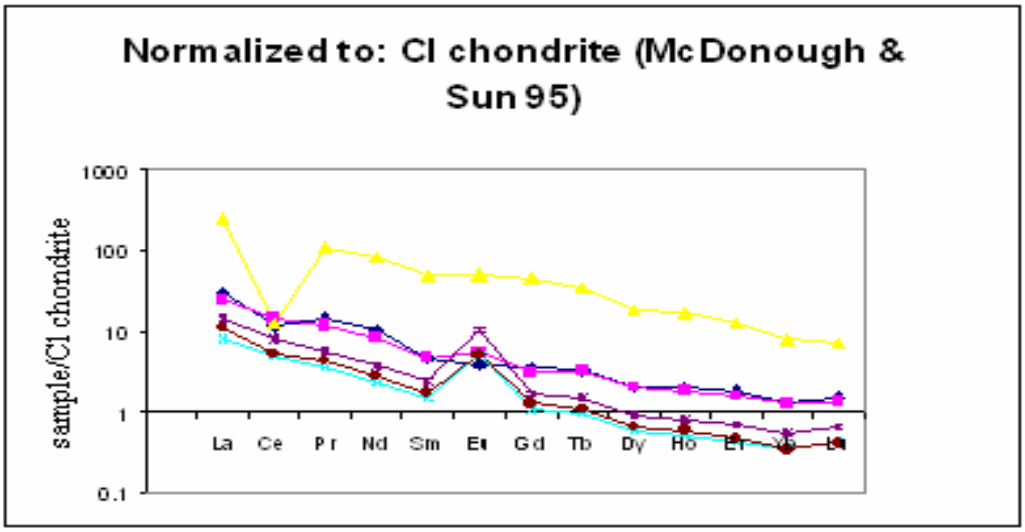

Fig 4.21a REE Distribution in *A. karroo* found in mineralized area

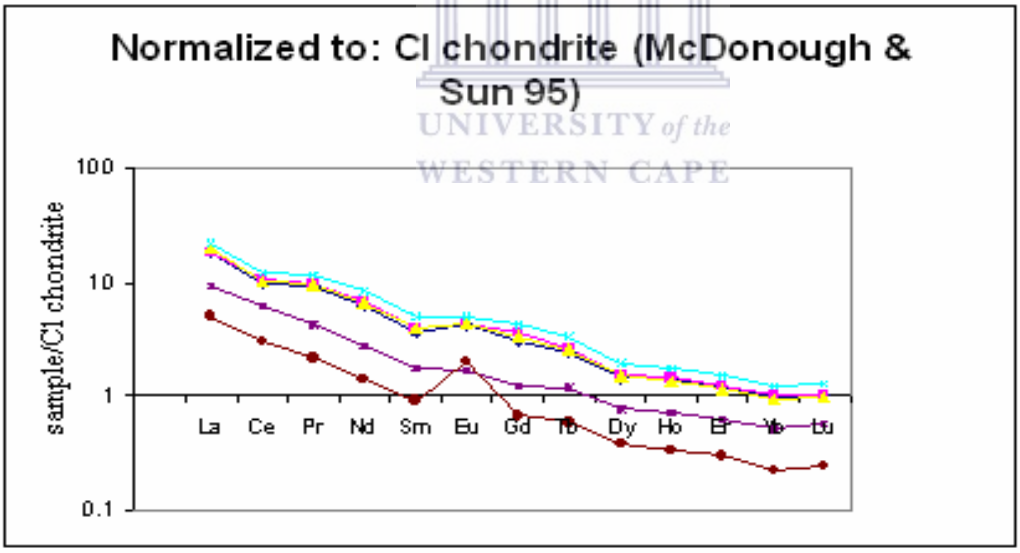

Fig 4.21b REE Distribution in *B albitrunca* found in mineralized area

4.2.3.4 REE Distribution in non-mineralized areas

The distribution pattern in *A. karroo* in non-mineralized areas is similar to the distribution pattern in greenstone. The *B. albitrunca* plot is characterized by a steep slope and a $(La/Yb)_N$ ratio of 21.79 that is slightly higher than *A. karroo*. The ∑LREE/∑HREE ratio is 11.11 which is similar to the *A. karroo* ratio of 10.73 above.

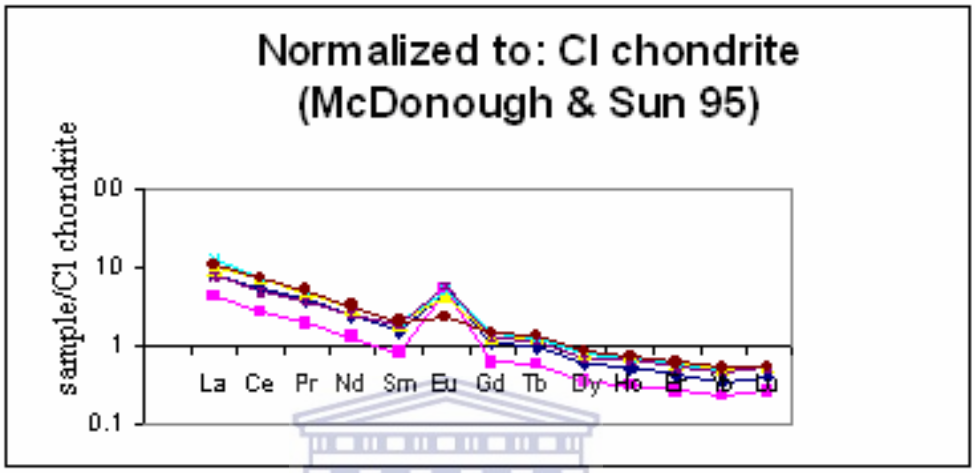

Fig 4.22a REE Distribution in *A. karroo* found in non mineralized area

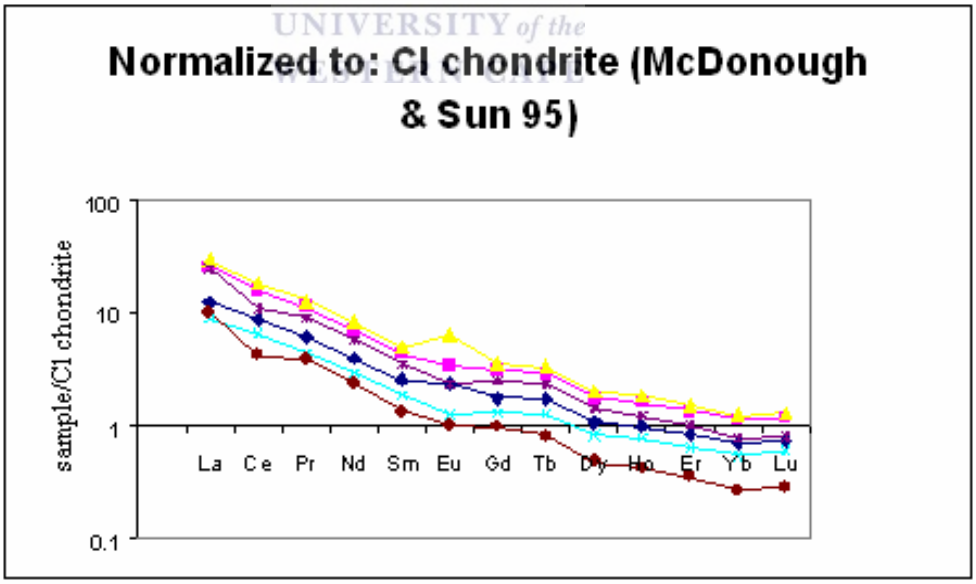

Fig 4.22b REE Distribution in *B albitrunca* found in non mineralized area

4.2.3.5 Summary

From the data and distribution patterns discussed above the following are evident:

- REEs are more prevalent in *A. karroo* compared to *B. albitrunca* given higher $(La/Yb)_N$ ratios
- REEs in *A. karroo* are more abundant in mineralized areas, granite, carbonate schist and poorly-drained areas
- REEs in *B. albitrunca* are abundant in granites, poorly-drained and non-mineralized areas. Well-drained show a depletion in REE content in both plants

4.3 Separation of background and anomalous element values

The element concentrations were separated into background, anomalous and threshold values, in order to appraise spatial geochemical patterns. The statistical parameters of the background, threshold and anomalous values were determined using boxplots (Figs 4.1-4.8). According to O' Connor & Reimann (1993), the boxplots are resistant to inconsistencies and disturbances typical of raw geochemical data. Therefore the above-mentioned technique is effective in aiding visualization of data. All values below the 50th percentile were regarded as background values while threshold values are those values that lie between the 50th percentile and the 75th percentile. The anomalous values are represented from the 75th percentile upwards. The results are presented in tables 4.9 and 4.10.

Element	Background	Threshold	Anomaly
Mg	4.2	4.2 - 4.8	>5
P	1.6	1.7 - 2.2	2.4
S	0.7	0.7 - 1.2	1.3
Ca	23	23.1 - 28	28.1
K	5.9	6 - 6.3	6.4
La	3	3.0 - 6	7
Ce	4.1	4.1 - 6.4	6.5
Pr	0.5	0.5 - 1	1.2
Nd	2	2.0 - 3.0	4
Sm	0.4	0.4 - 0.6	0.62
Eu	0.4	0.4 - 0.6	0.61
Gd	0.3	0.3 - 0.6	0.7
Tb	0.05	0.05 - 0.1	0.12
Dy	0.2	0.2 - 0.4	0.5
Ho	0.016	0.016 - 0.1	>0.1
Er	0.16	0.16 - 0.2	0.21
Tm	0.02	0.02 - 0.027	0.028
Yb	0.1	0.1 - 0.15	0.16
Lu	0.02	0.02 - 0.028	0.029
Sr	1100	1100 - 1500	1510
Ag	0.15	0.15 - 0.2	0.21
Sb	0.15	0.15 - 0.18	0.19
Te	0.1	0.10 - 0.122	0.123
Ba	750	750 - 1100	1200
W	0.38	0.38 - 0.42	0.43
Au	6	6.0 - 7.0	7.1
Hg	0.2	0.2 - 1.0	>1
Pb	8	8.0 -11.0	11.1
Bi	0.024	0.025 - 0.028	0.029
As	0.8	0.8 - 1.3	1.4
Se	2.8	2.8 - 3.1	3.2

Table 4.9 Estimated background-anomalous values various elements in *A. karroo* (all trace elements ppm except Au, in ppb; Major elements are in %)

Element	Background	Threshold	Anomaly
Mg	3.2	3.2 - 3.8	3.9
P	1.7	1.7 - 2.2	2.3
S	1.05	1.05 - 1.45	1.46
Ca	15	15.0 - 18.0	>18
K	7.2	7.2 - 9.2	>9.2
La	4	4.0 - 5.0	6
Ce	5.8	5.8 - 7.2	7.3
Pr	0.7	0.7 - 1	1.2
Nd	3	3 - 3.5	3.6
Sm	0.5	0.5 - 0.6	0.62
Eu	0.2	0.2 - 0.3	0.31
Gd	0.5	0.5 - 0.6	0.61
Tb	0.08	0.08 - 0.1	0.12
Dy	0.3	0.3 - 0.41	0.42
Ho	0.06	0.06 - 0.07	0.08
Er	0.2	0.2 - 0.3	0.31
Tm	0.023	0.023 - 0.03	0.031
Yb	0.13	0.13 - 0.18	0.19
Lu	0.022	0.022 - 0.027	0.028
Sr	450	450 - 750	>750
Ag	0.19	0.19 - 0.2	0.21
Sb	0.13	0.13 - 0.15	0.16
Te	0.06	0.06 - 0.082	0.083
Ba	150	150 - 300	>300
W	0.53	0.53 - 0.67	0.68
Au	2	2 - 4	6
Hg	1	1.0 - 2.0	2.1
Pb	12.5	12.5 - 16.5	17
Bi	0.028	0.028 - 0.03	0.031
As	1.22	1.23 - 1.42	1.5
Se	3.1	3.1 - 3.5	3.6

Table 4.10 Estimated background- for the Anomalous values for the various are in Elements in B. albitrunca

4.4 Geochemical maps

The geochemical maps plotted (Fig4.23-4.39), represent concentration ranges of the respective elements. As earlier stated in chapter 4.1, the element groupings from the factor analysis formed the basis of selection of elements to be plotted. These elements include the macronutrients (Ca, Mg, P and S), gold and pathfinder elements (Au, Ag, Hg, Pb, As, Te, Sb, W), trace elements (Se, and Sr) and REEs (La, Ce and Eu). In order to view the distribution patterns of these elements in relation to geology, drainage and mineralization, the raw data set of the individual elements was used together with SURFER 7 to prepare geochemical maps. Due to low sampling density in B. albitrunca, geochemical maps for this species could not be prepared.

4.4.1 Element distribution in *A. karroo*

4.4.1.1 Major elements

Calcium

Calcium is the most abundant macronutrient found in ***A. karroo,*** with a threshold value of 20% (2% dry wt) and an anomalous value of 27% (2.7% dry wt). Calcium is widely but unevenly distributed throughout the study area, with a number of elevated clusters concentrated towards the south, in close proximity to the Goudplaats mineralization (Fig 4.23). There is an obvious relationship between Ca in *A. karroo* and mineralization in Goudplaats and Abelskop. Furthermore, high Ca values occur within the ultramafic greenstones. Huge amounts of Ca are released during weathering of feldspars (Nagaraju & Karimulla, 2001), making it available for uptake by vegetation by way of hydromorphic dispersion.

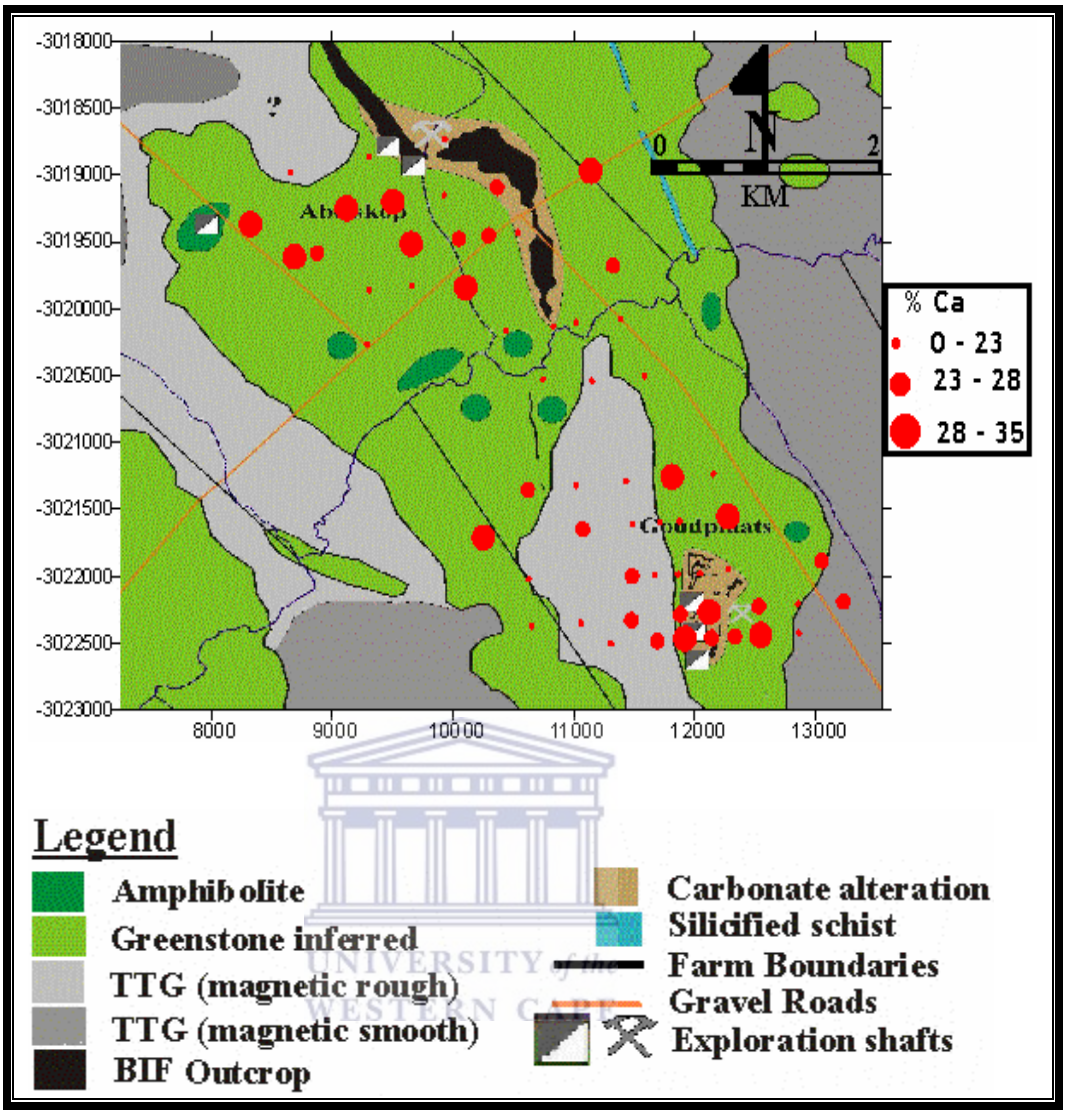

Fig. 4.23 Geochemical map of Ca in *A. karroo*

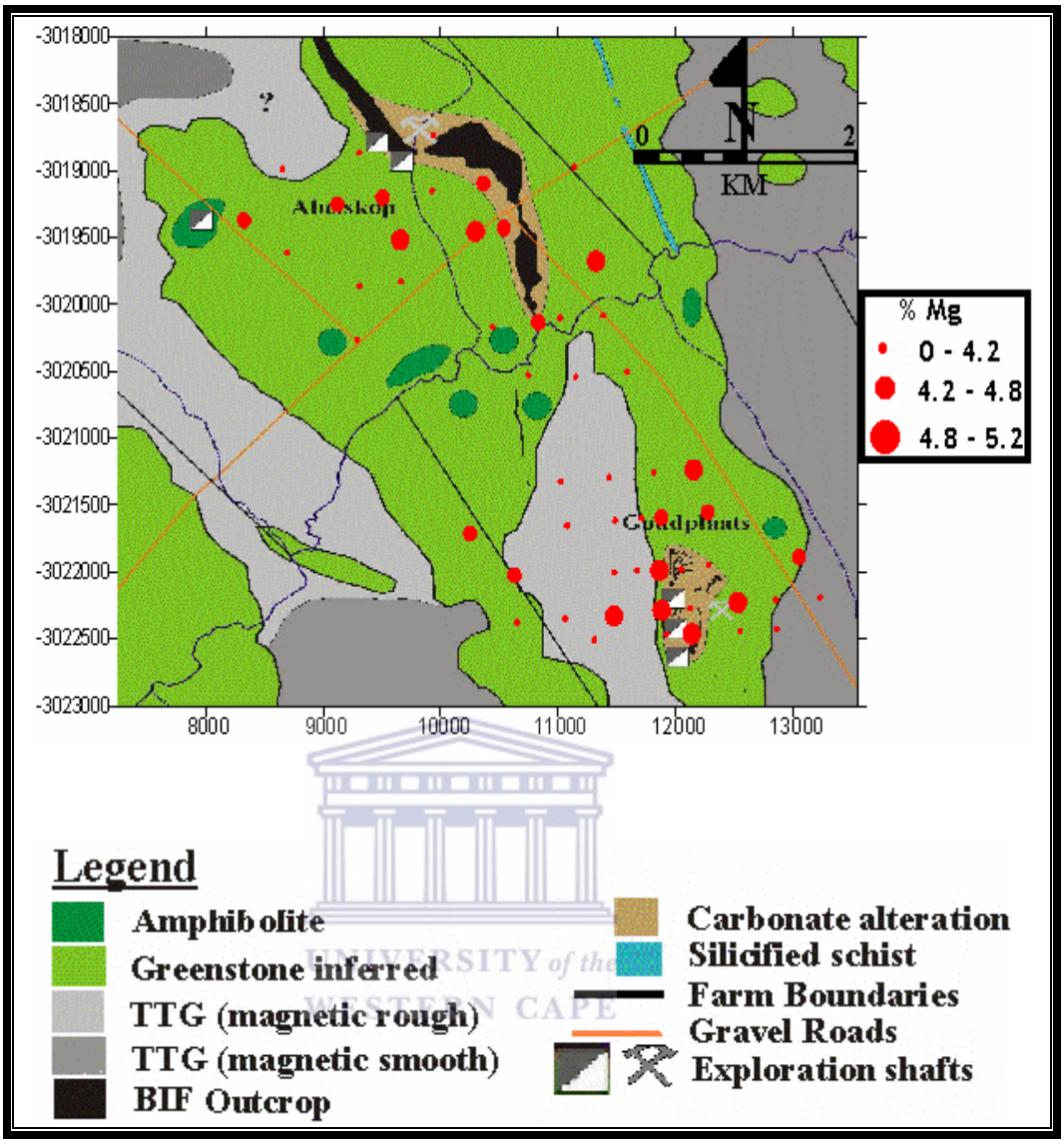

Fig. 4.24 Geochemical map of Mg in A. karroo

Magnesium

Magnesium is another abundant macronutrient in *A. karroo* with an anomalous value of 5.5% (0.5% dry wt). The distribution pattern of Mg and Ca show a high degree of similarity (Fig 4.24) in that they seem to be lithologically controlled. The similarities between Ca and Mg can be expected since they show a high degree of correlation (40.9%) in the factor analysis. Anomalous values occur in the southwards, in the

Goudplaats mineralized section with fewer clusters occurring in Abelskop and almost nothing in the BIF. There are some elevated clusters to the west of Abelskop, coinciding with an area of unknown mineralization. The high Mg values in the Blue Dot mine area could be attributed to the weathering of chlorite in the area.

Phosphorus

Phosphorus has an anomalous value of 3.7% (0.37% dry wt) with clusters of elevated P values occurring in the south, in Goudplaats area (Fig 4.25). A few elevated clusters also occur in the area west of Abelskop with very little occurring in the BIF. Once again the distribution pattern is similar to Mg and Ca however there a cluster that occurs on the Harts river.

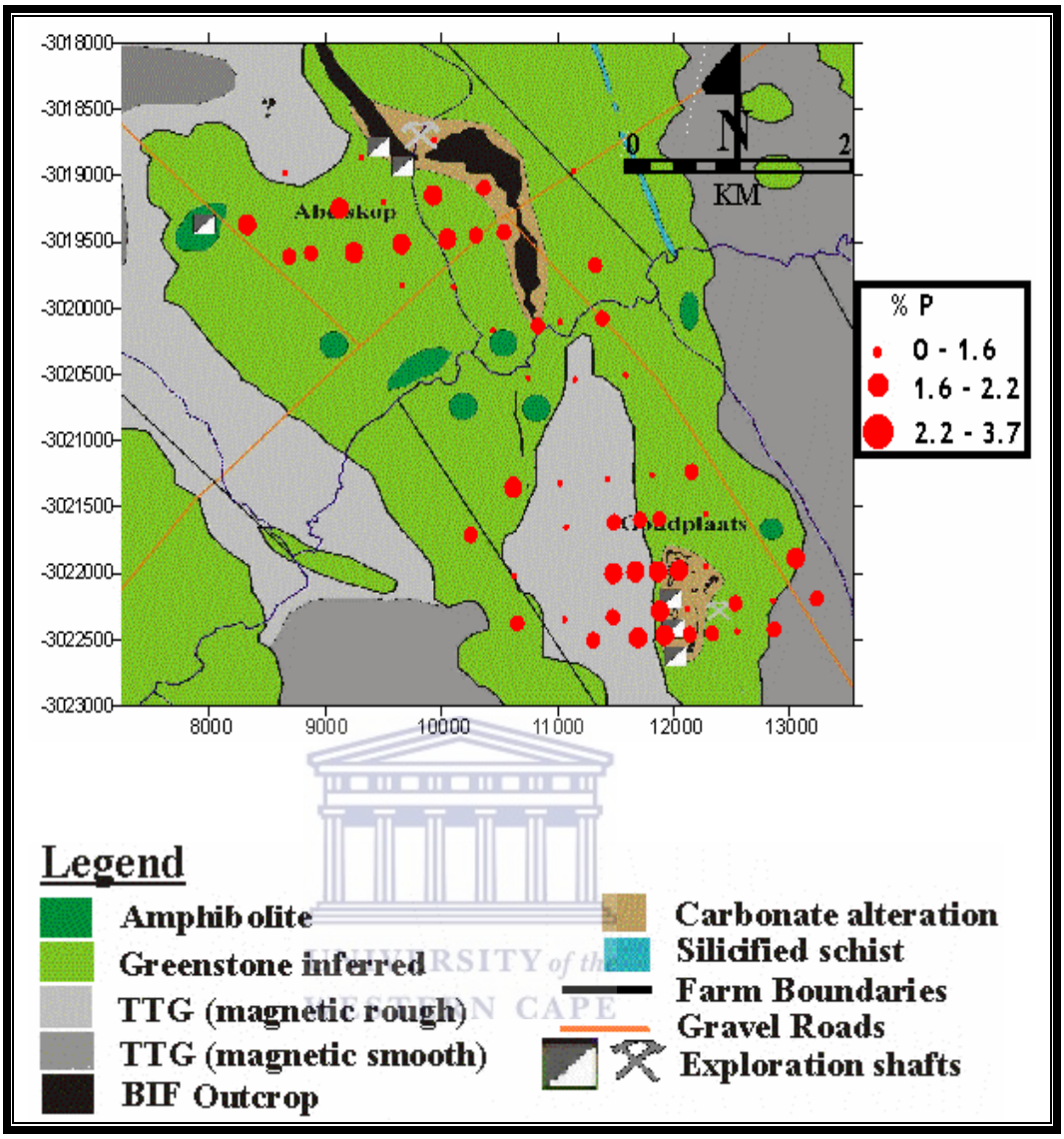

Fig. 4.25 Geochemical map of P in *A. karroo*

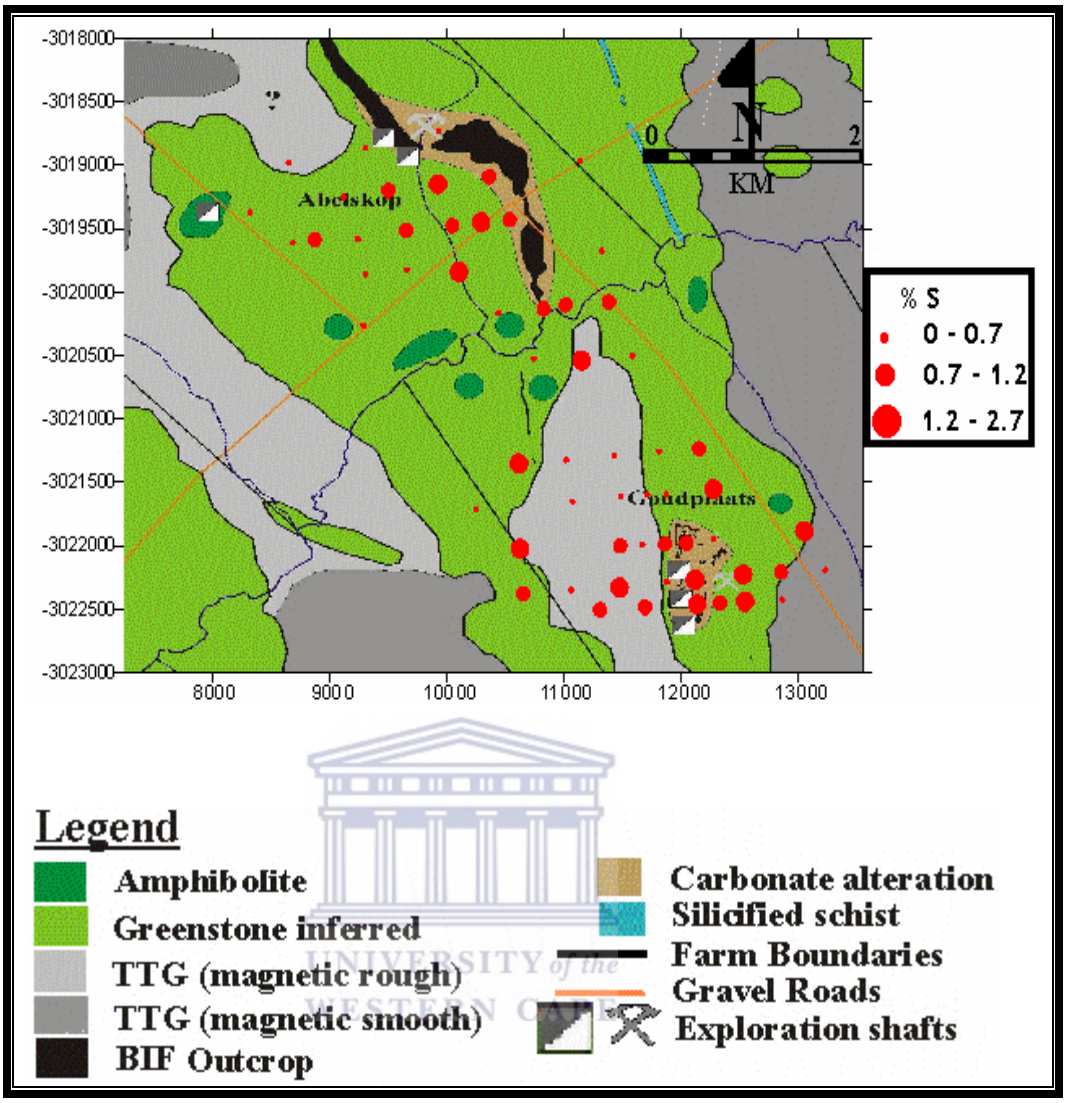

Fig 4.26 Geochemical map of S in *A. karroo*

Sulphur

Sulphur has an anomalous value of 2.7% (0.27% dry wt) and is widely distributed throughout the study area, with anomalous clusters occurring mainly in Goudplaats and some weaker anomalies occurring along the Harts River and west of Abelskop (Fig 4.26). Gold mineralization in the Blue Dot mine area occurs associated with pyrite, a major constituent of sulphur. There are elevated clusters along the drainage of Harts River especially in close proximity of Abelskop. Some anomalous clusters occur on the edges around Goudplaats and not directly on it as is the case in Ca, Mg and P. The area of unknown mineralization to the west of Abelskop also contains some strong S anomalies.

4.4.1.2 Gold and Pathfinder Elements

Gold

The gold geochemical map of *A. karroo* (Fig 4.27) shows a cluster of high gold values (up to a maximum of 79ppb), concentrated in the Goudplaats. These elevated gold values correlate well spatially with the carbonate altered schist of the Goudplaats mineralization and the siliceous BIF that host the economic gold deposits (Kiefer, 2004). A significant number of clusters occur in the area underlain by granites. High values also occur in the area west of the Abelskop BIF units, however fewer gold clusters occur on the carbonate altered schist in Abelskop. The results of factor analysis show a very low factor score (3%) for Au and no correlation with other elements. This is due to its low solubility and its lack of reaction with other elements.

Arsenic

Arsenic is an important trace element in gold prospecting as it is a major pathfinder for gold. The geochemical map (Fig 4.28) of As shows a cluster of anomalous values in the area west of the Abelskop BIF unit. These clusters extend into the carbonate altered rocks that envelope the BIF. Goudplaats mineralization contains background values and well defined anomalies occur along the Harts River.

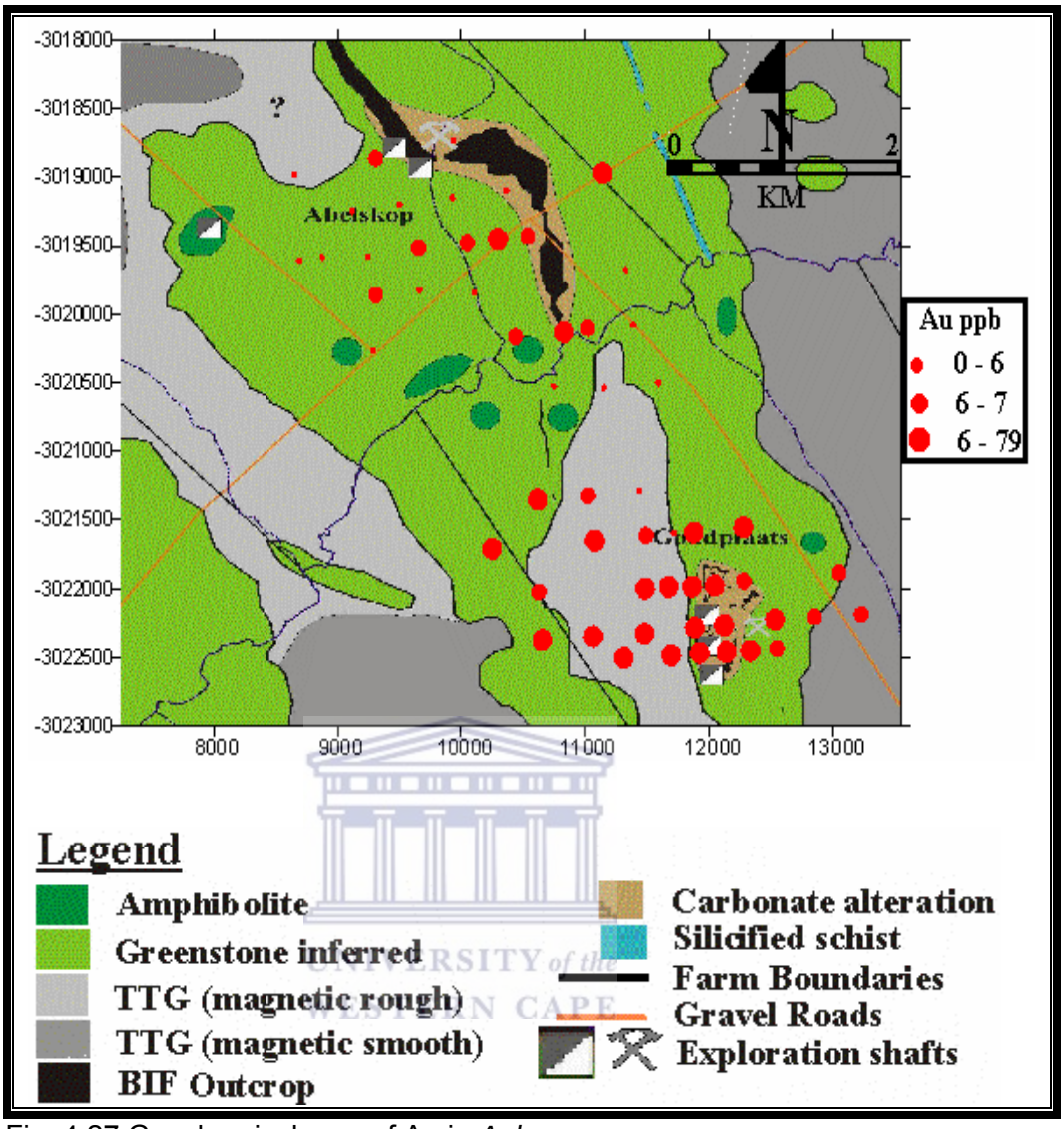

Fig. 4.27 Geochemical map of Au in *A. karroo*

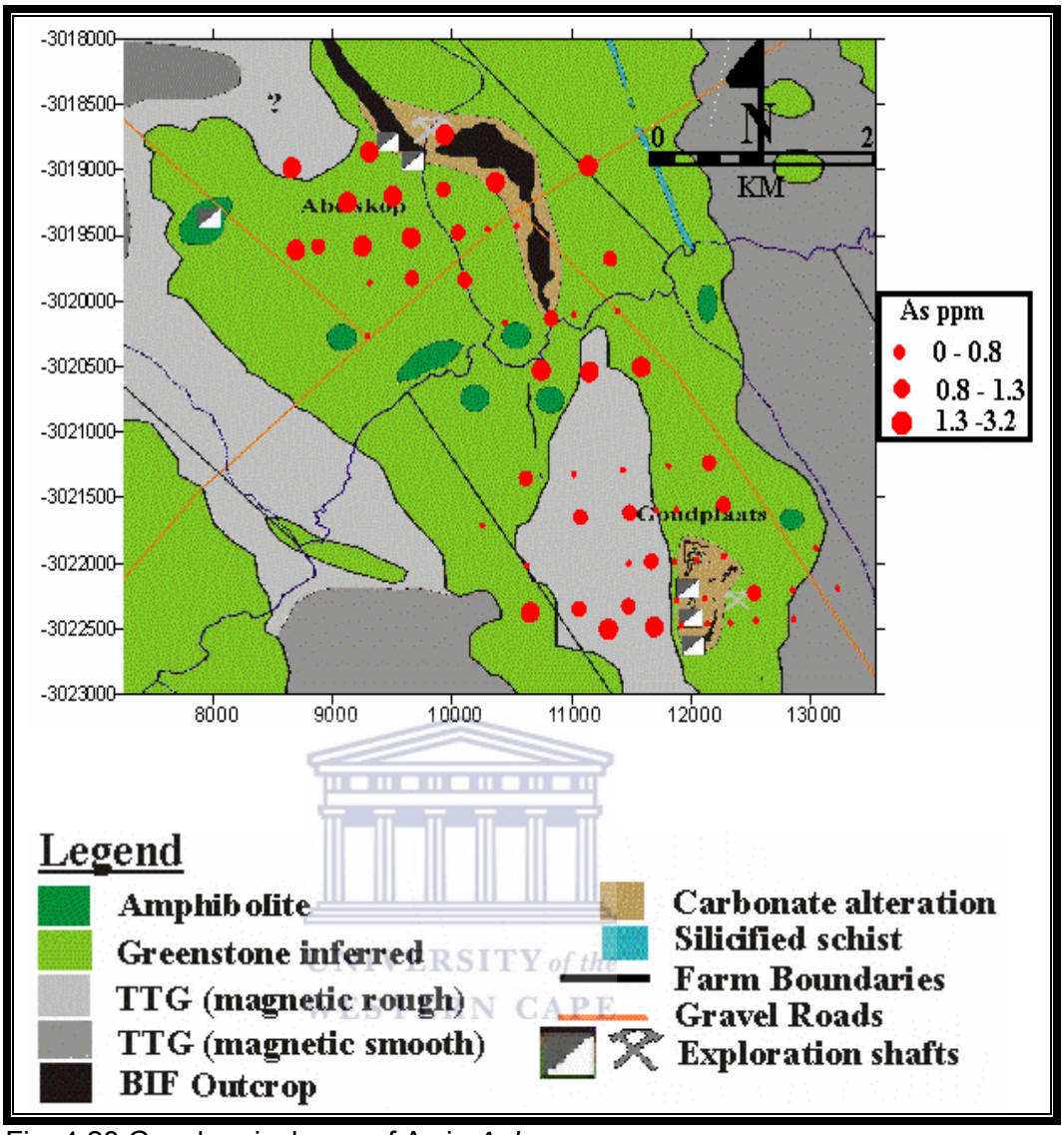

Fig. 4.28 Geochemical map of As in *A. karroo*

Silver

Silver has a threshold value of 0.13ppm (0.013ppm dry wt) and an anomalous value of 0.56ppm (0.056ppm, dry wt). Silver is an element associated with ores particularly gold, hence a number of anomalous values occur in the mineralized Goudplaats. The Ag geochemical map (Fig 4.29) shows a distribution pattern similar gold above. The occurrence of Ag in the BIF unit in Abelskop is insignificant. Silver is seemingly more abundant in areas covered in greenstones as compared to areas underlain by granites.

Lead

The geochemical map of Pb (Fig 4.30) shows a well-defined cluster of lead anomalies (maximum 29ppm) located on the granite and extending over the carbonate altered schist mineralized rocks in Goudplaats. The area west of Abelskop BIF also contains a number of high Pb clusters, which extend along the Harts river.

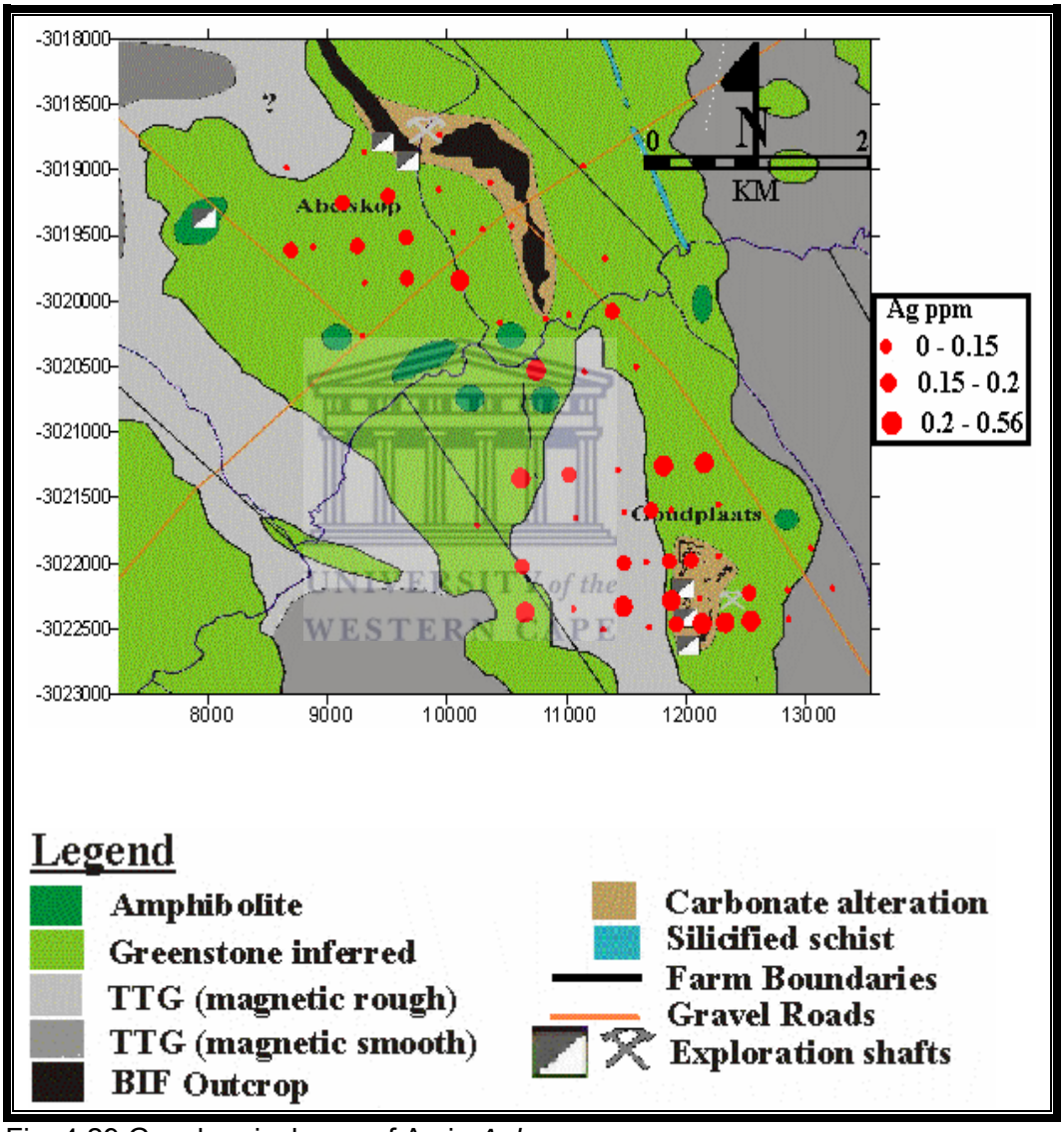

Fig. 4.29 Geochemical map of Ag in *A. karroo*

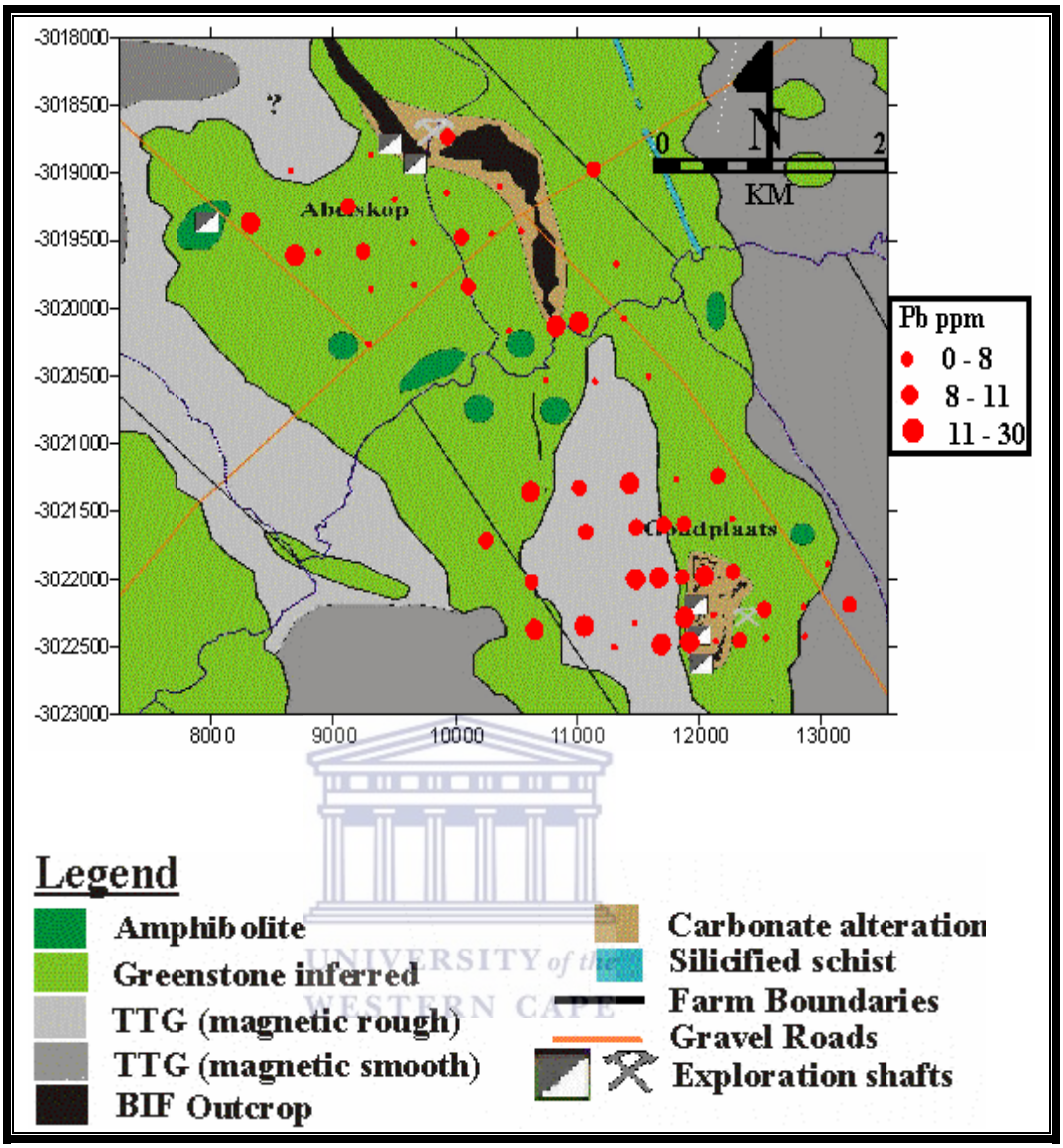

Fig. 4.30 Geochemical map of Pb in *A. karroo*

Mercury

The Hg geochemical map (Fig 4.31) shows a wide distribution of enhanced Hg values. These anomalous clusters (maximum 21ppm) correlate well with the Goudplaats mineralization, which is located in the southwest of the study area. Another cluster of anomalies occurs in Abelskop, extending into the BIF units. Elevated clusters also occur along the Harts river and into the granite area. The distribution of Hg is similar to Ag, showing an affinity for ultramafic greenstones.

Antimony

Antimony is another pathfinder with a threshold value of 0.175ppm (0.0175ppm dry wt) and an anomalous value of 0.245ppm (0.0245ppm dry wt). The geochemical map of Sb (Fig 4.32) shows a major southeast trending cluster of Sb anomalies centred in Goudplaats. These anomalous clusters occur mainly in the carbonate rocks, which are known to host economic gold. Other elevated Sb clusters occur in Abelskop mineralization and along the Harts river.

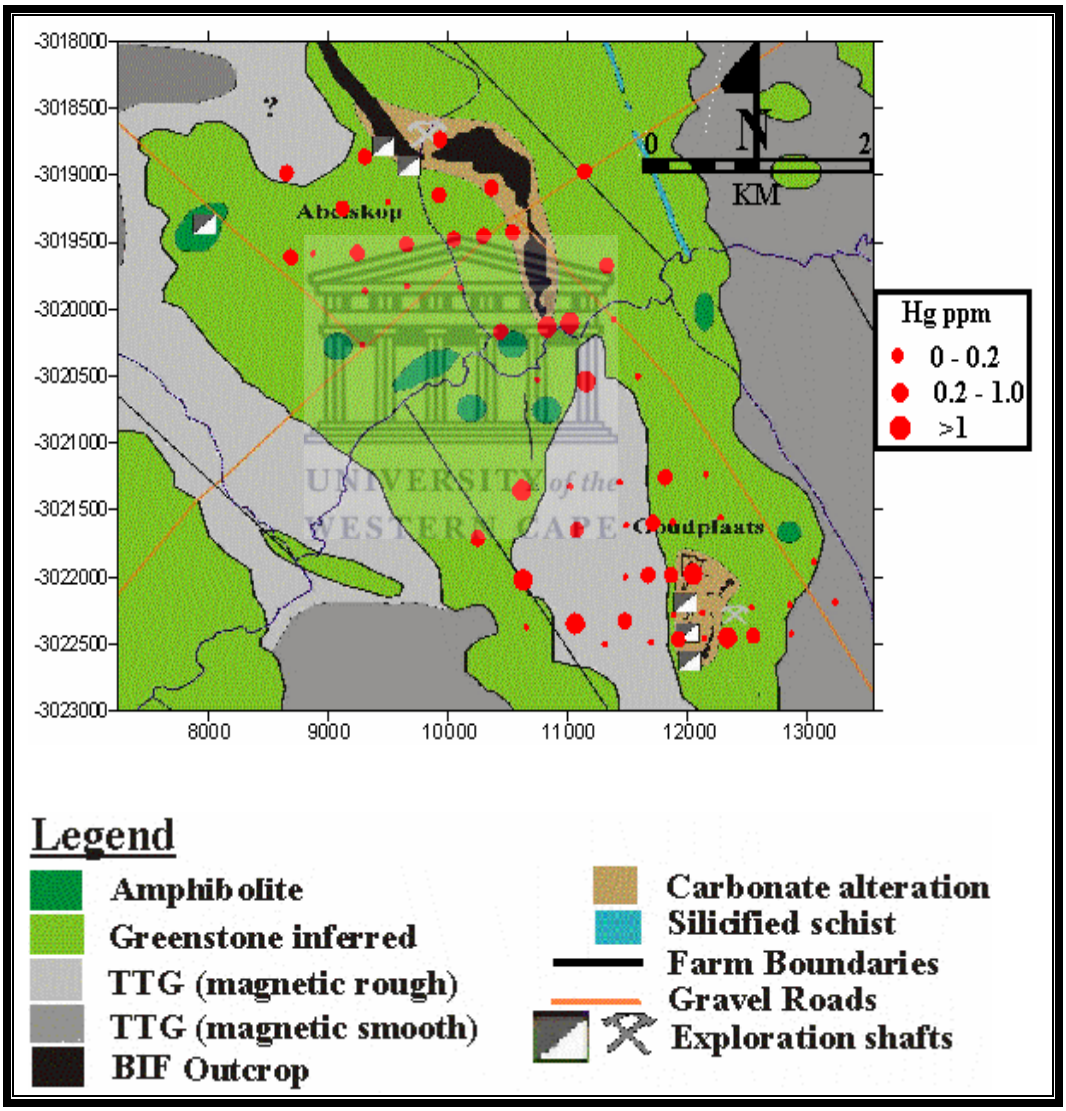

Fig. 4.31 Geochemical map of Hg in *A. karroo*

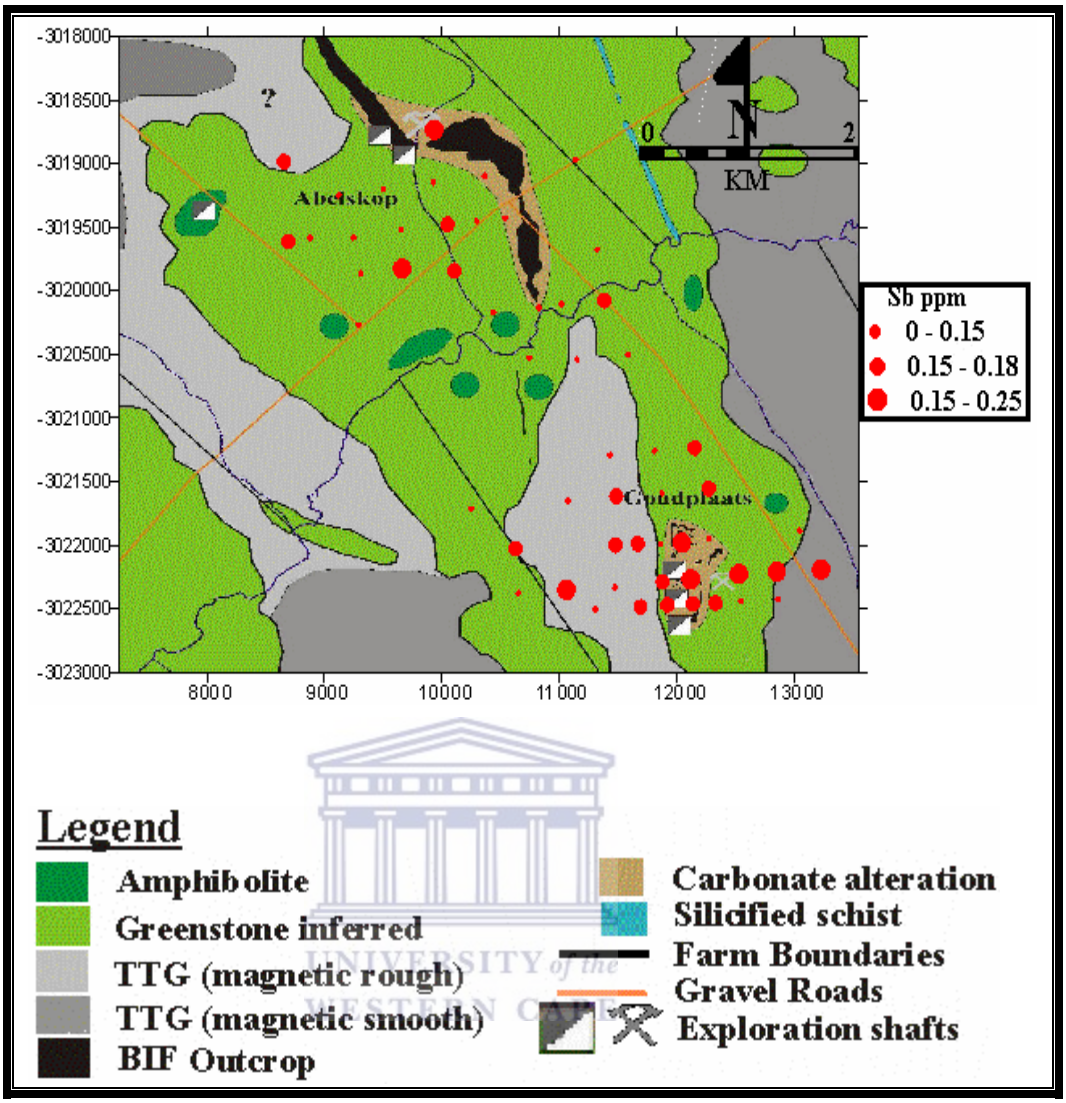

Fig. 4.32 Geochemical map of Sb in *A. karroo*

Tellurium

The geochemical map of Te (Fig 4.33) shows a strong association with granite, located in the southeast near Goudplaats mineralization. Elevated clusters are also seen in the carbonate rocks of the Goudplaats mineralization, extending into the area underlain by greenstones. The area west of Abelskop is characterized by background values, with the some anomalies occurring along the Harts river drainage. Tellurium has a threshold value of 0.12ppm (0.012ppm dry wt) and an anomalous value of 0.16ppm (0.016ppm dry wt).

Tungsten

The distribution pattern of W (Fig 4.34) is characterized by elevated anomalous clusters along the drainage pattern of the Harts river. Anomalous clusters also occur in the southeast, in Goudplaats where the carbonate rocks occur. The distribution of W shows similar trends to Ag and Hg. Few enhanced W clusters occur in the granite, just as in Ag and Hg. Abelskop has wide distribution of anomalous clusters, which extends into the BIF unit. Tungsten has an anomalous value of 1.14ppm (0.114ppm dry wt) and 0.75ppm (0.075ppm dry wt).

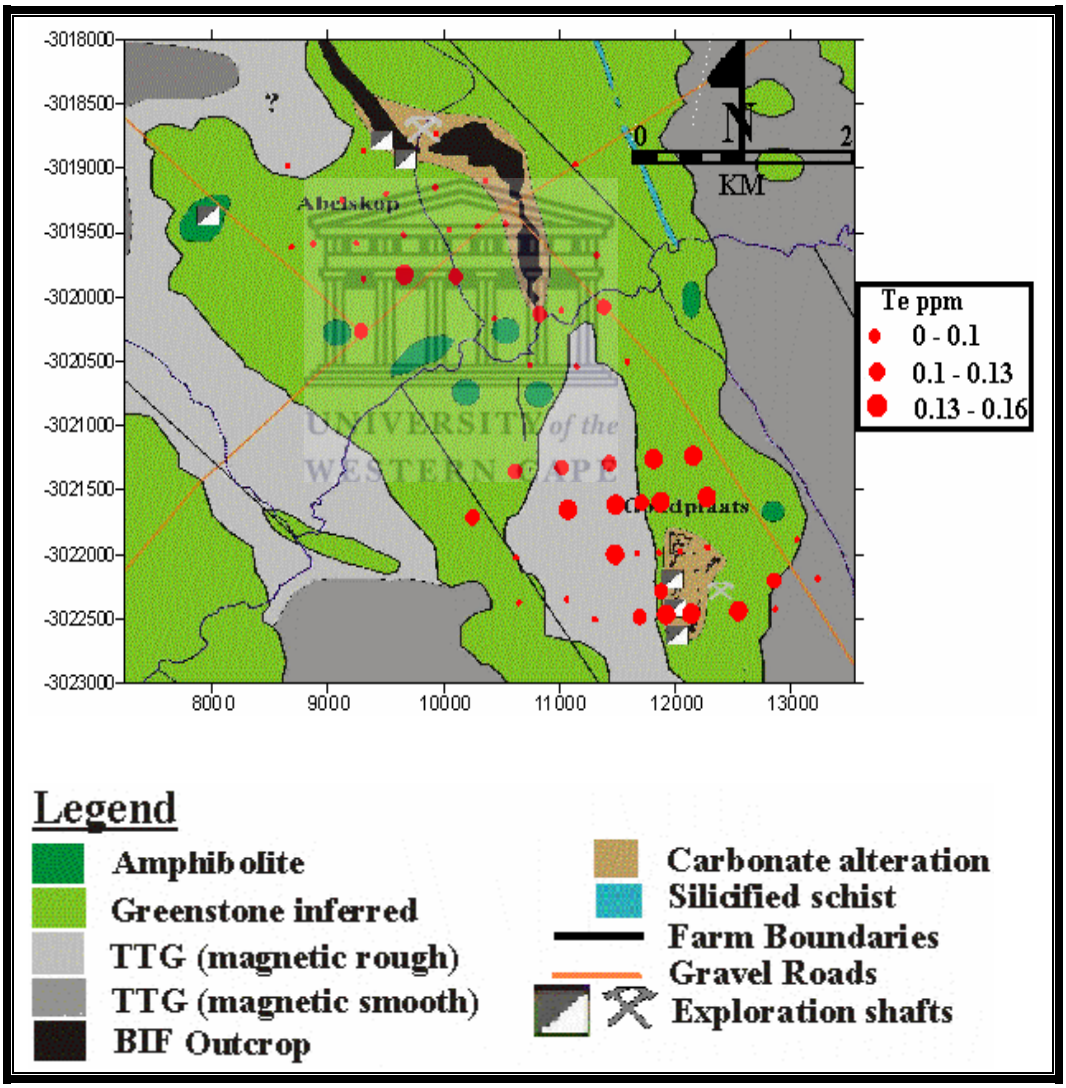

Fig. 4.33 Geochemical map of Te in *A. karroo*

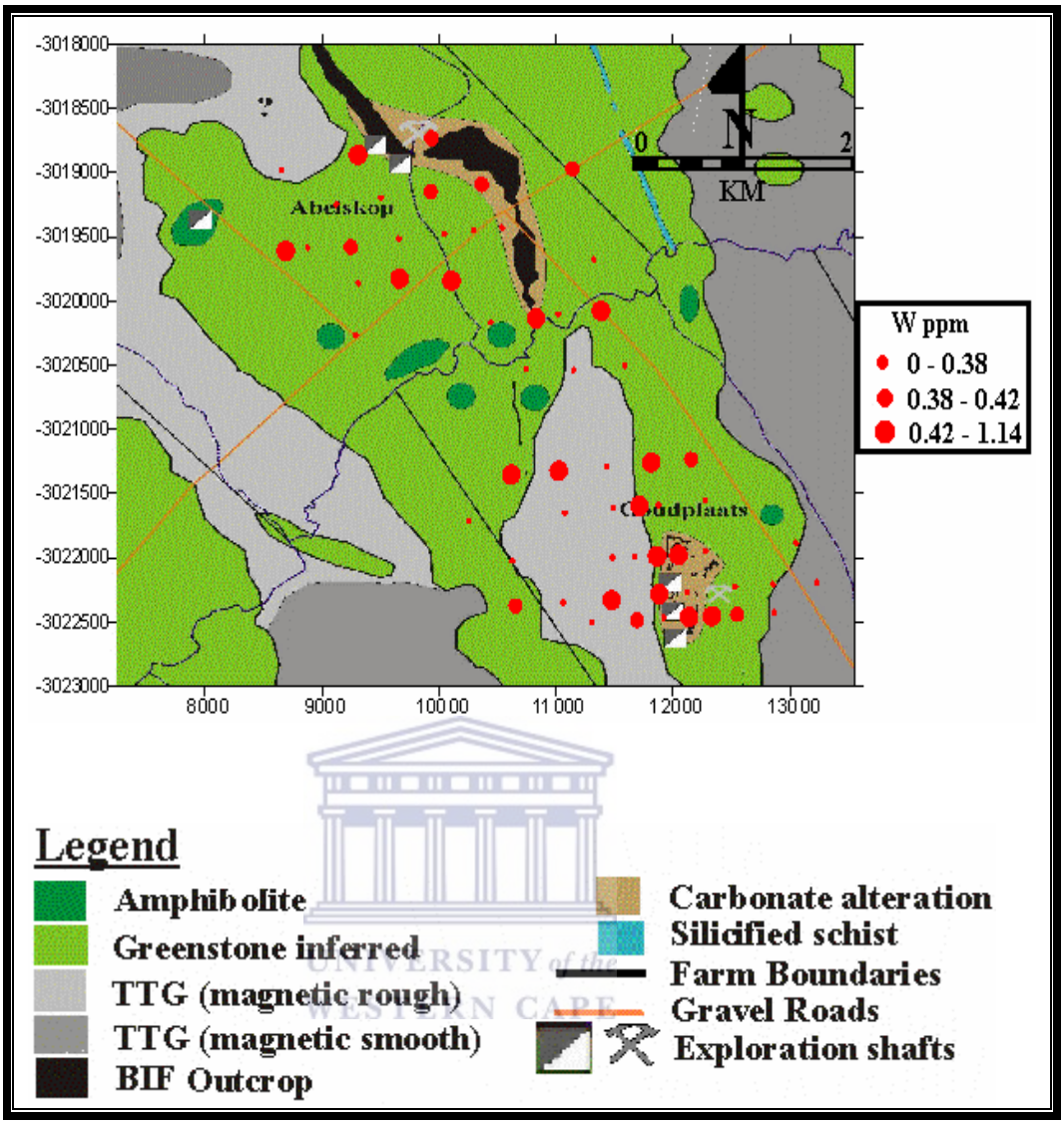

Fig. 4.34 Geochemical map of W in *A. karroo*

4.4.1.3 Other Trace Elements

Selenium

Selenium has an anomalous value of 5ppm (0.5ppm dry wt) and a threshold value of 4.2ppm (0.42ppm dry wt). The geochemical map of Se (Fig 4.35) shows a major NE-NW linear anomaly cluster, in close proximity to Abelskop and along the drainage of the Harts river. There is lack high Se values in Goudplaats mineralization, especially on the

granite. Anomalous values are concentrated in the area of unknown mineralization, to the west of Abelskop.

Strontium

The geochemical map of Sr (Fig 4.36) shows similarities to gold. The difference is the absence of anomalous clusters along the drainage pattern of the Harts river. Two clusters of anomalous values, one occurring in the southeast in Goudplaats and the other in the northwest, near the BIF outcrops of Abelskop.

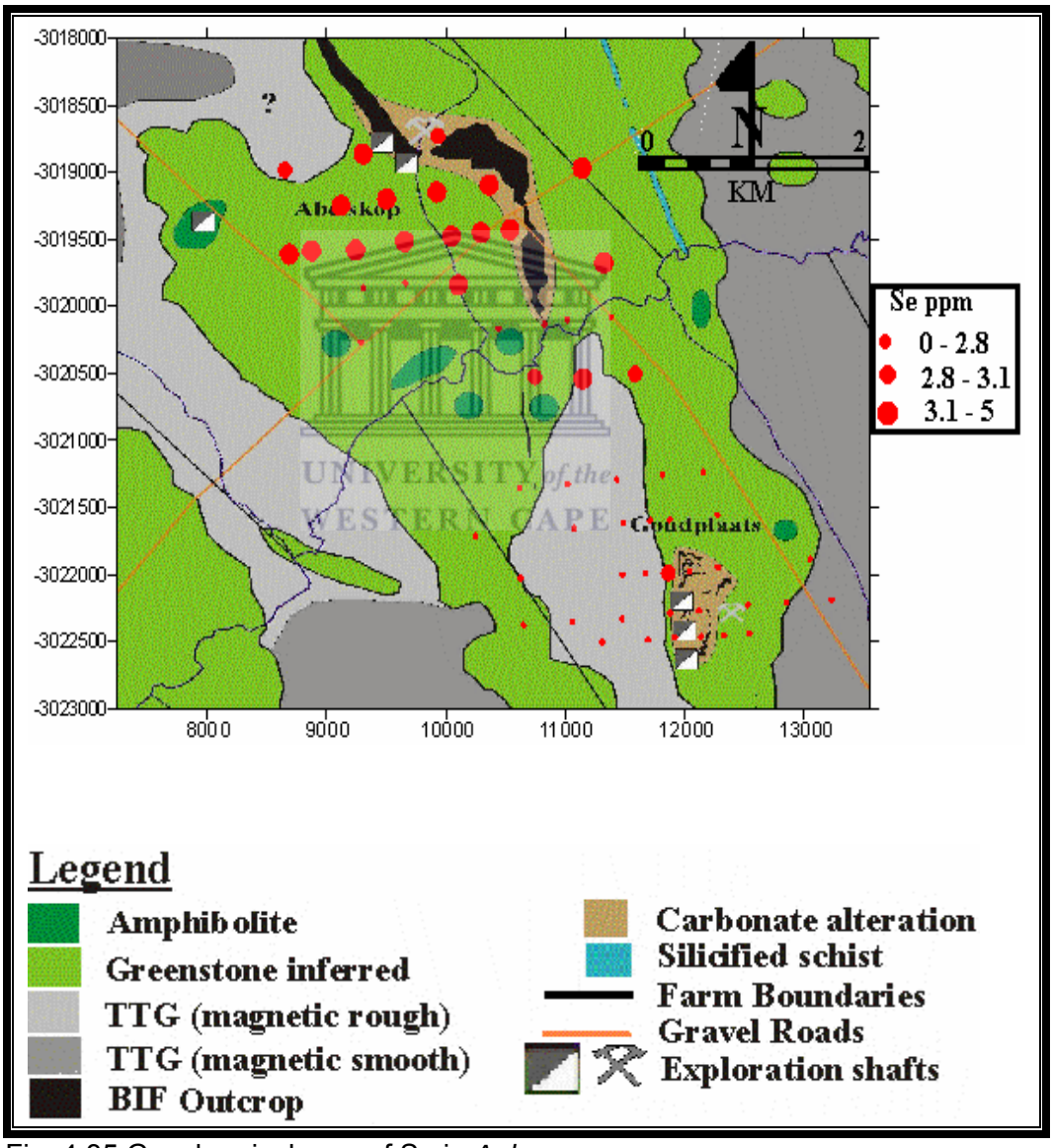

Fig. 4.35 Geochemical map of Se in *A. karroo*

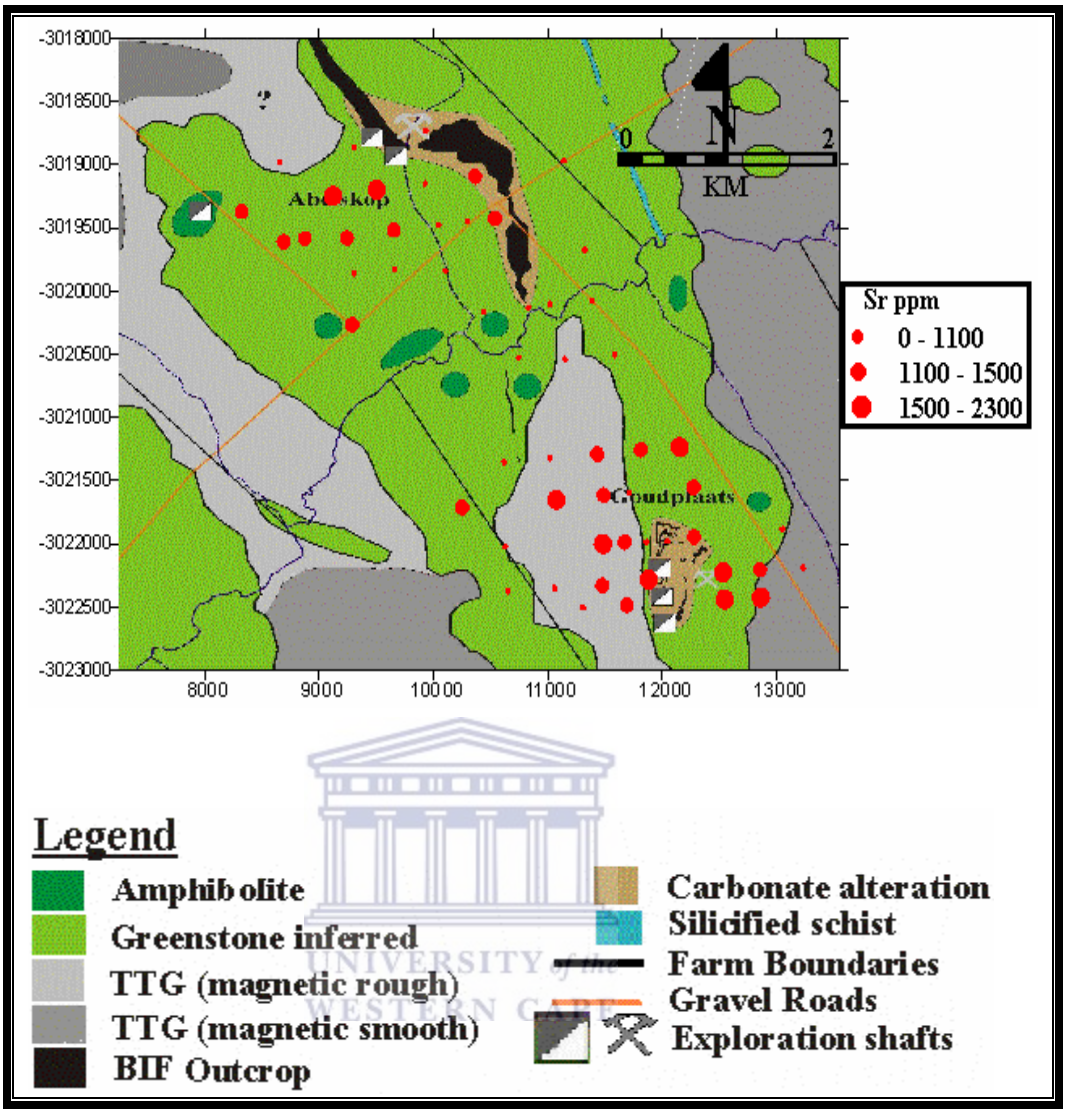

Fig. 4.36 Geochemical map of Sr in *A. karroo*

4.4.1.4 Rare Earth Elements

Lanthanum

The geochemical map of La (Fig 4.37) shows high values (up to 59ppm max) of La in areas underlain by granites and extending into the carbonate Goudplaats mineralization and greenstones. Lanthanum distribution seems to be associated with mineralization.

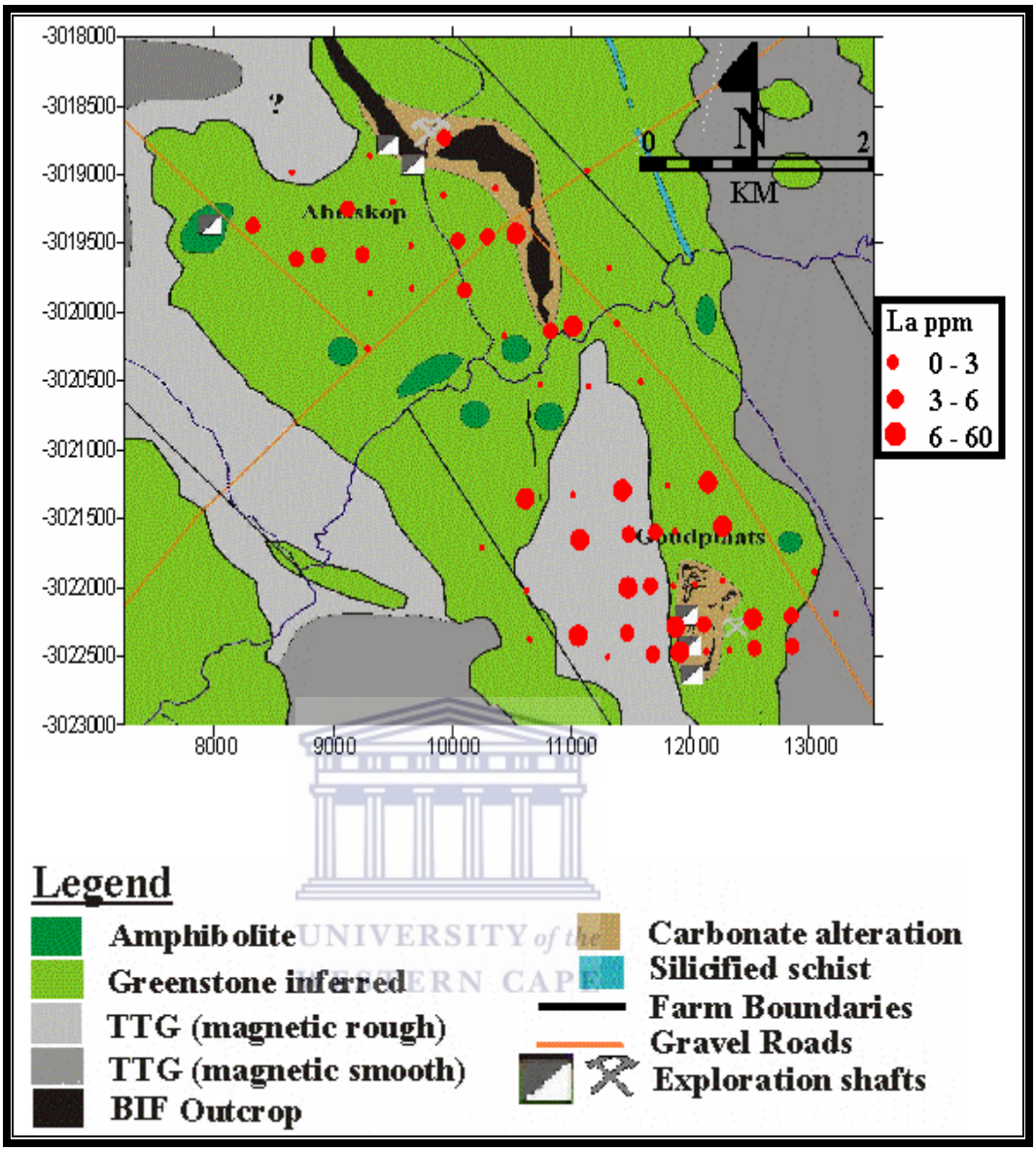

Fig. 4.37 Geochemical map of La in *A. karroo*

Cerium

The geochemical map of Ce (Fig 4.38) shows similar trends as La above, with a preference for granites. Elevated clusters occur towards the southeast and extend over Goudplaats and Abelskop mineralizations. Abelskop also contains a high number of elevated Ce values, which extend into the BIF outcrops.

Europium

The Eu distribution map (Fig 4.39) shows this element also has strong affinity for granites. These anomalous clusters extend across into Goudplaats mineralization. Abelskop also has enhanced Eu values including along the Harts river. The Eu distribution is similar to La and Ce above. The rest of the REEs (not included here) also show similar distribution trends and will not be dealt with further in this study.

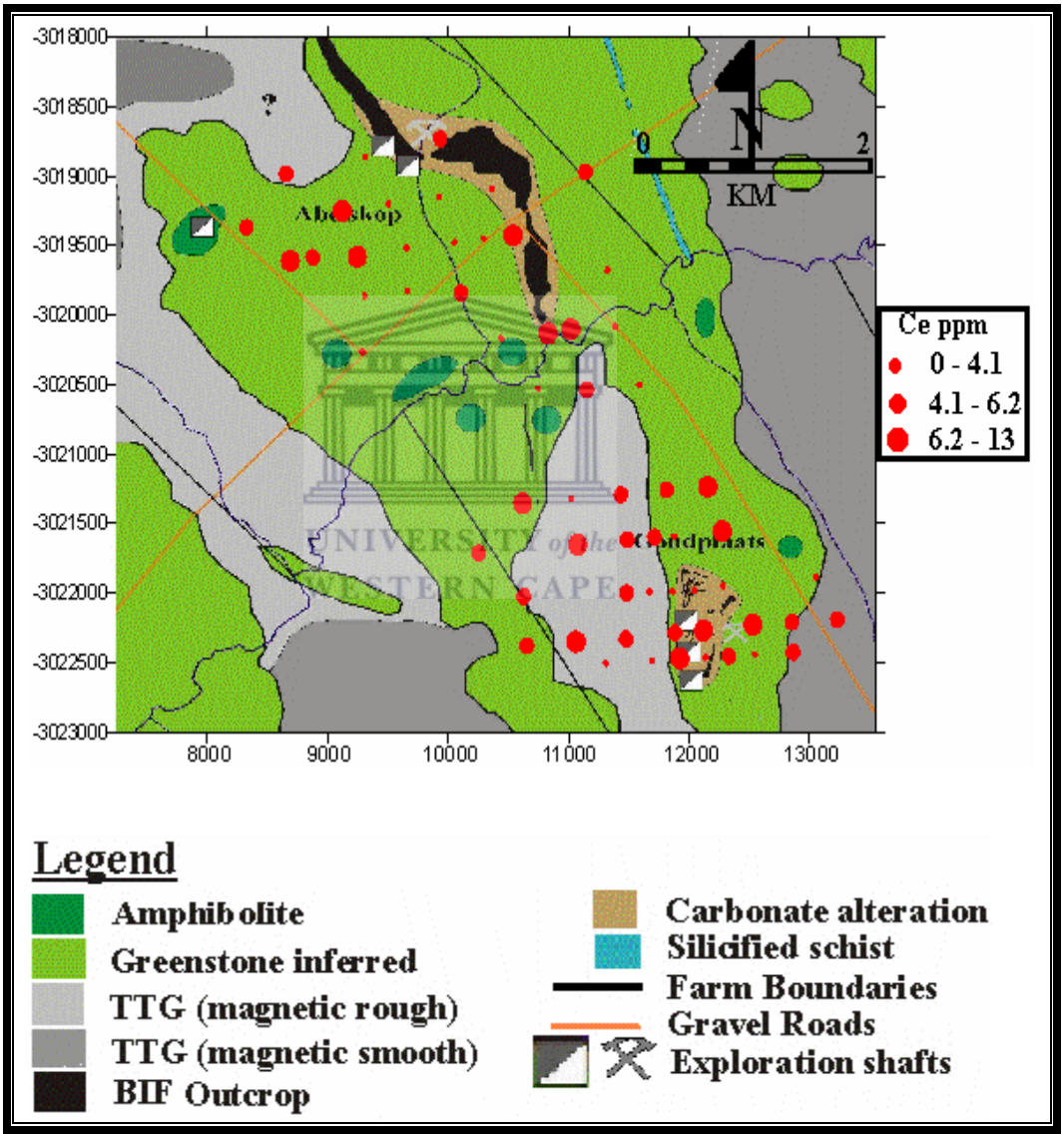

Fig. 4.38 Geochemical map of Ce in *A. karroo*

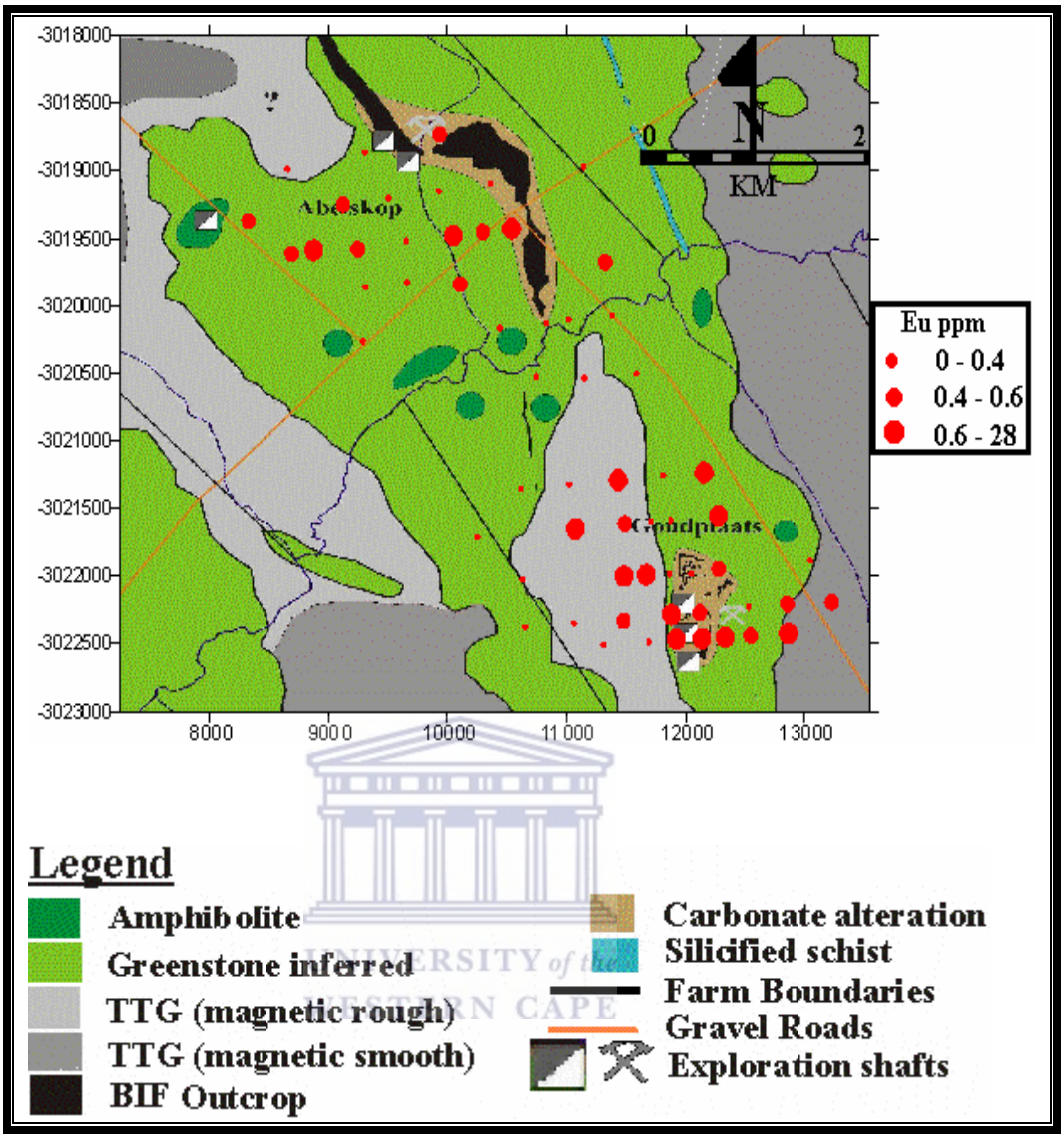

Fig. 4.39 Geochemical map of Eu in *A. karroo*

CHAPTER 5

5. Discussion, Conclusions and Recommendations

5.1 Discussion

The main focus of this investigation is to determine the suitability of *A. karroo* and *B. albitrunca* for biogeochemical prospecting for gold in the Blue Dot Mine area. The appraisal of the suitability for both plant species requires an understanding of their element absorption and distribution patterns in relation to variable composition of bedrock and associated underlying gold mineralization. Worldwide studies have been carried out using various plant species in order to ascertain their suitability for biogeochemical prospecting. Acacia species in Western Australia and the United States of America have been proven to be suitable sampling media for gold exploration (Arne et al., 1999) but nothing has been reported on *B. albitrunca*. There are also no published studies in Southern Africa that deal with the suitability of either for biogeochemical prospecting.

The Blue Dot Mine area is mainly covered by transported regolith of varying thickness of less than 1m to 5m and this regolith mainly comprises aeolian sand and calcrete, which has interacted with local bedrock and mineralization. The area is also characterized by sparse vegetation consisting mainly of grasses, shrubs and trees, with *A. karroo* as the most widespread tree species and *B. albitrunca* as the second most abundant species. The distribution of these species renders them suitable for biogeochemical sampling, as there is a presence of at least one species at each sampling point (Brooks, 1972). *A karroo* has an extensive and deep-rooting (as much as 65m) system that operates over a large surface area. This species grows well in heavy clay and loose sand and is also tolerant of highly saline, acidic and very basic soils (Otieno et al., 2005). *B. albitrunca* on the other hand favours sandy, loamy and calcrete soils. This species' deep rooting system is particularly suited to arid, sandy areas, perhaps because it is easier to extend deep roots into sand. It also grows against the dune slopes of the inner veld, but tends to grow as a shrubby,

tangled thicket in these areas, as it has difficulty anchoring itself in the loose sands (Alias & Milton, 2003).

The average gold content for *A karroo* is 9.15ppb and it ranges from 1ppb to a high value of 74ppb, while *B. albitrunca* has gold values that range from 1ppb to 10ppb with an average of 5.36ppb. The gold levels in *A. karroo* are similar to those reported for plants (Hall & Dunn, 1999). There is a marked difference in the distribution of gold in Abelskop and Goudplaats sections, with anomalous Au values generally restricted to Goudplaats. This may be attributed to the proximity of the Harts river with respect to Goudplaats and Abelskop. Abelskop is freely drained as the Harts river extends into the Abelskop valley while Goudplaats is poorly drained. Furthermore, studies show that stable minerals such as gold in soil or bedrock, may be solubilized, released to the secondary environment and made available to plants through organic and biologic processes (Stednick et al., 1987). Results from factor analysis show a poor correlation of gold with other pathfinder elements such As, Pb Ag, W, Hg and Te. Similar results were obtained in the Ballarat East Goldfield where low values of gold and decoupling of gold with other elements was attributed to dust contamination (Arne et al., 1999).

Uptake of gold in *B. albitrunca* (average 5.36ppb) is lower compared to *A. karroo.* The low values in *B. albitrunca* may be due to the "barrier effect" that inhibits the uptake of Au by plant (Erdman & Olson, 1985) or the high concentration of Ca because a high concentration Ca means a low intake of heavy metals such as Fe and Au (Reading et al., 1987).

The distribution and absorption patterns of gold pathfinder elements such as As, Sb, Te, Hg, Ag, Pb and W are significant in geochemical prospecting, hence the need to consider such elements in biogeochemical prospecting. Uptake of As is similar in *A. karroo* and *B. albitrunca*, with a mean concentration of 1.05ppm in *A. karroo* and a concentration of 1.15ppm in *B. albitrunca*. The distribution pattern of As is associated with mineralization, given the anomalous As values that occur in Goudplaats and Abelskop. This siliceous BIF is of economic importance as it is wherein the gold ores are located

(Kiefer, 2004). The non-mineralized areas contain low values, which by differ 2-3 times that of the anomalous values.

Low values of W were found in both species (*A karroo*, averaging at 0.41ppm and B albitrunca averaging at 0.60 ppm). The distribution of W in *A. karroo* is similar to gold distribution, where anomalous clusters occur in the mineralized Goudplaats. High values of 5-100ppm (dry wt) have been reported in trees and shrubs in the Rocky Mountains (Greger, 2004). However tungsten values of <1 are quite common in a number of plant types as it moderately toxic in plants (Greger, 2004).

The distribution of Sb in *A. karroo* is related to mineralization as anomalous clusters occur mainly in Goudplaats and few occur in Abelskop. Some weakly anomalous clusters also occur along the Harts river. Background and anomalous values differ by a factor of 2. Antimony is highly mobile in the environment since it occurs in water, carbon and in Fe hydroxides. As a result, it is easily taken up by plants and translocated to other parts of the plant. *B. albitrunca* also has low concentrations of Sb, with a mean concentration of 0.14ppm (range 0.10-0.24ppm). The distribution of Sb in *B. albitrunca* is uniform throughout showing no marked difference between the mineralized and non-mineralized areas.

Silver is an element commonly associated with gold in ores. Both species have an average Ag concentration of 0.17ppm and similar ranges. The distribution in *A karroo* is associated with mineralization as anomalies occur in Goudplaats. The difference between background anomalous values is not much (factor of 2).

In summary, there are similar levels of absorption of As, Ag, Hg, and Pb by both *A. karroo* and *B. albitrunca* which show elevated values over mineralized areas. *A. karroo* has a higher average concentration of Te and Sb while *B. albitrunca* shows higher absorption pattern with regards to W. The ability of *A. karroo* and *B. albitrunca* to absorb appreciable amounts of pathfinder elements, more especially from mineralized areas shows potential value of these species for biogeochemical prospecting for gold.

In this present study the accumulation of LREE (La, Ce, Pr, Nd, Sm and Eu) is more than that of the HREEs (Gd, Tb, Dy, Ho, Er,Tm, Yb and Lu) in both plants. In addition to this, the REE of even atomic number (Ce, Nd, Sm, Gd, Dy, Er, and Yb) are more abundant than those odd atomic numbers (La, Pr, Eu, Tb, Tm, Ho, and Lu). Such behaviour was also noticed by some earlier workers (Market, 1987). This pattern of depletion of HREEs compared to LREEs is typical of plants and soils (Angelica & Costa, 1993; Market, 1987).

The variations in REE are controlled by the original parent rock, fluid and secondary products involved in physico-chemical conditions of weathering and alteration (Raju & Raju, 1999). The REE group undergoes fractionation in aqueous solutions during a variety of geological processes including hydrothermal ore formation, carbonatite evolution, wall-rock alteration and weathering (Wood, 1990). In this study, this is clearly evident in the distribution pattern of REE in *A karroo* and *B. albitrunca* is closely associated with the areas underlain by granites and carbonate schist wherein the mineralization occurs. Enrichment also occurs in mineralized areas and poorly drained areas. High values of Ce and La (mean of 4.93ppm) in *A. karroo* in particular Elevated REE values may indicate an increase in detrital heavy minerals such as zircon, apatite, allanite and monazite due to the dissolution of quartz (Kiefer, 2004). Alternatively this could be the result of dissolution of apatite during weathering causing the release of elements such Ce, La, and Nb (Dill, 1994). The above-mentioned plots are characterized by high $(La/Yb)_N$ as opposed to the plots where the gradients are rather flat, such as those in non-mineralized areas.

In general uptake of REEs by plants is high for La, Ce and Nd, moderate for Pr, Sm, Eu and Gd and low for the other elements (Raju & Raju, 1999). REE enrichment in plants and soils may mainly be attributed to granitic parent material or alkaline igneous rocks (Wood, 1990; Raju & Raju, 1999). The overall REE concentration in *A. karroo* is in agreement with the values in literature according to Hall & Dunn, 1999) thus making this species suitable for biogeochemical analysis of REEs.

Distribution patterns of Ca and Mg in the study area are similar, showing elevated values in and around Goudplaats mineralization. Fewer clusters occur in Abelskop mineralization and along the Harts river. The high degree of association between Mg and Ca as shown by the high factor loadings (40%) in the factor analysis is indicative of a mafic association. This factor represents the greenstones that occur throughout the study area. These greenstones are tholeiitic basalts with a compositional range of 20%>CaO+MgO>12% (Kiefer, 2004). Therefore the high uptake of Ca and Mg seems to lithologically controlled, since anomalous values occur on the greenstones. The high concentration of these elements could also be related to the weathering trends in the Blue Dot mine area. The weathering of K-feldspars leads to high Ca levels (Nagaraju & Karimulla, 2001), while the weathering of chlorite explains the high uptake of Mg (Bain, 1994). Cluster analysis results also clearly indicate higher concentration in areas covered in greenstone and mineralized areas especially in Goudplaats.

The other of the macronutrients (P, S,) have similar distribution patterns to Mg and Ca, showing a clear association to mineralization, especially in Abelskop and an area west of Goudplaats that is of unknown mineralization. Both species also show similar absorption patterns with regard to P and S even though their concentrations (S & K) are significantly lower than the reported literature values by Bowen, (1964) and Hall & Dunn (1999).

5.2 Conclusions

This study has investigated the potential for biogeochemical prospecting using the two most widely distributed tree species, *A. karroo* and *B. albitrunca* in the Blue Dot Mine area. Geochemical maps for *A. karroo* show anomalous levels (maximum, 74ppb) of Au in the Goudplaats mineralization. The element absorption patterns of pathfinder elements such as Ag, Pb, As, Sb, Te and Hg further reinforces the potential of *A. karroo* for biogeochemical prospecting in the Blue Dot Mine area. *A. karroo* has also shown the ability to appreciably absorb REEs which are otherwise rarely available to plants and translocate these elements to its aerial parts such as the leaves. The wide distribution *A.*

karroo throughout the study area gives it an even greater advantage due to its accessibility.

B. albitrunca on the other hand has shown capabilities in absorbing significant amounts of gold pathfinders such as Ag, As, Pb, W and Hg. Although geochemical maps for this species could not be plotted due to low sampling density, the absorption of the pathfinders was comparable to *A. karroo.* This also holds true for the REEs in that B. albitrunca demonstrated the ability for optimum uptake of REEs, particularly in mineralized areas and in granitic rocks. That being said, it is a common occurrence in biogeochemistry, that the species with the highest metal concentrations are not the most widespread (Dunn, et. al., 1996).

In spite of the lesser distribution of *B. albitrunca* when compared to *A. karroo*, this study has demonstrated the suitability of the two species for biogeochemical prospecting in the Blue Dot Mine area.

5.3 Recommendations

Despite the small size of the Blue Dot Mine deposit, there is potential for the discovery of further economic deposits. Conventional soil sampling in the area has given unsatisfactory results. It is therefore recommended that biogeochemical prospecting become an integral part in search of further targets in the future. Since the suitability of the two species has been established, perhaps other plant organs such as the bark and twigs also be sampled, especially in *B. albitrunca* where the gold concentration is not as high.

References

Ackon, P., 2001. Selective leach techniques as a tool for prospecting gold deposits concealed by aeolian regolith. A case study at Blue Dot Mine, Amalia, Northwest Province, South Africa. M.Sc. Thesis (unpublished), University of the Western Cape, Cape Town, 127pp.

Alias, D., Milton, S., 2003. A collation of and overview of research information on *Boscia albitrunca* and identification of relevant research gaps to inform protection of the species. Department of Water Affairs and Forestry No. 2003/089 150pp.

Angelica, R.L., Da Costa, M.L., 1993. Geochemistry of rare-earth elements in surface lateritic rocks and soils from the Maicuru Complex, Para, Brazil. Journal of Geochemical Exploration 47, 165-182.

Anhaeusser, C.R., Walraven, F., 1999. Episodic granitoid emplacement in the western Kaapvaal Craton: evidence from the Archean Kraaipan granite-greenstone terrane, South Africa. Journal of African Earth Sciences 28, 289-309.

Arne, D.C., Stott, J.E., Waldron, H.M., 1999. Biogeochemistry of the Ballarat east goldfield, Victoria, Australia. Journal of Geochemical Exploration 67, 1-14.

Beus, A.A., Grigorian, S.V., 1975. Geochemical exploration methods for mineral deposits. Applied Publishing Ltd, Illinois, USA, 287pp.

Bowen, H.J.M., 1964. Trace elements in biochemistry. Academic Press, London, 241pp.

Brooks R.R., 1972. Geobotany and biogeochemistry in mineral exploration. Harper and Row, New York, NY, 290pp.

Brooks, R.R., 1982. Biological methods of prospecting for gold. Journal of Geochemical Exploration 17, 109-122.

Brooks, R.R., Baker, A., J., M., Malaisse, F., 1992. Copper flowers. Res. Explor., 8, 338-351.

Cheng, H.K., Yang, M.S., 1996. On a class of fuzzy c-numbers clustering procedures for fuzzy data. Fuzzy Sets and Systems 84, 49-60.

Chiarenzelli, J., Aspler, L., Dunn, C., Cousens, B., Ozarko, D., Powis, K., 2001. Multi-element and rare earth element composition of lichens, mosses and vascular plants from the Central Barrenlands, Nunavut, Canada. Applied Geochemistry 16, 245-270.

Clare, A.P., Cohen, D.R., 2001. Geochemistry: Exploration, Environment, Analysis 1, 119-164.

Cohen, D.R., Hoffman, E.L., Nichol, I., 1987. Biogeochemistry: a geochemical method for gold exploration in the Canadian Shield. Journal of Geochemical Exploration 29, 49-73.

Cohen, D.R., Shen, X.C., Dunlop, A.C. and Rutherford, N.F., 1989. A comparison of selective soil geochemistry and biogeochemistry in the Cobar area, New South Wales. Journal of Geochemical Exploration 98, 173-189.

Dill, H.G., 1994. Can REE patterns and U-Th variations be used as a tool to determine the origin of apatite in clastic rocks? Sediment. Geol. 92, 175-196.

Dunn, C.E., Brooks, R.R., Edmondson, J., Leblanc M., Reeves, R.D., 1996. Biogeochemical studies of metal-tolerant plants from Morocco. Journal of Geochemical Exploration, 56, 13-22.

Greger, M. 2004. Uptake of nuclides by plants. Technical Report TR-04-14. 70pp.

Erdman, J.A., Olson, J.C., 1985. The use of plants in prospecting for gold: a brief overview with a selected bibliography and topic index. Journal of Geochemical Exploration 24, 281-304.

Hall, G.E.M., Dunn, C.E., 1999. Biogeochemistry applied to mineral exploration and environmental studies and recent developments in the analysis of organic and other surficial materials. Short course. Association of Exploration Geochemists, 150pp.

Hoffmann, E.L., 1989. Instrumental neutron activation analysis as an analytical technique for gold exploration. Journal of Geochemical Exploration 32, 301-308.

Hou, Z., 1987. Influence of the siliceous components in determination of gold in plant materials. Journal of Geochemical Exploration 27, 323-328.

Hu, Z., Richter, H., Sparovek, G., Schnug, E., 2004. Physiological and biochemical effects of rare earth elements on plants and their agricultural significance: A review. Journal of Plant Nutrition 27, 183-220.

Hunt, J.P., 1996. Aspects of the geology and mineralization of the Abelskop section, Amalia Gold Mine and the geochemical signatures related to mineralization. Dept of Geology, University of the Witwatersrand, South Africa, (Unpublished).

Johnson, S.F., 1995. Geology and gold mineralization of part of the farm Goudplaats 96HO, Amalia Greenstone Belt, South Africa, Dept. of Geology, University of the Witwatersrand, 3pp, (Unpublished).

Jones, I.M., Anhaeusser, C.R., 1993. Accretionary lapilli associated with Archean banded iron formations of the Kraaipan Group, Amalia greenstone belt, South Africa. Precambrian Research 61, 117-136.

Jones, I.M., Anhaeusser, C.R., 1991. The Kraaipan Group-Amalia Greenstone Belt, southwestern Transvaal. In: C.R. Anhaeusser (Editor), The Archean Kraaipan Group volcano-sedimentary rocks associated with granites and gneisses of the southwestern Transvaal, North-Western Cape Province and Bophuthatswana excursion guide book, Information circular, Economic Geology Research Unit, University of the Witwatersrand, Johannesburg, 244: 13-25.

Kiefer, R.D., 2004. Regional geology, tectonic evolution and controls of gold mineralization in the Archean Amalia Greenstone Belt, Kraaipan Terrane, South Africa. PhD Thesis (unpublished), University of the Witwatersrand, Johannesburg, 515pp.

Leavitt, S.W., Deuser, R.D., Goodell, H.G., 1979. Plant regulation of essential and non-essential heavy metals. Journal of Applied Ecology 16, 203-212.

Liang, T., Yan, B., Zheng, S., Wang, L., Wang, N., Liu, H., 2001. Contents and biogeochemical characteristics of rare earth elements in wheat seeds. Biogeochemistry 54, 41-49.

Lintern, M.J., Butt, C.R.M., Scott, K.M., 1997. Gold in vegetation and soil- three case studies from the goldfields of southern Western Australia. Journal of Geochemical Exploration 58, 1-14.

Markert, B., 1987. The pattern of distribution of lanthanide elements in soil and plants. Phytochemistry 26, 3167-3170.

Markett, B., Li, Z.D., 1991. Natural background concentrations of rare earth elements in a forest ecosystem. Sci. Total Environ. 103, 23-35.

Markett, B., Deli, Z., 1991. Inorganic chemical investigations in the forest biosphere reserve near Kalinin, USSR. Vegetation 97, 57-62.

Marschner, H., 1995. Mineral nutrition in higher plants, 2nd edn. Academic Press, London, 889pp.

McDonough, W.F., Sun, S., 1995. The chemical composition of the Earth. Chemical Geology 120, 223-253.

Nagaraju, A., Karimulla, S., 2001. Geobotany and biogeochemistry of *Gymnosporia montana* – a case study from Nellore Mica Belt, Andhra Pradesh. Environmental Geology 41, 167-173.

O' Connor, P.J., Reimann, C., 1993. Multielement regional geochemical reconnaissance as an aid to target selection in Irish Caledonian terrains. Journal of Geochemical Exploration 47, 63-87.

Okujeni, C.D., Olidapo A.O., 1994. The use of U/Th ratios and REE pattern in savannah trees as a guide to uranium mineralization in the Benue Trough, Nigeria. Discov. Innovat. 6, 152-156.

Okujeni, C.D., Ackon, P., Baugaard, W., Langa, N., 2005. Controls of element dispersion in aeolian sand and calcrete dominated regolith associated with gold mineralization in the Kraaipan greenstone belt, South Africa. Geochemistry, Exploration, Environment, Analysis 5, 1-9.

Otieno, D., Schmidt, M.U.I., Adiku, S.T.K., Tenhunen, J.D., 2005. Physiological and morphological responses to water stress in two acacia species from contrasting habitats, Tree Physiology 25, 361-371.

Ozaki, T., Enomoto, S., 2001. Uptake of rare earth elements by *Dryopteris erythrosara* (autumn fern). Riken Review 35, 84-87.

Poujol, M., Anhaeusser, C.R., & Armstrong, R.A., 2002. Episodic granitoid emplacement in the Archean Amalia-Kraaipan terrane, South Africa. Journal of African Earth Sciences 35, 147-161.

Raju, K.K., Raju, A.N., 1999. Biogeochemical investigation in south eastern Andhra Pradesh: the distribution of rare earths, thorium and uranium in plants and soils. Environmental Geology 39, 1102-1106.

Reading, K.A.L., Brooks, R.R., Naidu, S.D., 1987. Biogeochemical prospecting for gold in the Canadian Arctic. Journal of Geochemical Exploration 27, 143-155.

Reimann, C., Filzmoser, P., Garrett, R.G., 2002. Factor analysis applied to regional geochemical data: problems and possibilities. Applied Geochemistry 17, 185-206.

Smith, B.H. and Keele, R.A., 1984. Some observations on the geochemistry of gold mineralization in the weathered zone of Norseman, Western Australia. Journal of Geochemical Exploration 22**,** 1-20.

South African Committee for Stratigraphy (SACS), 1980. Stratigraphy of South Africa. Part 1. (Compiler, L.E. Kent). Lithostratigrphy of the Republic of South Africa, South West Africa/Namibia and the Republic of Bophuthatswana, Transkei and Venda. Handbook, Geological Survey of South Africa, 8, 690p.

Stednick, J.D., Klem, R.B., Riese, W.C., 1987. Temporal variation of metal concentrations in biogechemical samples over the Royal Tiger mine, Colorado, part 1: within year variation. Journal of Geochemical Exploration 28, 75-88.

Tyler, G., 2004. Rare earth elements in soil and plant systems- A review. Plant and Soil: 267, 191-206.

Van Eeden, O.R., de Wet, N.P., Strauss, C.A., 1963. The geology of the area around Schweizer-Reneke. Explanation sheets 2427B (Pudimoe) and 2725A (Schweizer-Reneke). Geological Survey, South Africa, pp76.

Vearncombe, J.R., 1986. Structural veins in a gold-pyrite deposit in banded iron formation, Amalia Greenstone Belt, South Africa. Geological Magazine, 123, 601-604.

Visser, D.J.L., 1989. The geology of the republics of South Africa, Transkei, Bophuthatswana, Venda and Ciskei and the kingdoms of Lesotho and Swaziland. Geological survey, Republic of South Africa, 491pp.

Warren, H.V., Delavault, R.E., (1950b), History of biogeochemical prospecting in British Colombia: Canadian Inst.Mining Metallurgy Trans., 61, 236-242.

White, W.M., 1997. Geochemistry. John-Hopkins University Press, New York, 750pp.

Wood, S.A., 1990. The aqueous geochemistry of the rare-earth elements and yrittium. Chemical Geology 82, 159-186.

Xu, X., Zhu, W., Wang, Z., Witkamp, G.J., 2003. Accumulation of rare earth elements in maize plants (*Zea mays L.*) after applications of mixtures of rare earth elements and lanthanum. Plant and Soil: 252, 267-277.

Zhihui, H., 1987. Influence of the siliceous component in determination of gold in plant materials. Journal of Geochemical Exploration 27, 323-328.

Zimmerman, O.T., Anhaeusser, C.R., 1991. In: C.R. Anhaeusser (editor), The Archean Kraaipan Group volcano-sedimentary rocks and associated granites and gneisses of the southwestern Transvaal, North-Western Cape Province and Bophuthatswana excursion guide book, information circular, Economic Geology Research Unit, University of the Witwatersrand, Johannesburg 244: 26-42.

APPENDIX 1

Raw analytical data for *A. karroo*

Sample ID	Mg	P	S	Ca	K
2.1	2.61	1.73	0.66	19.4	6.45
2.2	4.08	1.30	1.67	31.7	5.98
2.2i	7.90	2.09	0.99	27.8	5.21
2.3	5.32	1.68	1.27	26.0	6.26
2.3i	3.82	2.40	5.94	28.0	7.50
2.4i	7.62	3.47	0.76	24.3	6.23
2.5	3.40	1.78	1.13	17.4	5.11
3.1	3.04	2.05	1.11	13.2	9.88
3.2	4.15	1.15	0.64	13.9	8.61
3.3	4.86	2.03	1.74	23.4	5.29
3.4	5.25	2.46	0.44	24.4	6.52
3.4i	3.99	1.44	1.35	30.1	5.40
3.5i	5.05	1.85	2.50	25.1	4.35
3.6	3.14	1.32	0.85	21.1	4.36
3.7	3.61	1.95	0.37	25.2	6.14
4.1	4.52	2.73	1.70	24.2	6.16
4.3	3.05	1.14	0.24	15.5	7.15
4.3i	3.59	2.62	1.12	19.5	5.83
4.4	4.89	2.55	0.90	22.8	6.10
4.4i	4.02	2.25	0.48	22.2	6.14
4.5	4.17	2.56	0.77	24.3	5.76
4.7	4.32	1.50	1.78	19.7	6.85
5.1	4.45	1.72	0.53	29.3	4.69
5.3	3.82	1.54	0.32	23.1	5.82
5.4	2.77	1.61	0.41	21.1	3.31
5.4i	4.17	1.65	0.37	22.5	4.04
5.5	4.69	1.66	0.64	21.0	5.53
5.6	4.32	1.37	2.08	31.7	4.37
6.2	5.04	1.62	0.73	20.8	4.60
6.3	3.68	1.10	0.48	28.7	3.73
6.4	2.43	1.47	0.41	17.9	5.58
6.5	3.52	1.26	0.43	21.3	4.66
6.6	6.15	2.58	2.35	25.9	8.08
8.2	4.07	1.60	0.94	20.9	4.81
8.3	3.96	1.59	1.04	13.1	6.29
8.3i	4.53	1.88	0.97	17.0	5.37
8.4	2.40	1.08	0.29	16.5	5.30
8.7	2.43	8.58	0.19	19.5	4.86
9.2	2.62	8.08	0.22	13.7	5.36
9.3	3.07	1.24	0.47	18.3	4.60
9.4	5.50	1.58	2.06	28.6	6.54

Sample ID	Mg	P	S	Ca	K
9.7	4.96	1.73	0.57	25.2	6.68
10.3	4.38	2.04	0.84	22.6	7.85
10.3i	4.91	2.04	1.52	25.8	6.52
10.4	6.34	3.00	0.97	25.2	6.95
10.5	5.22	2.24	0.70	29.4	6.71
10.6	6.29	2.55	0.63	39.6	5.26
10.7	5.84	1.95	0.92	26.2	7.19
10.8	3.16	1.66	0.56	32.2	11.7
11.1	4.31	2.60	0.65	29.8	20.0
11.3	4.62	2.27	0.57	30.8	6.77
11.4	4.42	1.11	0.95	34.7	5.97
11.5	2.81	2.36	1.84	14.2	9.89
11.6	4.38	1.69	0.70	27.5	5.98
11.8	2.77	1.43	0.55	28.7	4.73
12.2	3.22	1.43	0.38	21.9	5.36
12.3	2.76	0.74	0.37	21.1	5.58
12.4	2.53	0.99	0.35	16.5	4.80
13.2	2.43	1.02	0.59	18.2	4.77
13.3	3.39	1.39	1.55	10.9	5.93
13.4	2.41	0.80	0.34	21.1	4.14

Sample ID	B	Al	V	Mn	Fe	Co	Ni	Cu	Zn
2.1	309.2	4091.7	7.93	418.0	4310.8	1.46	29.0	44.7	272.6
2.2	426.1	3442.7	6.79	589.9	3341.0	1.42	49.7	53.3	207.3
2.2i	385.8	4196.8	8.35	530.2	4611.2	1.98	72.0	95.4	211.0
2.3	498.3	2529.5	5.12	637.0	2768.2	1.37	47.4	71.9	209.2
2.3i	713.1	4055.4	8.25	784.0	4479.0	1.64	52.4	42.6	533.4
2.4i	708.9	2235.3	5.64	987.9	6943.9	9.68	61.2	36.1	419.6
2.5	706.8	2519.6	5.60	296.2	4419.2	1.96	23.2	63.2	228.7
3.1	344.3	5976.5	15.09	286.1	7475.8	3.19	42.7	18.4	241.6
3.2	263.8	9806.0	19.29	649.8	9687.1	4.50	68.1	82.7	194.2
3.3	613.7	7613.1	16.23	411.9	7952.5	4.21	48.7	67.6	260.7
3.4	357.6	2848.4	5.85	1066.7	3556.0	1.55	49.6	46.7	604.0
3.4i	697.3	6244.3	12.80	765.3	5651.3	2.47	49.4	67.8	236.2
3.5i	609.9	5035.7	10.11	496.6	6385.5	2.12	35.1	98.9	277.6
3.6	414.6	3418.1	7.01	463.6	3821.4	1.34	54.5	43.8	202.4
3.7	437.5	2897.5	6.25	826.9	3446.8	1.45	40.1	29.6	227.0
4.1	739.0	3383.8	9.51	442.5	4711.8	2.86	31.2	78.5	222.5
4.3	303.0	1528.2	3.43	310.4	1818.0	0.89	40.3	25.0	137.2
4.3i	246.9	2145.9	5.27	421.0	3670.7	2.08	61.2	79.4	255.5
4.4	483.6	1799.5	4.26	942.8	2812.2	1.60	88.6	16.5	195.2
4.4i	543.7	2084.2	4.83	991.8	6984.9	2.31	41.0	38.7	417.0
4.5	748.7	3420.6	7.64	973.6	4821.1	2.24	68.9	56.2	467.2
4.7	485.1	4744.2	9.77	324.9	4406.8	1.78	37.7	63.2	193.1
5.1	289.7	2857.0	6.59	541.8	3130.2	1.30	35.9	42.0	179.1
5.3	297.1	4150.7	8.94	535.6	4123.6	1.77	32.2	32.0	193.6
5.4	409.9	4240.7	9.07	406.0	4496.6	1.84	37.9	27.3	259.1
5.4i	258.4	4686.6	12.15	856.4	5876.2	3.31	39.2	38.5	284.2
5.5	382.8	2310.1	5.10	550.7	2679.0	1.03	27.8	30.1	176.5
5.6	361.1	4665.4	10.24	523.5	4760.2	2.00	41.6	49.2	216.6
6.2	342.1	5155.0	11.27	589.0	5919.0	2.52	49.2	77.9	377.9
6.3	389.2	3309.3	7.43	415.9	3710.4	1.55	39.7	41.5	179.8
6.4	365.0	2483.2	5.94	610.9	3253.2	1.10	31.2	29.7	283.9
6.5	187.7	2672.2	6.85	508.9	3624.3	1.75	53.3	40.2	202.3
6.6	360.6	9222.4	20.09	789.3	8782.7	3.32	78.8	170.7	387.5
8.2	243.9	2059.7	4.73	385.6	2540.3	1.11	29.6	60.2	153.0

Sample ID	B	Al	V	Mn	Fe	Co	Ni	Cu	Zn
8.3	396.4	2995.9	6.91	2105.0	3695.0	5.41	102.9	204.0	261.3
8.3i	732.8	4382.0	10.81	2416.4	5362.1	4.28	69.0	132.4	556.9
8.4	417.9	1977.4	7.09	276.1	3652.4	1.72	16.7	26.9	98.1
8.7	252.3	1597.6	4.01	233.0	2039.0	0.97	15.2	20.8	92.1
9.2	197.5	1380.3	3.33	401.1	1729.9	1.21	20.9	17.2	122.2
9.3	325.7	1362.5	3.29	598.0	1832.4	1.71	35.6	53.8	153.2
9.4	243.2	2967.8	6.40	236.0	3522.8	1.50	70.6	72.8	199.7
9.7	344.9	1701.4	3.74	592.5	2050.6	1.25	56.7	28.6	291.4
10.3	409.0	2668.3	5.56	303.7	2750.5	1.69	50.0	70.7	207.7
10.3i	662.6	2356.2	5.09	410.5	2702.2	1.51	38.2	65.5	190.3
10.4	658.1	2710.6	5.79	900.5	3135.8	1.51	52.5	71.8	338.0
10.5	716.6	2619.0	5.57	441.2	2722.9	1.22	56.1	78.9	177.3
10.6	492.9	4772.4	10.88	1016.8	4417.1	1.72	54.5	56.5	280.5
10.7	661.4	2527.4	5.86	732.8	2497.6	1.51	58.3	44.1	237.1
10.8	496.1	5076.5	11.66	792.6	4787.0	2.95	90.3	48.3	217.6
11.1	448.8	5527.9	12.63	1078.7	5243.2	3.66	146.8	96.0	387.9
11.3	300.9	6107.6	13.46	928.5	5238.8	2.37	80.2	43.0	285.3
11.4	463.5	2131.3	5.31	621.6	2079.9	1.01	20.2	59.8	161.7
11.5	298.5	1118.2	2.84	324.9	1529.6	1.32	62.4	80.7	236.1
11.6	317.0	1686.8	4.55	627.2	1909.2	1.08	59.2	45.0	222.8
11.8	218.5	2430.1	6.48	501.6	2444.4	1.12	23.7	43.0	238.3
12.2	251.3	2367.2	6.48	554.8	2388.9	1.27	56.4	41.2	288.0
12.3	166.2	1145.9	3.05	589.5	1314.0	0.85	46.3	29.1	133.3
12.4	167.0	1775.6	4.80	567.2	1811.9	1.08	40.4	39.7	186.7
13.2	159.0	2682.9	11.72	212.3	4853.7	3.08	34.2	38.3	99.0
13.3	143.0	2548.7	6.93	282.6	2657.3	2.26	50.2	33.3	141.9
13.4	146.6	1959.5	5.55	361.2	1976.3	1.25	19.1	27.8	111.8

Sample ID	Sr	Ag	Sb	Te	W	Au	Hg	Pb	As	Se
2.1	1507.9	0.12	0.00	0.06	0.24	0.001	0.03	7.69	0.40	0.42
2.2	1711.9	0.22	0.13	0.15	0.40	0.007	0.21	4.52	0.54	1.62
2.2i	2024.5	0.31	0.17	0.17	1.08	0.009	1.24	9.27	0.72	1.72
2.3	2366.2	0.32	0.17	0.14	0.50	0.008	0.19	6.17	0.50	1.74
2.3i	2138.8	0.16	0.18	0.14	0.33	0.012	0.20	21.20	0.75	2.01
2.4i	1384.5	0.15	0.15	0.12	0.41	0.025	0.18	12.21	2.50	1.84
2.5	666.3	0.13	0.13	0.09	0.30	0.012	0.16	7.99	1.55	1.98
3.1	513.6	0.20	0.14	0.08	0.38	0.012	0.15	11.41	1.44	1.92
3.2	654.7	0.11	0.25	0.07	0.35	0.009	1.80	12.70	1.10	1.52
3.3	1427.7	0.24	0.15	0.18	0.43	0.009	0.23	7.03	0.95	1.91
3.4	1647.4	0.22	0.17	0.12	0.48	0.007	0.17	20.98	0.54	1.73
3.4i	2372.5	0.14	0.19	0.16	0.25	0.008	0.15	6.46	0.72	1.76
3.5i	1583.4	0.17	0.20	0.16	0.30	0.010	0.15	10.62	0.98	1.72
3.6	1112.7	0.12	0.20	0.11	0.26	0.007	0.14	6.38	0.62	1.72
3.7	892.1	0.11	0.24	0.09	0.31	0.006	0.14	8.04	0.47	1.58
4.1	832.4	0.13	0.15	0.09	0.37	0.007	0.14	7.03	0.40	1.82
4.3	1120.8	0.13	0.10	0.07	0.35	0.006	5.84	8.41	0.32	1.57
4.3i	536.8	0.19	0.22	0.09	1.07	0.011	2.12	20.07	0.62	1.87
4.4	847.3	0.19	0.15	0.09	0.59	0.007	0.35	10.63	0.62	2.88
4.4i	1210.6	0.11	0.15	0.09	0.34	0.008	0.22	17.25	0.94	1.68
4.5	1973.0	0.16	0.15	0.16	0.36	0.009	0.18	15.22	0.75	1.74
4.7	495.4	0.16	0.16	0.07	0.34	0.006	1.82	8.93	0.71	1.63
5.1	1356.7	0.13	0.13	0.11	0.30	0.008	0.22	9.34	0.42	1.54
5.3	1782.3	0.10	0.13	0.12	0.28	0.008	0.23	8.12	1.27	1.66
5.4	1229.5	0.11	0.17	0.14	0.28	0.007	0.18	8.57	0.91	1.67
5.4i	643.2	0.19	0.25	0.12	0.43	0.006	0.22	10.36	0.72	1.67
5.5	2026.2	0.12	0.13	0.16	0.29	0.007	0.16	8.14	0.46	1.91
5.6	1368.3	0.15	0.16	0.13	0.31	0.009	0.19	5.83	1.03	1.77
6.2	1547.3	0.20	0.15	0.14	0.39	0.074	0.16	9.35	0.91	1.52
6.3	1434.2	0.23	0.13	0.14	0.47	0.027	0.21	6.45	0.78	1.65

Sample ID	Sr	Ag	Sb	Te	W	Au	Hg	Pb	As	Se
6.4	1280.4	0.11	0.14	0.11	0.28	0.005	0.17	15.15	0.49	1.69
6.5	899.2	0.19	0.37	0.11	0.49	0.007	0.17	9.79	0.76	1.62
6.6	638.1	0.44	0.42	0.12	0.45	0.009	1.18	14.47	1.04	2.29
8.2	861.4	0.19	0.17	0.10	0.47	0.006	0.15	5.69	0.56	1.69
8.3	646.5	0.09	0.14	0.10	0.35	0.007	1.82	15.59	0.53	1.43
8.3i	641.7	0.12	0.14	0.11	0.46	0.008	4.50	13.39	0.96	1.62
8.4	591.7	0.10	0.14	0.07	0.20	0.006	0.29	5.49	0.58	1.49
8.7	1399.1	0.08	0.14	0.10	0.23	0.004	0.19	7.28	0.50	1.52
9.2	530.0	0.10	0.14	0.10	0.32	0.007	0.16	7.49	0.39	1.43
9.3	1026.0	0.19	0.23	0.13	0.47	0.005	0.17	5.10	0.88	1.60
9.4	976.9	0.23	0.16	0.10	0.45	0.003	0.20	8.54	0.88	3.74
9.7	751.4	0.12	0.11	0.07	0.29	0.004	0.24	4.63	0.81	3.13
10.3	1218.4	0.10	0.13	0.07	0.38	0.007	0.63	5.48	0.64	3.35
10.3i	1005.9	0.14	0.11	0.07	0.36	0.008	0.20	5.32	0.66	3.45
10.4	743.6	0.13	0.15	0.05	0.36	0.006	0.27	9.73	1.00	3.39
10.5	1256.6	0.17	0.09	0.07	0.33	0.006	0.23	4.59	1.31	3.33
10.6	1404.1	0.17	0.14	0.09	0.40	0.005	0.22	9.36	1.42	3.53
10.7	1240.5	0.14	0.10	0.06	0.37	0.005	0.17	5.48	1.22	3.29
10.8	1129.6	0.17	0.17	0.07	0.47	0.006	0.97	13.44	1.79	4.51
11.1	1165.8	0.80	0.39	0.18	1.69	0.047	20.32	28.09	3.20	14.65
11.3	1701.9	0.15	0.13	0.10	0.33	0.005	0.30	9.69	1.72	3.46
11.4	1736.6	0.18	0.09	0.10	0.32	0.005	0.17	4.15	2.69	3.27
11.5	646.5	0.10	0.10	0.06	0.41	0.005	0.80	6.62	1.01	3.25
11.6	1448.2	0.11	0.12	0.09	0.39	0.004	0.73	7.32	2.17	3.44
11.8	864.3	0.14	0.12	0.06	0.39	0.007	0.24	10.91	2.27	3.51
12.2	978.1	0.10	0.22	0.07	0.42	0.005	0.63	9.79	2.02	3.04
12.3	922.7	0.06	0.26	0.06	0.43	0.006	0.36	7.17	2.09	3.15
12.4	847.9	0.11	0.15	0.05	0.28	0.004	0.25	7.20	1.33	2.89
13.2	972.4	0.10	0.09	0.06	0.37	0.004	0.16	6.07	1.59	2.99
13.3	298.9	0.12	0.11	0.05	0.37	0.005	1.05	5.94	1.35	3.21
13.4	915.4	0.30	0.14	0.07	0.31	0.005	0.19	7.55	1.48	3.09

Sample ID	Li	Be	Rb	Y89	Zr	Nb	Pd	Cd	In	Sn	Cs
2.1	11.88	0.08	39.9	2.16	0.16	0.83	0.01	0.04	0.00	0.19	0.68
2.2	5.47	0.09	19.6	2.11	2.15	0.33	0.04	0.10	0.05	0.31	0.32
2.2i	9.92	0.10	21.9	1.43	6.84	0.61	0.13	0.30	0.04	1.09	0.95
2.3	6.36	0.07	31.0	1.12	1.40	0.35	0.03	0.12	0.05	0.29	5.81
2.3i	10.18	0.11	39.6	4.04	0.16	0.41	0.01	0.03	0.06	0.36	0.74
2.4i	13.65	0.08	35.7	1.23	0.20	0.29	0.01	0.04	0.07	0.41	0.83
2.5	5.52	0.08	12.4	0.97	0.65	0.28	0.02	0.04	0.07	0.26	0.29
3.1	16.52	0.13	25.9	1.57	0.65	0.36	0.02	0.05	0.08	0.59	0.43
3.2	9.32	0.20	22.9	3.42	0.15	0.19	0.03	0.12	0.08	0.36	0.66
3.3	10.74	0.16	22.6	2.78	0.52	0.45	0.02	0.07	0.09	0.47	0.56
3.4	9.73	0.09	20.3	2.84	0.18	0.27	0.02	0.03	0.08	0.37	0.50
3.4i	10.44	0.16	16.1	2.62	0.27	0.32	0.02	0.13	0.10	0.41	1.08
3.5i	5.79	0.13	22.8	3.88	0.54	0.31	0.02	0.05	0.11	0.44	0.41
3.6	7.17	0.10	15.4	2.71	0.29	0.28	0.01	0.03	0.09	0.26	0.41
3.7	12.16	0.08	28.0	1.30	0.15	0.27	0.01	0.06	0.09	0.29	1.05
4.1	4.34	0.07	19.4	0.97	0.30	0.19	0.02	0.11	0.09	0.24	1.11
4.3	6.39	0.05	16.7	0.63	0.23	0.07	0.04	0.08	0.07	0.24	0.15
4.3i	8.30	0.07	11.0	0.80	2.07	0.27	0.06	0.11	0.09	1.20	1.24
4.4	21.49	0.07	33.8	0.74	0.62	0.26	0.02	0.06	0.09	0.45	5.02
4.4i	12.59	0.07	44.8	1.51	0.17	0.29	0.01	0.03	0.09	0.54	1.72
4.5	8.39	0.10	28.7	4.46	0.12	0.25	0.01	0.03	0.09	0.42	4.23
4.7	4.19	0.11	14.3	1.53	0.17	0.18	0.03	0.08	0.10	0.28	0.56
5.1	4.68	0.08	18.3	1.26	0.10	0.18	0.01	0.03	0.08	0.27	0.66
5.3	6.58	0.09	22.5	2.93	0.10	0.16	0.01	0.03	0.07	0.29	0.62
5.4	11.14	0.10	15.2	1.90	0.12	0.30	0.01	0.04	0.08	0.29	2.21
5.4i	9.33	0.09	21.9	1.58	0.17	0.25	0.02	0.04	0.08	0.36	1.25
5.5	6.65	0.07	24.3	1.03	0.17	0.20	0.02	0.14	0.07	0.28	0.26
5.6	5.59	0.11	38.5	7.08	0.36	0.26	0.02	0.07	0.07	0.33	0.56
6.2	5.19	0.11	22.3	4.25	0.53	0.33	0.02	0.06	0.07	0.47	0.62
6.3	3.88	0.07	14.8	1.56	0.39	0.23	0.03	0.10	0.05	0.32	1.87
6.4	4.55	0.06	26.1	2.50	0.13	0.21	0.01	0.03	0.05	0.26	0.81
6.5	5.46	0.05	26.2	1.30	0.23	0.19	0.02	0.03	0.04	0.33	0.48
6.6	5.74	0.18	14.7	3.89	0.21	0.25	0.03	0.13	0.08	0.58	1.05
8.2	3.88	0.05	63.0	0.92	0.35	0.21	0.02	0.06	0.04	0.28	3.19
8.3	5.92	0.10	41.0	4.11	0.23	0.19	0.04	0.12	0.05	0.20	0.78
8.3i	6.57	0.10	28.5	2.79	0.12	0.14	0.03	0.23	0.05	0.33	0.66
8.4	2.24	0.04	74.2	0.85	0.43	0.13	0.01	0.03	0.04	0.20	15.60
8.7	3.38	0.05	28.0	0.71	0.14	0.10	0.01	0.02	0.04	0.21	1.10
9.2	3.84	0.04	25.2	0.77	0.15	0.11	0.01	0.03	0.04	0.22	0.30
9.3	2.76	0.04	12.4	0.73	0.27	0.16	0.02	0.11	0.05	0.28	1.93
9.4	2.94	0.09	87.8	2.88	1.25	0.48	0.03	0.07	0.08	0.31	2.42

Sample ID	Li	Be	Rb	Y89	Zr	Nb	Pd	Cd	In	Sn	Cs
9.7	4.34	0.06	51.6	0.81	0.15	0.25	0.01	0.03	0.09	0.23	27.34
10.3	3.79	0.08	44.8	33.23	0.08	0.21	0.02	0.08	0.08	0.25	1.51
10.3i	3.88	0.07	98.6	2.42	0.13	0.23	0.02	0.04	0.08	0.35	227.48
10.4	4.18	0.07	27.6	1.82	0.09	0.23	0.03	0.15	0.10	0.29	3.69
10.5	2.93	0.07	18.7	1.12	0.11	0.20	0.03	0.09	0.10	0.28	0.68
10.6	6.07	0.12	9.4	1.85	0.11	0.23	0.04	0.20	0.14	0.36	0.68
10.7	7.82	0.13	36.0	1.19	0.11	0.19	0.03	0.03	0.16	0.27	4.57
10.8	8.62	0.23	27.4	2.13	0.22	0.22	0.04	0.06	0.25	0.33	1.27
11.1	13.94	0.75	33.3	2.29	1.29	0.61	0.34	0.56	0.75	1.46	0.59
11.3	9.29	0.22	33.8	2.26	0.14	0.20	0.03	0.06	0.21	0.40	0.76
11.4	6.11	0.22	16.6	0.93	0.14	0.13	0.03	0.07	0.22	0.27	0.41
11.5	12.27	0.21	54.2	0.52	0.28	0.20	0.03	0.04	0.24	0.22	24.38
11.6	3.03	0.21	66.5	0.84	0.06	0.14	0.03	0.04	0.22	0.21	8.31
11.8	5.10	0.19	20.8	0.98	0.18	0.23	0.02	0.03	0.22	0.32	10.48
12.2	5.54	0.18	42.6	1.23	0.09	0.14	0.03	0.05	0.18	0.28	2.75
12.3	3.62	0.18	27.7	0.99	0.15	0.10	0.03	0.04	0.16	0.15	9.36
12.4	5.03	0.15	17.4	1.04	0.12	0.16	0.02	0.03	0.16	0.23	6.25
13.2	2.22	0.15	25.2	1.05	0.15	0.08	0.02	0.06	0.16	0.23	3.31
13.3	1.65	0.14	42.3	0.99	0.11	0.15	0.03	0.04	0.16	0.24	16.60
13.4	3.15	0.15	46.2	0.88	0.14	0.16	0.02	0.04	0.15	0.23	17.83

Sample ID	Ba	Hf	Ta	Tl	Bi	Th	U	Na	Sc	Ti	Cr	Ga	Ge
2.1	1713.8	0.010	0.003	0.01	0.02	0.65	0.14	1537.4	0.94	171.7	31.2	7.55	0.01
2.2	1003.9	0.074	0.002	0.02	0.02	0.46	0.09	960.8	0.78	82.2	54.2	6.18	0.02
2.2i	1924.5	0.188	0.004	0.02	0.03	0.57	0.18	2069.3	0.96	150.7	100.9	7.56	0.02
2.3	1788.0	0.038	0.002	0.02	0.02	0.39	0.11	946.4	0.59	83.9	50.7	7.50	0.02
2.3i	1387.2	0.012	0.003	0.01	0.03	0.65	0.14	1999.2	0.93	156.7	42.0	8.17	0.02
2.4i	472.8	0.010	0.002	0.02	0.02	0.33	0.40	1590.8	0.59	65.2	38.3	2.31	0.01
2.5	118.6	0.014	0.002	0.01	0.02	0.37	0.09	698.7	0.61	79.0	29.3	0.72	0.02
3.1	482.6	0.016	0.002	0.03	0.02	0.66	0.11	1330.9	1.59	177.7	68.6	4.02	0.02
3.2	695.1	0.010	0.003	0.02	0.03	1.07	0.19	1146.0	2.45	306.4	85.3	4.02	0.03
3.3	1086.9	0.015	0.003	0.02	0.04	0.88	0.22	1436.1	2.07	239.1	91.8	4.94	0.03
3.4	2727.3	0.017	0.002	0.02	0.02	0.48	0.14	1223.0	0.68	91.4	53.8	15.46	0.01
3.4i	969.6	0.011	0.003	0.03	0.03	0.99	0.18	956.0	1.46	185.5	51.9	5.08	0.03
3.5i	400.8	0.015	0.003	0.02	0.03	0.75	0.16	1047.4	1.14	131.2	41.3	2.77	0.02
3.6	1406.9	0.014	0.002	0.01	0.02	0.53	0.11	826.8	0.80	118.0	30.4	6.76	0.02

Sample ID	Ba	Hf	Ta	Tl	Bi	Th	U	Na	Sc	Ti	Cr	Ga	Ge
3.7	971.0	0.009	0.002	0.01	0.02	0.50	0.10	1129.3	0.74	114.2	30.9	5.16	0.01
4.1	384.1	0.009	0.002	0.01	0.03	0.30	0.06	895.6	1.37	82.8	61.7	2.54	0.02
4.3	1088.2	0.012	0.002	0.01	0.01	0.24	0.15	762.0	0.36	58.5	32.1	7.08	0.01
4.3i	272.7	0.060	0.002	0.01	0.03	0.41	0.08	2166.3	0.57	81.1	91.0	1.81	0.02
4.4	471.9	0.014	0.002	0.01	0.04	0.33	0.07	1694.4	0.48	78.9	53.4	3.35	0.02
4.4i	1503.2	0.011	0.002	0.01	0.02	0.42	0.19	1549.1	0.53	119.6	29.3	8.99	0.03
4.5	2317.6	0.016	0.003	0.01	0.02	0.65	0.16	1759.0	0.86	147.4	46.4	13.06	0.03
4.7	81.1	0.006	0.002	0.02	0.03	0.75	0.11	658.9	1.14	142.6	48.5	1.18	0.02
5.1	738.1	0.007	0.002	0.01	0.06	0.55	0.12	925.0	0.75	103.3	34.2	3.31	0.02
5.3	2948.3	0.017	0.003	0.02	0.02	0.84	0.16	1045.0	1.03	159.9	42.4	29.46	0.02
5.4	1336.7	0.010	0.002	0.02	0.03	0.84	0.23	844.1	1.08	181.9	33.3	8.94	0.02
5.4i	494.0	0.008	0.002	0.02	0.03	0.81	0.16	1059.5	1.55	160.7	71.8	3.28	0.02
5.5	716.1	0.007	0.002	0.01	0.01	0.49	0.15	1075.9	0.58	96.2	30.2	4.24	0.01
5.6	381.2	0.016	0.004	0.02	0.03	0.98	0.17	1358.2	1.18	131.4	42.0	2.32	0.02
6.2	1796.8	0.023	0.003	0.04	0.03	1.05	0.17	883.6	1.31	155.0	56.8	9.77	0.02
6.3	695.3	0.014	0.002	0.02	0.02	0.78	0.12	597.1	0.85	115.6	51.7	2.91	0.01
6.4	1729.1	0.013	0.003	0.01	0.03	0.68	0.16	952.1	0.70	107.7	28.2	7.01	0.02
6.5	727.1	0.010	0.003	0.02	0.02	0.62	0.13	743.2	0.82	107.7	51.5	2.51	0.02
6.6	94.5	0.012	0.004	0.04	0.06	1.90	0.30	1115.5	2.32	407.2	57.2	2.47	0.03
8.2	560.3	0.010	0.002	0.01	0.02	0.49	0.12	625.1	0.55	73.7	46.0	3.52	0.02
8.3	125.7	0.009	0.003	0.02	0.03	0.63	0.13	713.4	0.83	131.8	54.2	0.94	0.02
8.3i	347.3	0.008	0.003	0.02	0.04	0.89	0.18	999.6	1.33	186.0	75.0	2.55	0.02
8.4	215.2	0.014	0.002	0.02	0.02	0.40	0.10	622.8	0.72	60.6	29.5	0.87	0.02
8.7	774.4	0.008	0.002	0.01	0.01	0.45	0.10	791.0	0.47	66.9	23.2	2.95	0.01
9.2	529.6	0.007	0.001	0.01	0.01	0.42	0.09	841.6	0.41	56.1	24.4	2.02	0.01
9.3	587.6	0.009	0.002	0.01	0.02	0.43	0.11	486.6	0.35	54.2	38.6	1.65	0.01
9.4	599.1	0.029	0.003	0.03	0.02	0.47	0.11	648.3	0.72	72.7	55.6	2.29	0.03
9.7	841.1	0.007	0.002	0.01	0.02	0.31	0.07	717.9	0.41	68.1	27.9	2.42	0.01
10.3	936.8	0.045	0.013	0.03	0.02	0.51	0.10	913.2	0.63	96.4	33.2	1.62	0.02
10.3i	757.1	0.009	0.003	0.04	0.02	0.49	0.09	1165.8	0.57	82.1	32.9	0.75	0.02
10.4	1045.2	0.009	0.003	0.01	0.02	0.54	0.09	1127.4	0.63	109.0	37.1	1.81	0.02
10.5	586.3	0.006	0.002	0.01	0.02	0.52	0.10	776.9	0.61	84.8	42.7	2.09	0.02
10.6	986.0	0.008	0.002	0.01	0.02	0.85	0.14	1490.2	1.10	174.2	74.8	3.83	0.02
10.7	1557.6	0.008	0.002	0.01	0.02	0.49	0.10	908.6	0.64	97.1	46.8	6.77	0.02
10.8	1083.8	0.010	0.003	0.03	0.02	0.66	0.15	1655.6	1.35	162.0	67.2	5.25	0.04
11.1	833.3	0.034	0.007	0.03	0.04	0.81	0.23	3470.3	1.10	207.2	145.2	6.19	0.01
11.3	867.5	0.008	0.002	0.04	0.03	1.11	0.17	1203.0	1.40	174.5	64.7	3.14	0.03
11.4	604.5	0.007	0.002	0.01	0.02	0.49	0.09	684.8	0.50	62.9	39.7	2.08	0.02
11.5	769.4	0.009	0.002	0.01	0.01	0.27	0.05	940.9	0.30	48.7	33.0	2.19	0.02
11.6	700.0	0.005	0.002	0.01	0.01	0.38	0.07	737.7	0.47	65.4	43.8	2.25	0.03

Sample ID	Ba	Hf	Ta	Tl	Bi	Th	U	Na	Sc	Ti	Cr	Ga	Ge
11.8	613.3	0.008	0.002	0.01	0.02	0.75	0.12	913.8	0.62	94.1	36.3	1.29	0.03
12.2	1810.6	0.010	0.003	0.01	0.02	0.70	0.13	1030.4	0.62	96.0	48.8	2.72	0.03
12.3	777.8	0.007	0.001	0.02	0.02	0.34	0.09	510.9	0.31	39.9	33.0	1.28	0.02
12.4	858.4	0.006	0.002	0.01	0.02	0.64	0.13	801.6	0.46	74.2	28.3	1.14	0.02
13.2	999.0	0.010	0.002	0.01	0.04	0.45	0.10	566.8	1.15	61.9	58.2	1.09	0.03
13.3	247.5	0.006	0.002	0.03	0.03	0.72	0.13	607.3	0.70	84.6	37.5	0.85	0.02
13.4	422.9	0.006	0.002	0.02	0.03	0.87	0.14	677.0	0.54	68.8	32.7	0.71	0.02

Sample ID	La	Ce	Pr	Nd	Sm	Eu	Gd	Tb	Dy	Ho	Er	Tm	Yb	Lu
2.1	5.12	5.29	0.91	3.14	0.59	0.62	0.68	0.10	0.39	0.07	0.19	0.02	0.17	0.03
2.2	4.68	4.06	0.81	2.81	0.50	0.41	0.59	0.09	0.33	0.06	0.14	0.02	0.11	0.02
2.2i	2.50	4.43	0.54	1.88	0.37	0.67	0.40	0.06	0.26	0.05	0.13	0.02	0.12	0.02
2.3	2.52	3.71	0.45	1.55	0.28	0.60	0.33	0.05	0.18	0.04	0.09	0.01	0.08	0.01
2.3i	10.18	6.56	1.59	5.46	0.96	0.66	1.22	0.17	0.59	0.11	0.24	0.03	0.18	0.03
2.4i	3.63	3.53	0.56	1.90	0.34	0.25	0.39	0.06	0.20	0.04	0.09	0.01	0.08	0.01
2.5	1.51	2.68	0.34	1.21	0.24	0.10	0.26	0.04	0.17	0.03	0.08	0.01	0.07	0.01
3.1	2.58	4.65	0.59	2.12	0.42	0.25	0.42	0.07	0.29	0.06	0.14	0.02	0.13	0.02
3.2	8.41	7.74	1.43	4.84	0.77	0.39	0.92	0.13	0.50	0.10	0.26	0.04	0.22	0.04
3.3	5.84	6.14	1.07	3.73	0.67	0.46	0.75	0.11	0.44	0.09	0.21	0.03	0.17	0.03
3.4	6.32	4.18	1.00	3.69	0.70	1.05	0.82	0.12	0.40	0.07	0.16	0.02	0.12	0.02
3.4i	5.89	8.36	1.06	3.62	0.66	0.45	0.73	0.11	0.44	0.09	0.21	0.03	0.17	0.03
3.5i	7.75	7.30	1.37	4.85	0.87	0.33	1.00	0.15	0.59	0.11	0.26	0.03	0.19	0.03
3.6	5.35	4.38	0.92	3.23	0.58	0.57	0.67	0.10	0.40	0.08	0.18	0.02	0.14	0.02
3.7	2.61	4.43	0.52	1.79	0.34	0.41	0.37	0.06	0.23	0.05	0.12	0.02	0.10	0.02
4.1	1.75	2.34	0.33	1.20	0.22	0.19	0.24	0.04	0.15	0.03	0.08	0.01	0.07	0.01
4.3	1.16	1.96	0.24	0.85	0.17	0.42	0.17	0.03	0.11	0.02	0.06	0.01	0.05	0.01
4.3i	1.41	2.74	0.31	1.08	0.21	0.14	0.20	0.04	0.15	0.03	0.07	0.01	0.06	0.01
4.4	1.53	2.46	0.28	0.98	0.19	0.21	0.18	0.03	0.13	0.03	0.06	0.01	0.06	0.01
4.4i	4.80	3.80	0.64	2.11	0.36	0.61	0.40	0.06	0.23	0.04	0.10	0.01	0.09	0.02
4.5	7.55	6.24	1.29	4.53	0.93	1.08	0.99	0.17	0.65	0.12	0.27	0.03	0.19	0.03
4.7	2.98	5.27	0.61	2.11	0.40	0.12	0.38	0.07	0.28	0.05	0.13	0.02	0.11	0.02
5.1	2.46	4.10	0.49	1.71	0.33	0.34	0.32	0.05	0.23	0.04	0.11	0.02	0.09	0.02
5.3	7.87	6.78	1.27	4.34	0.77	1.30	0.75	0.12	0.47	0.09	0.21	0.03	0.17	0.03
5.4	4.31	6.22	0.77	2.62	0.49	0.58	0.46	0.08	0.34	0.07	0.17	0.02	0.15	0.03
5.4i	3.03	5.97	0.64	2.27	0.43	0.29	0.38	0.07	0.30	0.06	0.15	0.02	0.14	0.02
5.5	2.47	3.35	0.43	1.48	0.27	0.33	0.25	0.04	0.18	0.04	0.09	0.01	0.08	0.01
5.6	15.33	11.59	2.62	9.40	1.79	0.65	1.73	0.30	1.15	0.22	0.46	0.06	0.29	0.04
6.2	7.66	8.20	1.37	4.86	0.95	0.90	0.89	0.16	0.65	0.13	0.28	0.04	0.21	0.04

Sample ID	La	Ce	Pr	Nd	Sm	Eu	Gd	Tb	Dy	Ho	Er	Tm	Yb	Lu
6.3	2.96	5.26	0.62	2.15	0.42	0.38	0.37	0.07	0.29	0.06	0.14	0.02	0.12	0.02
6.4	7.79	5.32	1.20	4.19	0.74	0.90	0.70	0.11	0.42	0.08	0.18	0.02	0.14	0.02
6.5	2.23	3.91	0.47	1.71	0.33	0.39	0.29	0.06	0.25	0.05	0.13	0.02	0.12	0.02
6.6	8.14	12.61	1.59	5.46	1.03	0.28	0.92	0.17	0.72	0.14	0.36	0.05	0.30	0.05
8.2	2.02	3.33	0.38	1.31	0.24	0.29	0.22	0.04	0.17	0.03	0.08	0.01	0.07	0.01
8.3	6.91	7.15	1.34	4.76	0.72	0.22	0.71	0.12	0.51	0.11	0.30	0.04	0.22	0.04
8.3i	5.79	8.88	1.11	3.86	0.70	0.30	0.63	0.12	0.50	0.10	0.26	0.04	0.21	0.03
8.4	1.52	2.69	0.33	1.19	0.24	0.16	0.20	0.04	0.18	0.04	0.09	0.01	0.08	0.01
8.7	1.44	2.89	0.31	1.09	0.21	0.38	0.18	0.03	0.15	0.03	0.07	0.01	0.07	0.01
9.2	1.71	3.03	0.34	1.21	0.23	0.30	0.20	0.04	0.16	0.03	0.08	0.01	0.07	0.01
9.3	1.62	2.77	0.31	1.06	0.20	0.31	0.17	0.03	0.13	0.03	0.07	0.01	0.06	0.01
9.4	4.74	4.25	0.95	3.33	0.65	0.42	0.73	0.10	0.40	0.08	0.18	0.02	0.13	0.02
9.7	1.81	2.30	0.31	1.04	0.22	0.43	0.24	0.03	0.14	0.03	0.07	0.01	0.06	0.01
10.3	59.17	7.73	10.20	37.68	7.38	2.82	9.16	1.23	4.59	0.92	2.04	0.24	1.25	0.18
10.3i	3.63	4.04	0.73	2.63	0.59	0.47	0.66	0.10	0.41	0.08	0.18	0.02	0.13	0.02
10.4	3.00	3.75	0.57	2.00	0.43	0.62	0.46	0.07	0.28	0.06	0.13	0.02	0.10	0.02
10.5	2.42	3.55	0.43	1.43	0.30	0.35	0.28	0.04	0.18	0.03	0.08	0.01	0.07	0.01
10.6	3.77	6.49	0.70	2.26	0.48	0.51	0.45	0.07	0.30	0.06	0.15	0.02	0.12	0.02
10.7	3.17	4.20	0.48	1.49	0.31	0.68	0.29	0.04	0.18	0.04	0.08	0.01	0.07	0.01
10.8	4.26	6.49	0.71	2.31	0.47	0.51	0.45	0.08	0.31	0.06	0.16	0.02	0.13	0.02
11.1	5.16	6.29	0.87	2.72	0.53	0.45	0.52	0.08	0.34	0.07	0.15	0.02	0.14	0.02
11.3	5.51	9.00	0.93	2.94	0.59	0.44	0.55	0.09	0.36	0.07	0.17	0.03	0.14	0.02
11.4	1.95	3.32	0.35	1.14	0.23	0.26	0.22	0.04	0.14	0.03	0.07	0.01	0.06	0.01
11.5	1.01	1.72	0.18	0.59	0.13	0.29	0.13	0.02	0.09	0.02	0.04	0.01	0.04	0.01
11.6	1.92	3.10	0.33	1.06	0.22	0.29	0.21	0.03	0.14	0.03	0.07	0.01	0.06	0.01
11.8	2.26	4.43	0.44	1.41	0.29	0.24	0.27	0.05	0.20	0.04	0.10	0.01	0.08	0.01
12.2	3.39	4.99	0.53	1.71	0.36	0.59	0.34	0.05	0.23	0.04	0.11	0.02	0.09	0.02
12.3	2.57	3.17	0.39	1.30	0.26	0.29	0.26	0.04	0.16	0.03	0.07	0.01	0.06	0.01
12.4	3.00	4.40	0.48	1.48	0.30	0.28	0.29	0.05	0.20	0.04	0.10	0.01	0.07	0.01
13.2	1.86	2.95	0.35	1.17	0.27	0.32	0.25	0.04	0.18	0.04	0.09	0.01	0.07	0.01
13.3	2.49	4.46	0.46	1.50	0.31	0.13	0.29	0.05	0.21	0.04	0.10	0.02	0.08	0.01
13.4	2.53	3.99	0.42	1.29	0.26	0.17	0.25	0.04	0.18	0.03	0.08	0.01	0.07	0.01

APPENDIX 2

Raw analytical data for *B. albitrunca*

Sample ID	Mg	P	S	Ca	K
2.1	4.5	2.3	0.5	28.1	6.0
6.5	3.5	1.4	0.3	20.1	5.1
8.2	4.1	2.8	1.4	16.6	4.9
8.3	3.3	1.5	0.3	17.5	5.1
8.3i	3.4	1.5	0.9	18.0	5.5
8.4	2.6	2.1	0.5	9.6	7.0
9.2	2.9	1.2	0.3	15.1	5.4
9.3	2.9	2.1	1.6	12.5	11.4
10.3	5.5	2.2	2.3	23.0	7.7
10.3i	5.2	2.0	1.2	24.8	6.7
10.4	3.9	2.2	1.0	19.6	7.9
10.5	2.1	3.7	0.8	7.9	7.2
10.6	3.0	2.8	1.4	12.2	4.9
10.7	2.6	2.1	1.3	8.8	14.9
11.1	4.4	2.1	1.7	23.4	5.2
11.3	4.3	1.9	1.1	16.6	17.9
11.5	3.2	0.9	0.9	18.3	9.1
11.6	1.5	1.7	0.9	8.2	12.8
11.8	1.5	1.7	1.6	9.5	10.9
12.3	2.5	1.6	1.6	9.0	9.3
12.4	0.7	0.8	0.3	3.6	11.5
13.3	1.2	0.7	0.5	7.7	8.0

Sample ID	B	Al	V	Mn	Fe	Co	Ni	Cu	Zn
2.1	405.7	2695.3	5.68	988.9	4476.1	1.28	78.1	53.0	426.8
6.5	463.3	3042.1	6.84	1068.4	3481.4	1.34	74.7	36.9	297.0
8.2	492.3	5144.4	11.20	525.9	5286.9	2.04	68.7	184.0	387.7
8.3	126.5	1767.9	4.54	517.1	2499.6	1.19	39.0	31.7	234.5
8.3i	218.0	2469.1	5.99	303.2	3028.4	2.06	52.0	53.6	141.2
8.4	216.9	2679.3	7.52	487.6	4101.0	1.79	40.5	76.5	185.1
9.2	194.3	1910.2	4.58	661.3	2439.6	1.47	31.0	33.3	199.7
9.3	366.1	2723.9	6.96	1220.2	5388.4	3.36	117.0	206.9	429.3
10.3	808.1	3591.2	7.26	1670.4	3789.7	4.63	97.0	390.1	272.1
10.3i	1052.0	4801.1	9.94	1564.4	5085.8	4.12	60.4	233.4	455.7
10.4	990.9	3893.7	8.21	1513.2	4194.8	2.91	73.3	267.8	637.1
10.5	247.4	3252.3	6.62	591.4	3357.3	2.85	108.1	217.5	491.3
10.6	412.9	5030.8	12.00	1838.0	5212.6	4.32	123.4	224.1	504.9
10.7	298.4	4489.2	9.85	419.9	3954.9	3.19	74.0	220.0	333.6
11.1	426.7	10166.8	21.79	597.3	8375.2	4.40	55.5	486.9	347.2
11.3	580.1	5011.0	11.96	2417.5	4806.9	4.93	227.2	200.6	386.5
11.5	745.4	3935.9	9.39	1364.8	3653.1	4.15	72.7	333.2	337.3
11.6	328.2	2279.2	5.73	419.9	2276.8	2.13	43.7	130.9	280.1
11.8	185.8	2119.2	5.69	395.0	2256.6	3.14	58.1	193.0	374.5
12.3	173.8	1550.0	4.00	313.7	1743.1	2.44	75.3	175.9	251.4
12.4	72.0	891.1	2.45	253.3	1009.8	1.04	31.4	63.0	177.1
13.3	127.6	3159.0	13.14	217.1	5467.2	3.53	63.1	113.9	147.0

Sample ID	La	Ce	Pr	Nd	Sm	Eu	Gd	Tb	Dy	Ho	Er	Tm	Yb	Lu
2.1	7.47	5.44	1.39	4.86	0.87	0.73	1.04	0.15	0.52	0.10	0.21	0.03	0.16	0.03
6.5	5.49	4.21	0.76	2.54	0.44	0.68	0.43	0.07	0.30	0.06	0.15	0.02	0.12	0.02
8.2	5.09	7.91	0.93	3.14	0.57	0.16	0.51	0.10	0.40	0.08	0.20	0.03	0.17	0.03
8.3	1.73	3.10	0.34	1.19	0.23	0.22	0.20	0.04	0.15	0.03	0.08	0.01	0.07	0.01
8.3i	10.24	8.23	2.50	9.72	2.06	0.86	1.93	0.39	1.68	0.34	0.78	0.10	0.48	0.07
8.4	1.96	3.29	0.39	1.37	0.27	0.22	0.23	0.04	0.19	0.04	0.10	0.02	0.09	0.01
9.2	2.17	3.72	0.43	1.54	0.29	0.48	0.26	0.05	0.20	0.04	0.11	0.02	0.09	0.02
9.3	2.09	3.55	0.46	1.58	0.32	0.14	0.34	0.05	0.22	0.04	0.12	0.02	0.10	0.02
10.3	4.81	6.32	0.89	3.03	0.59	0.25	0.67	0.09	0.37	0.07	0.18	0.03	0.15	0.02
10.3i	5.26	7.40	1.10	3.77	0.76	0.28	0.85	0.12	0.49	0.10	0.24	0.03	0.20	0.03
10.4	5.79	6.93	1.11	3.77	0.72	0.23	0.78	0.12	0.47	0.10	0.23	0.03	0.19	0.03
10.5	2.33	3.93	0.46	1.50	0.31	0.14	0.30	0.05	0.21	0.04	0.11	0.02	0.10	0.02
10.6	3.82	6.91	0.75	2.46	0.50	0.19	0.48	0.08	0.35	0.07	0.18	0.03	0.15	0.02
10.7	2.96	5.34	0.57	1.83	0.38	0.13	0.36	0.06	0.27	0.05	0.14	0.02	0.11	0.02
11.1	6.06	9.71	1.03	3.26	0.64	0.20	0.61	0.11	0.44	0.09	0.22	0.03	0.18	0.03
11.3	6.91	11.29	1.18	3.78	0.74	0.36	0.71	0.12	0.49	0.10	0.24	0.04	0.20	0.03
11.5	6.68	8.46	1.04	3.28	0.61	0.19	0.59	0.10	0.39	0.08	0.19	0.03	0.15	0.02
11.6	2.16	3.83	0.40	1.26	0.26	0.09	0.25	0.04	0.19	0.04	0.10	0.02	0.08	0.01
11.8	2.11	4.05	0.41	1.34	0.28	0.07	0.26	0.05	0.20	0.04	0.10	0.02	0.09	0.01
12.3	2.19	3.27	0.38	1.22	0.24	0.08	0.23	0.04	0.17	0.04	0.09	0.01	0.07	0.01
12.4	2.39	2.58	0.36	1.11	0.20	0.06	0.19	0.03	0.12	0.02	0.06	0.01	0.04	0.01
13.3	2.91	5.09	0.55	1.77	0.37	0.11	0.34	0.06	0.27	0.05	0.14	0.02	0.12	0.02

Sample ID	Sr	Ag	Sb	Te	W	Au	Hg	Pb	As	Se
2.1	2322.5	0.15	0.17	0.14	0.37	0.006	0.21	22.06	0.51	1.68
6.5	724.3	0.12	0.14	0.09	1.39	0.004	0.14	10.68	0.49	1.65
8.2	333.4	0.25	0.14	0.08	0.56	0.006	3.63	20.58	0.68	1.51
8.3	548.6	0.15	0.12	0.09	0.39	0.005	0.22	5.86	0.42	1.68
8.3i	791.8	0.15	0.15	0.10	0.45	0.006	0.32	6.73	0.42	1.66
8.4	304.9	0.11	0.12	0.07	0.42	0.003	2.25	7.55	0.46	1.43
9.2	797.3	0.11	0.13	0.09	0.31	0.005	0.17	5.68	0.47	1.48
9.3	387.1	0.12	0.14	0.05	0.51	0.004	1.80	8.57	1.01	3.72
10.3	1081.3	0.10	0.10	0.07	0.35	0.005	0.69	12.06	1.19	3.64
10.3i	901.0	0.24	0.11	0.07	0.23	0.008	1.63	17.70	1.19	3.67
10.4	587.8	0.21	0.10	0.06	0.57	0.007	1.30	12.58	1.91	3.26
10.5	318.7	0.17	0.11	0.08	1.12	0.004	1.91	18.49	0.90	3.03
10.6	397.7	0.18	0.13	0.06	1.00	0.004	2.33	11.98	1.48	3.16
10.7	416.9	0.14	0.14	0.05	0.64	0.003	0.59	8.11	1.34	3.06
11.1	746.6	0.28	0.23	0.07	0.37	0.004	2.28	15.79	3.34	3.46
11.3	880.1	0.13	0.24	0.10	0.95	0.005	0.56	16.92	1.99	4.79
11.5	847.3	0.20	0.14	0.09	0.44	0.007	2.65	15.83	1.77	3.45
11.6	381.7	0.10	0.15	0.06	0.64	0.005	0.92	6.35	1.00	3.23
11.8	111.3	0.10	0.13	0.06	0.71	0.007	1.25	12.78	1.34	3.15
12.3	422.8	0.14	0.13	0.05	0.65	0.005	0.97	9.24	1.40	3.00
12.4	178.2	0.55	0.12	0.03	0.57	0.005	1.88	13.92	0.60	2.83
13.3	330.1	0.12	0.11	0.05	0.52	0.010	1.68	7.19	1.34	2.82

Sample ID	Li	Be	Rb	Y	Zr	Nb	Pd	Cd	In	Sn	Cs
2.1	17.15	0.08	43.4	3.20	0.42	0.59	0.01	0.04	0.03	0.44	1.44
6.5	9.50	0.07	56.0	1.92	0.15	0.27	0.01	0.05	0.05	0.24	3.13
8.2	3.81	0.10	14.1	2.04	0.15	0.27	0.02	0.10	0.05	0.40	0.68
8.3	2.76	0.04	63.9	0.78	0.13	0.15	0.01	0.03	0.04	0.24	5.40
8.3i	3.18	0.06	60.9	10.56	0.94	0.19	0.02	0.07	0.04	0.35	1.26
8.4	2.76	0.05	35.6	0.99	0.13	0.19	0.04	0.15	0.05	0.26	3.35
9.2	2.32	0.05	28.4	1.08	0.08	0.11	0.01	0.03	0.04	0.22	0.40
9.3	2.68	0.08	61.1	1.21	0.99	1.00	0.09	0.54	0.07	0.28	0.81
10.3	3.99	0.11	27.4	2.12	0.18	0.29	0.05	0.33	0.10	0.27	1.75
10.3i	7.26	0.12	15.2	2.68	0.12	0.21	0.04	0.16	0.10	0.27	1.35
10.4	9.04	0.10	9.2	2.95	0.16	0.31	0.04	0.29	0.10	0.29	1.34
10.5	4.00	0.10	9.1	1.17	1.84	0.54	0.05	0.16	0.13	0.44	0.53
10.6	7.66	0.13	10.0	2.07	2.25	0.57	0.05	0.16	0.16	0.48	1.40
10.7	9.81	0.15	46.9	1.67	0.79	0.52	0.04	0.11	0.19	0.31	0.78
11.1	11.42	0.27	14.5	2.73	0.30	0.35	0.04	0.15	0.21	0.45	2.79

Sample ID	Li	Be	Rb	Y	Zr	Nb	Pd	Cd	In	Sn	Cs
11.3	6.02	0.35	46.1	3.15	0.96	0.55	0.10	0.43	0.38	0.52	5.24
11.5	5.57	0.23	21.8	2.74	0.40	0.28	0.05	0.10	0.24	0.35	1.03
11.6	6.06	0.21	48.2	1.08	1.09	0.42	0.06	0.10	0.24	0.28	5.36
11.8	1.58	0.16	20.1	1.05	0.41	0.30	0.04	0.13	0.22	0.35	1.84
12.3	1.76	0.17	19.2	0.97	1.58	0.27	0.07	0.21	0.17	0.30	0.91
12.4	1.84	0.14	19.4	0.68	0.33	0.15	0.08	0.71	0.17	0.36	0.22
13.3	2.62	0.13	23.0	1.46	0.14	0.12	0.04	0.08	0.16	0.27	0.94

Sample ID	Ba	Hf	Ta	Tl	Bi	Th	U	Na	Sc	Ti	Cr	Ga	Ge
2.1	1743.5	0.02	0.004	0.012	0.03	0.47	0.13	2737.0	0.65	119.3	33.9	5.49	0.02
6.5	1484.9	0.01	0.002	0.009	0.02	0.61	0.11	1240.8	0.89	143.0	31.0	8.94	0.02
8.2	71.6	0.01	0.002	0.020	0.03	1.05	0.17	739.7	1.33	209.9	55.5	1.41	0.02
8.3	380.6	0.01	0.002	0.011	0.02	0.46	0.09	659.4	0.53	62.1	40.2	1.56	0.01
8.3i	504.9	0.04	0.005	0.035	0.03	0.58	0.12	613.6	0.67	70.6	46.4	2.49	0.01
8.4	348.6	0.01	0.002	0.009	0.02	0.50	0.09	629.7	0.89	102.3	46.8	1.93	0.02
9.2	916.3	0.01	0.002	0.008	0.02	0.54	0.12	840.8	0.54	83.3	34.2	3.61	0.02
9.3	141.4	0.03	0.004	0.018	0.02	0.40	0.09	694.0	0.70	127.0	54.5	0.82	0.03
10.3	229.0	0.01	0.004	0.020	0.04	0.64	0.14	901.2	0.86	151.2	67.6	0.94	0.02
10.3i	221.2	0.01	0.004	0.017	0.04	0.76	0.17	1033.7	1.19	177.6	75.6	1.23	0.03
10.4	124.3	0.01	0.002	0.014	0.04	0.67	0.14	854.9	1.01	160.1	67.0	0.99	0.03
10.5	153.0	0.05	0.002	0.007	0.02	0.50	0.09	764.0	0.74	172.2	89.5	0.95	0.03
10.6	195.6	0.05	0.002	0.010	0.02	0.75	0.14	937.5	1.34	218.1	103.8	1.53	0.02
10.7	116.3	0.01	0.002	0.007	0.01	0.65	0.12	1056.0	1.10	221.1	71.5	1.29	0.03
11.1	133.2	0.01	0.003	0.029	0.05	1.34	0.20	1330.0	2.35	257.0	82.0	2.49	0.04
11.3	546.6	0.02	0.003	0.014	0.30	1.01	0.18	1692.4	1.23	207.1	94.6	2.79	0.04
11.5	153.4	0.01	0.002	0.014	0.03	0.86	0.17	1050.1	1.00	156.9	63.2	1.13	0.02
11.6	106.5	0.03	0.003	0.008	0.01	0.56	0.09	767.9	0.58	136.0	51.7	0.71	0.04
11.8	33.9	0.01	0.002	0.007	0.02	0.58	0.10	777.1	0.57	128.5	52.9	0.67	0.03
12.3	82.7	0.06	0.002	0.009	0.02	0.44	0.09	605.5	0.37	76.9	46.6	0.52	0.03
12.4	83.1	0.01	0.002	0.004	0.01	0.50	0.06	438.0	0.24	52.0	36.2	0.31	0.01
13.3	83.4	0.01	0.002	0.010	0.02	0.68	0.18	511.3	1.23	136.3	53.4	0.97	0.03

APPENDIX 3

Histograms for *A. karroo* and *B. albitrunca*

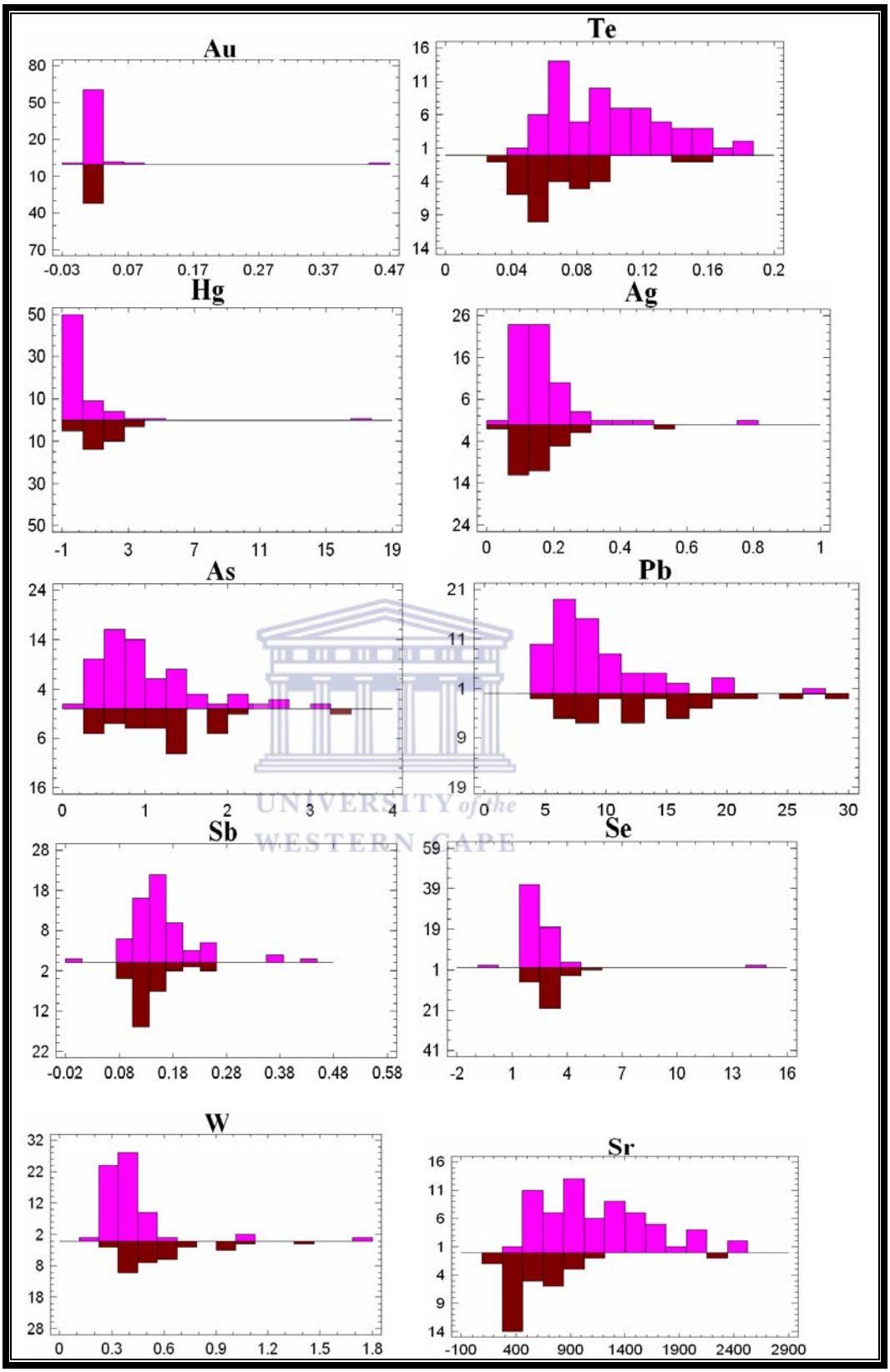

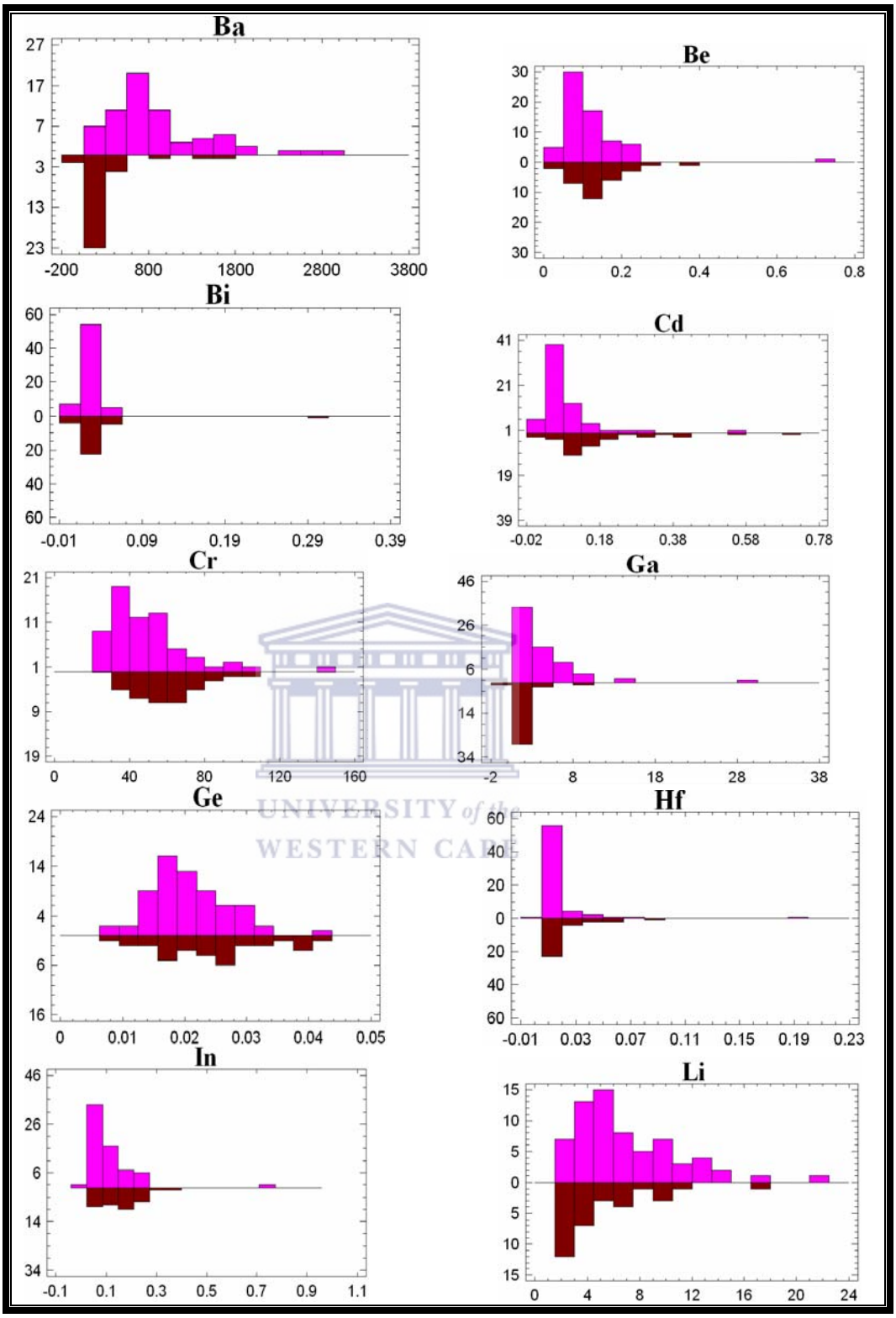

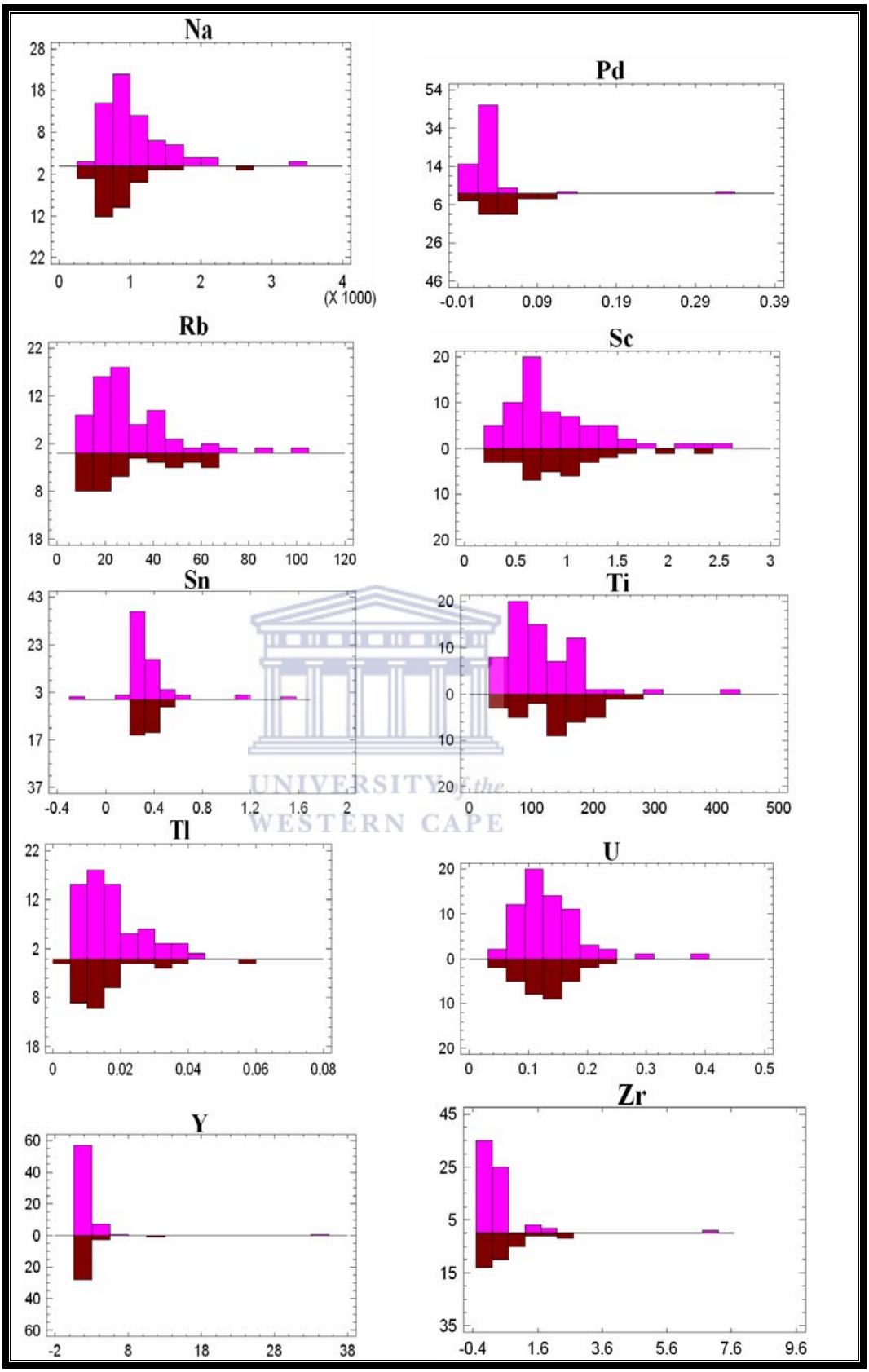

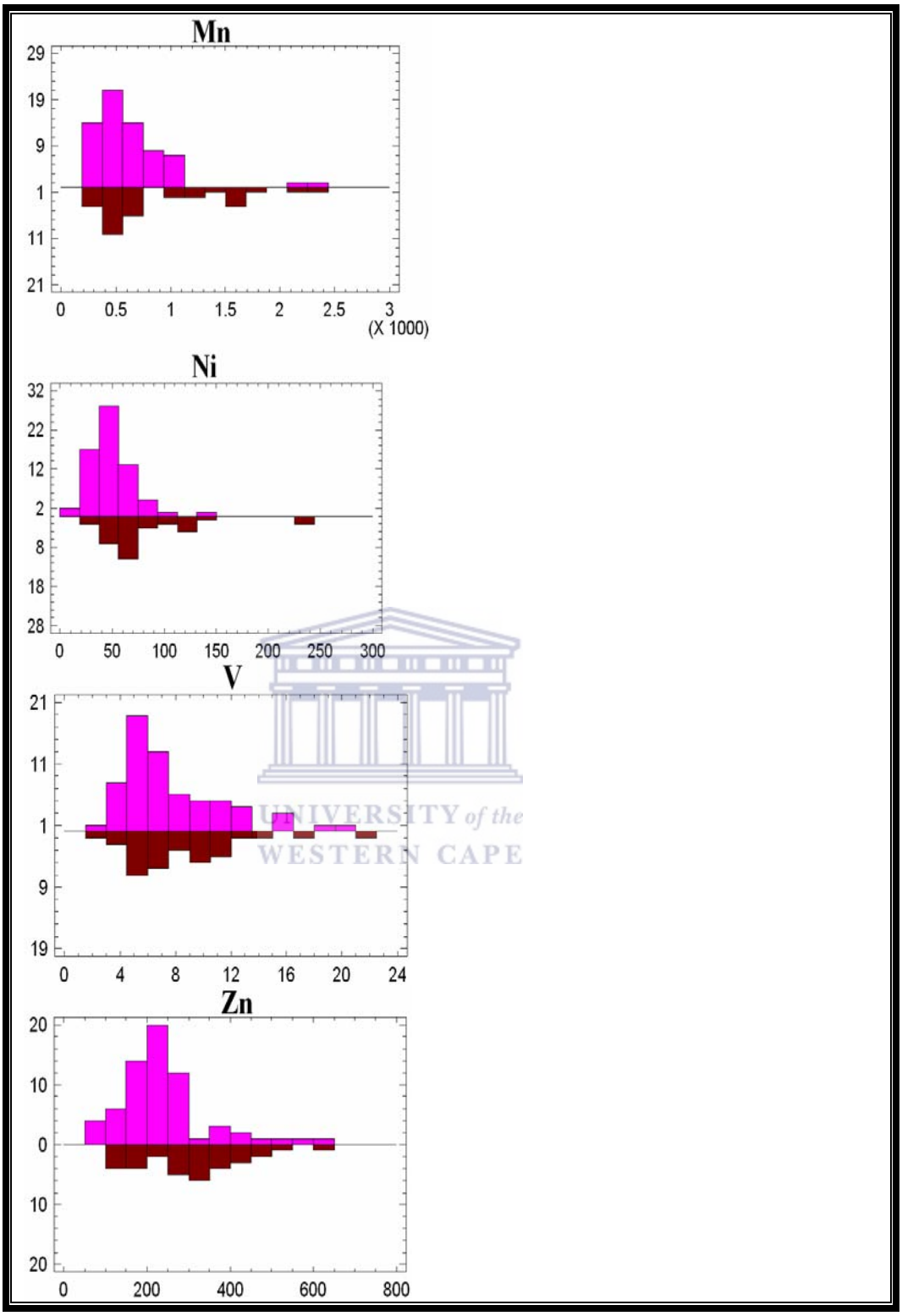

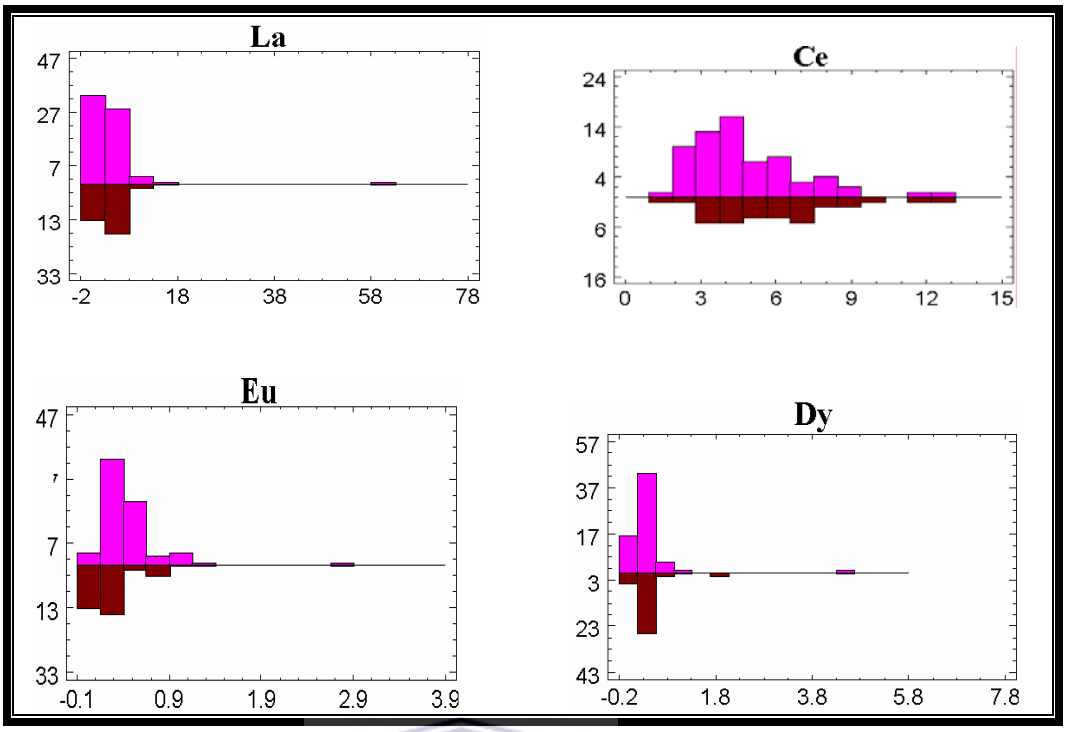

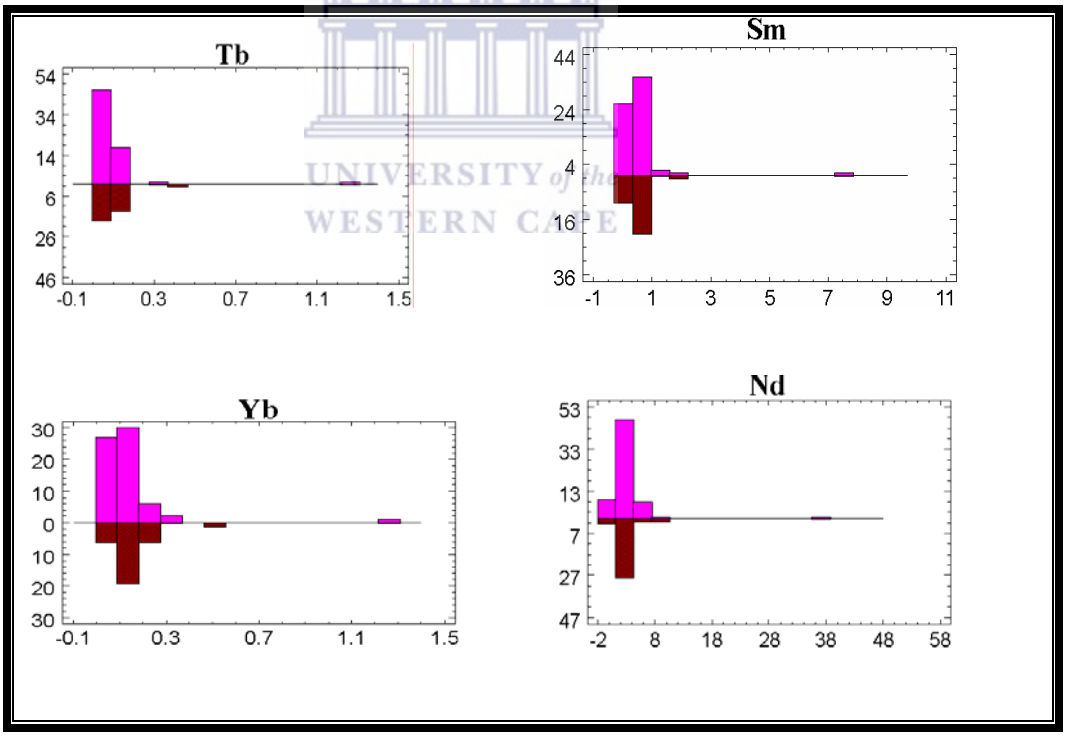

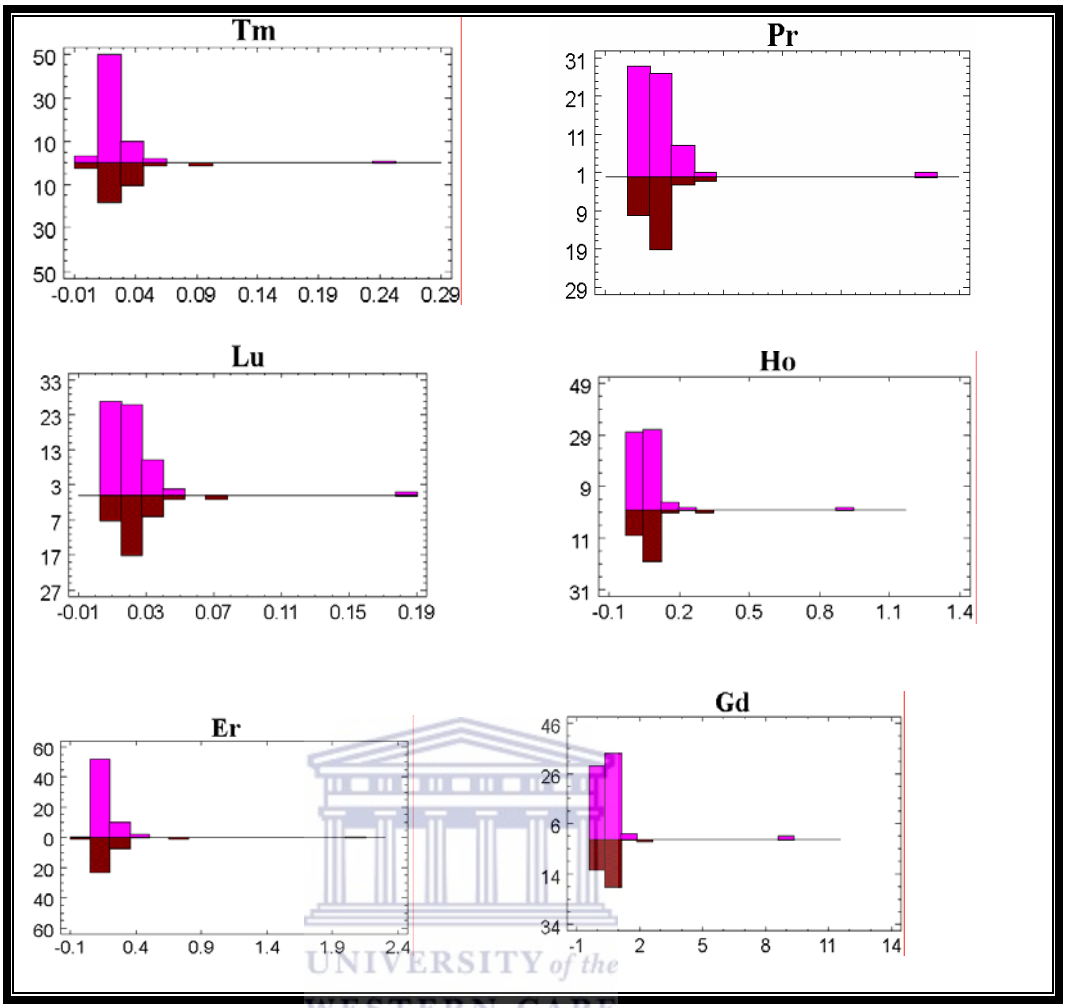

APPENDIX 4

Correlation matrices for *A. karroo* and *B. albitrunca*

Analysis of Macronutrients

Plant: *Acacia karroo*

	Mg	P	S	Ca	K
Mg	1.00000	0.63887	0.36030	0.48976	0.08131
P	0.63887	1.00000	0.28809	0.27547	0.36026
S	0.36030	0.28809	1.00000	0.12055	0.08614
Ca	0.48976	0.27547	0.12055	1.00000	0.08685
K	0.08131	0.36026	0.08614	0.08685	1.00000

Plant: *Boscia albitrunca*

	Mg	P	S	Ca	K
Mg	1.00000	0.37002	0.35368	0.85940	-0.19305
P	0.37002	1.00000	0.46912	0.14728	0.11784
S	0.35368	0.46912	1.00000	0.12873	0.24648
Ca	0.85940	0.14728	0.12873	1.00000	-0.37154
K	-0.19305	0.11784	0.24648	-0.37154	1.00000

Analysis of Element Group rare earth elements

Plant: *A. karroo*

	La	Ce	Pr	Nd	Sm	Eu	Gd
La	1.00000	0.43827	0.99847	0.99768	0.99564	0.85057	0.99260
Ce	0.43827	1.00000	0.44592	0.42929	0.41190	0.30548	0.35996
Pr	0.99847	0.44592	1.00000	0.99968	0.99799	0.83751	0.99417
Nd	0.99768	0.42929	0.99968	1.00000	0.99872	0.83695	0.99561
Sm	0.99564	0.41190	0.99799	0.99872	1.00000	0.84094	0.99731
Eu	0.85057	0.30548	0.83751	0.83695	0.84094	1.00000	0.84026
Gd	0.99260	0.35996	0.99417	0.99561	0.99731	0.84026	1.00000
Tb	0.99541	0.41500	0.99794	0.99875	0.99966	0.83871	0.99713
Dy	0.99386	0.42905	0.99756	0.99827	0.99927	0.83280	0.99529
Ho	0.99293	0.42378	0.99724	0.99808	0.99881	0.82684	0.99529
Er	0.99075	0.43593	0.99613	0.99677	0.99669	0.81951	0.99288
Tm	0.98643	0.46797	0.99307	0.99306	0.99174	0.80892	0.98636
Yb	0.98399	0.48375	0.99091	0.99057	0.98863	0.81257	0.98310
Lu	0.97770	0.51452	0.98508	0.98415	0.98085	0.81304	0.97332

	Tb	Dy	Ho	Er	Tm	Yb	Lu
La	0.99541	0.99386	0.99293	0.99075	0.98643	0.98399	0.97770
Ce	0.41500	0.42905	0.42378	0.43593	0.46797	0.48375	0.51452
Pr	0.99794	0.99756	0.99724	0.99613	0.99307	0.99091	0.98508
Nd	0.99875	0.99827	0.99808	0.99677	0.99306	0.99057	0.98415
Sm	0.99966	0.99927	0.99881	0.99669	0.99174	0.98863	0.98085
Eu	0.83871	0.83280	0.82684	0.81951	0.80892	0.81257	0.81304
Gd	0.99713	0.99529	0.99529	0.99288	0.98636	0.98310	0.97332
Tb	1.00000	0.99950	0.99885	0.99667	0.99174	0.98891	0.98132
Dy	0.99950	1.00000	0.99964	0.99822	0.99441	0.99170	0.98500
Ho	0.99885	0.99964	1.00000	0.99923	0.99606	0.99303	0.98649
Er	0.99667	0.99822	0.99923	1.00000	0.99855	0.99633	0.99114
Tm	0.99174	0.99441	0.99606	0.99855	1.00000	0.99873	0.99581
Yb	0.98891	0.99170	0.99303	0.99633	0.99873	1.00000	0.99835
Lu	0.98132	0.98500	0.98649	0.99114	0.99581	0.99835	1.00000

B. albitrunca

	La	Ce	Pr	Nd	Sm	Eu	Gd
La	1.00000	0.78765	0.94789	0.90760	0.87687	0.63058	0.88587
Ce	0.78765	1.00000	0.70475	0.62361	0.60936	0.19162	0.60458
Pr	0.94789	0.70475	1.00000	0.99215	0.98147	0.68601	0.98263
Nd	0.90760	0.62361	0.99215	1.00000	0.99511	0.72052	0.99087
Sm	0.87687	0.60936	0.98147	0.99511	1.00000	0.69134	0.98671
Eu	0.63058	0.19162	0.68601	0.72052	0.69134	1.00000	0.70214
Gd	0.88587	0.60458	0.98263	0.99087	0.98671	0.70214	1.00000
Tb	0.85105	0.56998	0.96624	0.98681	0.99634	0.69514	0.97436
Dy	0.82528	0.56181	0.94962	0.97354	0.98942	0.66870	0.95750
Ho	0.81688	0.56629	0.94438	0.96862	0.98637	0.65788	0.95220
Er	0.81689	0.58803	0.94368	0.96548	0.98432	0.63917	0.94970
Tm	0.83063	0.66238	0.94484	0.95666	0.97492	0.59848	0.93971
Yb	0.85352	0.69832	0.95884	0.96432	0.97669	0.61213	0.95325
Lu	0.85696	0.71167	0.95566	0.95905	0.97002	0.62115	0.94518

	Tb	Dy	Ho	Er	Tm	Yb	Lu
La	0.85105	0.82528	0.81688	0.81689	0.83063	0.85352	0.85696
Ce	0.56998	0.56181	0.56629	0.58803	0.66238	0.69832	0.71167
Pr	0.96624	0.94962	0.94438	0.94368	0.94484	0.95884	0.95566
Nd	0.98681	0.97354	0.96862	0.96548	0.95666	0.96432	0.95905
Sm	0.99634	0.98942	0.98637	0.98432	0.97492	0.97669	0.97002
Eu	0.69514	0.66870	0.65788	0.63917	0.59848	0.61213	0.62115
Gd	0.97436	0.95750	0.95220	0.94970	0.93971	0.95325	0.94518
Tb	1.00000	0.99697	0.99426	0.99087	0.97707	0.97177	0.96516
Dy	0.99697	1.00000	0.99933	0.99734	0.98503	0.97475	0.96829
Ho	0.99426	0.99933	1.00000	0.99904	0.98869	0.97774	0.97150
Er	0.99087	0.99734	0.99904	1.00000	0.99382	0.98416	0.97845
Tm	0.97707	0.98503	0.98869	0.99382	1.00000	0.99479	0.99173
Yb	0.97177	0.97475	0.97774	0.98416	0.99479	1.00000	0.99837
Lu	0.96516	0.96829	0.97150	0.97845	0.99173	0.99837	1.00000

Analysis of Element Group micronutrients

Plant: *A. karroo*

	B	Al	V	Mn	Fe	Co	Ni	Cu	Zn
B	1.00000	0.16807	0.10621	0.34897	0.29466	0.29415	0.14603	0.25296	0.45655
Al	0.16807	1.00000	0.96208	0.16065	0.85322	0.40876	0.34540	0.40149	0.28367
V	0.10621	0.96208	1.00000	0.14912	0.85949	0.45757	0.31520	0.36353	0.24032
Mn	0.34897	0.16065	0.14912	1.00000	0.21397	0.45348	0.52073	0.50950	0.62305
Fe	0.29466	0.85322	0.85949	0.21397	1.00000	0.65845	0.27020	0.33933	0.42045
Co	0.29415	0.40876	0.45757	0.45348	0.65845	1.00000	0.40223	0.37526	0.36852
Ni	0.14603	0.34540	0.31520	0.52073	0.27020	0.40223	1.00000	0.50542	0.39124
Cu	0.25296	0.40149	0.36353	0.50950	0.33933	0.37526	0.50542	1.00000	0.30390
Zn	0.45655	0.28367	0.24032	0.62305	0.42045	0.36852	0.39124	0.30390	1.00000

	B	Al	V	Mn	Fe	Co	Ni	Cu	Zn
B	1.00000	0.32202	0.12019	0.73095	0.28049	0.45610	0.22811	0.44561	0.45712
Al	0.32202	1.00000	0.92857	0.29694	0.89192	0.56944	-0.00444	0.67789	0.25565
V	0.12019	0.92857	1.00000	0.14381	0.89793	0.57046	-0.03798	0.57309	0.08139
Mn	0.73095	0.29694	0.14381	1.00000	0.31042	0.63622	0.46207	0.35313	0.51697
Fe	0.28049	0.89192	0.89793	0.31042	1.00000	0.53000	0.01532	0.52870	0.26238
Co	0.45610	0.56944	0.57046	0.63622	0.53000	1.00000	0.33050	0.69713	0.28718
Ni	0.22811	-0.00444	-0.03798	0.46207	0.01532	0.33050	1.00000	0.09962	0.30707
Cu	0.44561	0.67789	0.57309	0.35313	0.52870	0.69713	0.09962	1.00000	0.42144
Zn	0.45712	0.25565	0.08139	0.51697	0.26238	0.28718	0.30707	0.42144	1.00000

Analysis of Element Group trace elements

Plant: *A.karroo*

	Sb	Te	Cs	Ba	Hf	Ta	W	Au	Hg	Tl	Pb	Bi
Li	0.11728	0.22891	-0.13489	0.18009	0.11724	0.05048	0.30103	0.06815	0.21215	0.00444	0.43019	0.17388
Be	0.39327	0.17236	-0.05765	-0.03010	0.00994	0.33264	0.62162	0.04864	0.79500	0.29131	0.45191	0.30279
Rb	0.18204	-0.25988	0.56315	-0.08652	-0.07513	0.10452	-0.06752	-0.09078	-0.02308	0.13645	-0.12026	-0.22905
Sr	-0.14724	0.62960	-0.09707	0.58870	0.28303	0.08779	-0.01796	-0.08639	-0.08754	0.04759	0.02169	-0.04796
Y	0.00052	0.02346	-0.02625	0.06388	0.14079	0.89432	-0.03835	-0.02063	-0.00086	0.36883	-0.01410	0.06556
Zr	0.10195	0.35776	-0.06282	0.14268	0.97029	0.09148	0.57879	0.01331	0.14125	0.04533	0.08155	0.13020
Nb	0.04885	0.41516	-0.06300	0.24760	0.44985	0.24321	0.41828	0.13544	0.25336	0.16670	0.28732	0.17059
Pd	0.41699	0.31546	-0.05117	-0.01231	0.40784	0.38354	0.89466	0.06187	0.90672	0.18298	0.49822	0.28408
Ag	0.51193	0.44030	-0.06654	-0.03900	0.28981	0.31602	0.75369	0.35108	0.68165	0.37209	0.42422	0.44756
Cd	0.39200	0.39765	-0.10373	-0.06850	0.42441	0.37576	0.79290	0.09031	0.80322	0.19501	0.41394	0.33750
In	0.29292	0.03272	-0.00372	-0.04804	-0.05748	0.25977	0.60381	0.01430	0.76331	0.14716	0.38874	0.16261
Sn	0.50494	0.44940	-0.04293	0.00421	0.55021	0.27956	0.87521	0.10365	0.61053	0.28153	0.60904	0.43265
Sb	1.00000	0.32056	-0.13392	-0.12902	0.08362	0.22545	0.47224	-0.02259	0.39973	0.34059	0.45110	0.41142
Te	0.32056	1.00000	-0.19736	0.24570	0.35128	0.13920	0.32416	0.01699	0.23466	0.21401	0.28035	0.29583
Cs	-0.13392	-0.19736	1.00000	-0.06002	-0.06361	-0.00317	-0.04861	-0.03733	-0.04866	0.26059	-0.16461	-0.09177
Ba	-0.12902	0.24570	-0.06002	1.00000	0.23557	0.07576	0.00397	-0.03043	-0.07490	-0.04999	0.16812	-0.11930
Hf	0.08362	0.35128	-0.06361	0.23557	1.00000	0.25970	0.53802	-0.01024	0.11620	0.09894	0.07948	0.11955
Ta	0.22545	0.13920	-0.00317	0.07576	0.25970	1.00000	0.32009	0.01975	0.37428	0.47664	0.22798	0.22448
W	0.47224	0.32416	-0.04861	0.00397	0.53802	0.32009	1.00000	0.11742	0.75141	0.16211	0.54999	0.31793
Au	-0.02259	0.01699	-0.03733	-0.03043	-0.01024	0.01975	0.11742	1.00000	0.04562	0.05444	-0.01471	0.09402
Hg	0.39973	0.23466	-0.04866	-0.07490	0.11620	0.37428	0.75141	0.04562	1.00000	0.14774	0.54862	0.27011
Tl	0.34059	0.21401	0.26059	-0.04999	0.09894	0.47664	0.16211	0.05444	0.14774	1.00000	0.13999	0.44933
Pb	0.45110	0.28035	-0.16461	0.16812	0.07948	0.22798	0.54999	-0.01471	0.54862	0.13999	1.00000	0.34218
Bi	0.41142	0.29583	-0.09177	-0.11930	0.11955	0.22448	0.31793	0.09402	0.27011	0.44933	0.34218	1.00000
Th	0.42542	0.28251	-0.10690	-0.02318	-0.06082	0.21195	0.00844	-0.00644	0.09840	0.65513	0.21917	0.60341
U	0.35501	0.45418	-0.16680	0.10518	0.05801	0.18885	0.15199	-0.02208	0.23022	0.37486	0.39326	0.40727
Na	0.29248	0.38543	-0.02867	0.21413	0.36756	0.33548	0.72091	0.14766	0.58171	0.14636	0.71132	0.30276
Sc	0.35238	0.29876	-0.15294	-0.05983	0.01324	0.17778	0.03922	0.07244	0.08648	0.57325	0.20662	0.61889
Ti	0.45982	0.34196	-0.14063	0.05532	0.04710	0.27519	0.13972	0.04660	0.21351	0.56166	0.37550	0.61593
Cr	0.43063	0.39387	-0.14887	-0.00272	0.42643	0.27517	0.78867	0.10341	0.60858	0.37893	0.49940	0.50898
Ga	-0.03342	0.36994	-0.14880	0.83754	0.14925	0.03912	0.01679	0.01130	0.02727	0.02494	0.25217	-0.00344
Ge	0.07287	-0.15506	-0.02535	0.01796	-0.14809	0.02057	-0.19665	-0.02471	-0.23357	0.32384	0.05242	0.28904
As	0.15408	-0.10566	-0.05639	-0.10184	-0.12336	0.09151	0.30951	-0.01724	0.37842	0.12925	0.17548	0.03324
Se	0.33137	0.05721	0.09647	-0.08309	0.01852	0.39369	0.66774	0.01495	0.79812	0.21725	0.38185	0.17683

	Th	U	Na	Sc	Ti	Cr	Ga	Ge	As	Se
Li	0.03127	0.31038	0.63743	0.22608	0.31843	0.34576	0.27080	0.02434	0.07525	0.11138
Be	0.28713	0.24428	0.53692	0.23953	0.32043	0.60055	-0.01153	0.15159	0.70790	0.87629
Rb	-0.23918	-0.18422	-0.07119	-0.27146	-0.27449	-0.18147	-0.17539	0.08069	0.00375	0.15755
Sr	0.05048	0.22441	0.22054	-0.00652	0.05864	0.02682	0.49739	-0.04945	-0.02731	-0.06537
Y	0.11873	0.03618	0.03266	0.08677	0.11890	-0.03298	0.01217	0.03542	-0.11058	0.04392
Zr	-0.08328	0.04327	0.37343	0.01578	0.03117	0.46964	0.07678	-0.14920	-0.08545	0.04234
Nb	0.12422	0.25752	0.60255	0.23537	0.34194	0.41340	0.21286	-0.12767	-0.03783	0.15351
Pd	0.09294	0.18914	0.67184	0.08147	0.20484	0.73008	0.01281	-0.19281	0.42937	0.82936
Ag	0.31479	0.30162	0.58552	0.25923	0.37427	0.66099	0.04695	-0.13041	0.28437	0.63962
Cd	0.20059	0.23830	0.59643	0.22721	0.33685	0.75742	-0.02262	-0.19632	0.26143	0.65154
In	0.08332	0.08333	0.47657	0.00761	0.07751	0.48157	-0.06840	0.10252	0.73341	0.93423
Sn	0.18878	0.30411	0.75695	0.22497	0.31335	0.76775	0.09282	-0.07249	0.24575	0.52828
Sb	0.42542	0.35501	0.29248	0.35238	0.45982	0.43063	-0.03342	0.07287	0.15408	0.33137
Te	0.28251	0.45418	0.38543	0.29876	0.34196	0.39387	0.36994	-0.15506	-0.10566	0.05721
Cs	-0.10690	-0.16680	-0.02867	-0.15294	-0.14063	-0.14887	-0.14880	-0.02535	-0.05639	0.09647
Ba	-0.02318	0.10518	0.21413	-0.05983	0.05532	-0.00272	0.83754	0.01796	-0.10184	-0.08309
Hf	-0.06082	0.05801	0.36756	0.01324	0.04710	0.42643	0.14925	-0.14809	-0.12336	0.01852
Ta	0.21195	0.18885	0.33548	0.17778	0.27519	0.27517	0.03912	0.02057	0.09151	0.39369
W	0.00844	0.15199	0.72091	0.03922	0.13972	0.78867	0.01679	-0.19665	0.30951	0.66774
Au	-0.00644	-0.02208	0.14766	0.07244	0.04660	0.10341	0.01130	-0.02471	-0.01724	0.01495
Hg	0.09840	0.23022	0.58171	0.08648	0.21351	0.60858	0.02727	-0.23357	0.37842	0.79812
Tl	0.65513	0.37486	0.14636	0.57325	0.56166	0.37893	0.02494	0.32384	0.12925	0.21725
Pb	0.21917	0.39326	0.71132	0.20662	0.37550	0.49940	0.25217	0.05242	0.17548	0.38185
Bi	0.60341	0.40727	0.30276	0.61889	0.61593	0.50898	-0.00344	0.28904	0.03324	0.17683
Th	1.00000	0.55265	0.13020	0.75751	0.85421	0.32285	0.10756	0.37651	0.12150	0.04914
U	0.55265	1.00000	0.35672	0.47157	0.57933	0.27775	0.21727	0.11741	0.26793	0.06351
Na	0.13020	0.35672	1.00000	0.22243	0.37230	0.65450	0.25232	-0.04171	0.22093	0.49902
Sc	0.75751	0.47157	0.22243	1.00000	0.88423	0.55336	0.10363	0.47256	0.00979	-0.03534
Ti	0.85421	0.57933	0.37230	0.88423	1.00000	0.50314	0.21617	0.37402	0.02622	0.05735
Cr	0.32285	0.27775	0.65450	0.55336	0.50314	1.00000	0.06656	0.12252	0.27720	0.50415
Ga	0.10756	0.21727	0.25232	0.10363	0.21617	0.06656	1.00000	0.00995	-0.12933	-0.10200
Ge	0.37651	0.11741	-0.04171	0.47256	0.37402	0.12252	0.00995	1.00000	0.25569	0.00820
As	0.12150	0.26793	0.22093	0.00979	0.02622	0.27720	-0.12933	0.25569	1.00000	0.64350
Se	0.04914	0.06351	0.49902	-0.03534	0.05735	0.50415	-0.10200	0.00820	0.64350	1.00000

Plant: *B. albitrunca*

	Li	Be	Rb	Sr	Y	Zr	Nb	Pd	Ag	Cd	In	Sn
Li	1.00000	0.07289	0.05134	0.69454	0.17167	0.05733	0.39002	-0.23554	-0.01162	-0.21028	-0.08295	0.31084
Be	0.07289	1.00000	-0.10338	-0.08245	-0.07506	0.13218	0.05524	0.58692	0.13840	0.20196	0.94274	0.53248
Rb	0.05134	-0.10338	1.00000	0.18565	0.19580	-0.02458	0.20424	0.01166	-0.20938	-0.09607	-0.06534	-0.08101
Sr	0.69454	-0.08245	0.18565	1.00000	0.31870	-0.11428	0.18810	-0.26506	-0.13921	-0.20260	-0.25000	0.14969
Y	0.17167	-0.07506	0.19580	0.31870	1.00000	0.05950	-0.04710	-0.23706	-0.00648	-0.17177	-0.17383	0.16071
Zr	0.05733	0.13218	-0.02458	-0.11428	0.05950	1.00000	0.56632	0.34379	-0.09300	0.09782	0.19212	0.37920
Nb	0.39002	0.05524	0.20424	0.18810	-0.04710	0.56632	1.00000	0.39332	-0.21007	0.32622	0.02530	0.32272
Pd	-0.23554	0.58692	0.01166	-0.26506	-0.23706	0.34379	0.39332	1.00000	0.12533	0.78878	0.63127	0.34666
Ag	-0.01162	0.13840	-0.20938	-0.13921	-0.00648	-0.09300	-0.21007	0.12533	1.00000	0.37164	0.08526	0.14956
Cd	-0.21028	0.20196	-0.09607	-0.20260	-0.17177	0.09782	0.32622	0.78878	0.37164	1.00000	0.22297	0.14555
In	-0.08295	0.94274	-0.06534	-0.25000	-0.17383	0.19212	0.02530	0.63127	0.08526	0.22297	1.00000	0.48894
Sn	0.31084	0.53248	-0.08101	0.14969	0.16071	0.37920	0.32272	0.34666	0.14956	0.14555	0.48894	1.00000
Sb	0.34303	0.47443	0.15329	0.27417	0.21043	0.07299	0.32263	0.20761	-0.06102	0.05889	0.31598	0.51716
Te	0.42755	0.00290	0.41937	0.63539	0.20130	-0.01676	0.05959	-0.17326	-0.22594	-0.35837	-0.03807	0.38604
Cs	0.01210	0.31585	0.40477	-0.00461	-0.17926	-0.03608	-0.06738	0.30040	-0.15498	-0.03047	0.39811	0.38339
Ba	0.55700	-0.30634	0.40641	0.74200	0.18414	-0.12125	0.09788	-0.41180	-0.20433	-0.28713	-0.38158	0.01950
Hf	0.03212	0.01156	0.02647	-0.01302	0.22749	0.93832	0.45352	0.21804	-0.11775	0.01624	0.02725	0.27706
Ta	0.21767	0.00269	0.31448	0.45927	0.77518	0.05721	0.23850	0.06149	0.00779	0.13754	-0.11771	0.14965
W	0.08087	0.18946	0.14911	-0.22682	-0.16302	0.48302	0.26814	0.21052	-0.11725	0.03719	0.31664	0.38277
Au	-0.09622	0.13942	-0.14697	-0.02837	0.11870	-0.21553	-0.26290	0.02195	-0.11139	-0.04038	0.13650	0.17064
Hg	-0.14027	0.25710	-0.38073	-0.31938	-0.21220	-0.01485	-0.05707	0.17234	0.25117	0.02785	0.24669	0.35132
Tl	-0.06191	0.18257	0.06581	0.00136	0.44046	-0.23181	-0.22806	-0.01244	0.01227	-0.07025	0.09652	0.29133
Pb	0.25187	0.34372	-0.34634	0.25449	0.01254	-0.09252	0.01205	0.10773	0.18932	0.09203	0.25717	0.61167
Bi	0.09406	0.59399	0.08127	0.19425	0.17509	0.05841	0.18148	0.42034	-0.06970	0.28402	0.51030	0.40330
Th	0.12490	0.46980	-0.31085	-0.08134	0.22101	-0.22388	-0.18492	-0.09609	0.25254	-0.10146	0.29788	0.29413
U	0.18806	0.30521	-0.35704	0.12578	0.30062	-0.27011	-0.17103	-0.20094	0.02457	-0.19697	0.13087	0.16128
Na	0.85278	0.14116	0.15739	0.84912	0.15177	0.05534	0.44192	-0.12922	-0.12219	-0.13269	-0.01590	0.39532
Sc	0.32058	0.31655	-0.29129	-0.02414	0.20668	-0.12200	0.02507	-0.14034	0.08757	-0.13682	0.13906	0.29457
Ti	0.45661	0.33385	-0.35171	0.00029	0.07237	0.14287	0.36945	-0.01862	-0.03645	-0.03969	0.20020	0.37177
Cr	0.14819	0.50399	-0.29228	-0.15471	0.06597	0.44039	0.33236	0.33345	0.02693	0.11727	0.49210	0.60926
Ga	0.53142	-0.21682	0.37380	0.51491	0.20282	-0.15232	0.03934	-0.46492	-0.14212	-0.32885	-0.31457	-0.01184
Ge	0.26619	0.67960	-0.12147	-0.06291	-0.07888	0.21198	0.34892	0.30777	-0.13294	0.01124	0.61633	0.32561
As	0.19763	0.70955	-0.43415	-0.08180	-0.02086	0.02828	0.06482	0.32049	0.07093	0.14212	0.59581	0.29938
Se	-0.00272	0.71748	-0.23022	-0.12684	-0.14102	0.22568	0.32541	0.72406	0.00059	0.46884	0.72378	0.33757

	Sb	Te	Cs	Ba	Hf	Ta	W	Au	Hg	Tl	Pb	B
Li	0.34303	0.42755	0.01210	0.55700	0.03212	0.21767	0.08087	-0.09622	-0.14027	-0.06191	0.25187	0.09406
Be	0.47443	0.00290	0.31585	-0.30634	0.01156	0.00269	0.18946	0.13942	0.25710	0.18257	0.34372	0.59399
Rb	0.15329	0.41937	0.40477	0.40641	0.02647	0.31448	0.14911	-0.14697	-0.38073	0.06581	-0.34634	0.08127
Sr	0.27417	0.63539	-0.00461	0.74200	-0.01302	0.45927	-0.22682	-0.02837	-0.31938	0.00136	0.25449	0.19425
Y	0.21043	0.20130	-0.17926	0.18414	0.22749	0.77518	-0.16302	0.11870	-0.21220	0.44046	0.01254	0.17509
Zr	0.07299	-0.01676	-0.03608	-0.12125	0.93832	0.05721	0.48302	-0.21553	-0.01485	-0.23181	-0.09252	0.05841
Nb	0.32263	0.05959	-0.06738	0.09788	0.45352	0.23850	0.26814	-0.26290	-0.05707	-0.22806	0.01205	0.18148
Pd	0.20761	-0.17326	0.30040	-0.41180	0.21804	0.06149	0.21052	0.02195	0.17234	-0.01244	0.10773	0.42034
Ag	-0.06102	-0.22594	-0.15498	-0.20433	-0.11775	0.00779	-0.11725	-0.11139	0.25117	0.01227	0.18932	-0.06970
Cd	0.05889	-0.35837	-0.03047	-0.28713	0.01624	0.13754	0.03719	-0.04038	0.02785	-0.07025	0.09203	0.28402
In	0.31598	-0.03807	0.39811	-0.38158	0.02725	-0.11771	0.31664	0.13650	0.24669	0.09652	0.25717	0.51030
Sn	0.51716	0.38604	0.38339	0.01950	0.27706	0.14965	0.38277	0.17064	0.35132	0.29133	0.61167	0.40330
Sb	1.00000	0.19022	0.07113	0.20513	0.05490	0.18259	0.13369	-0.08003	0.04491	0.01607	0.20997	0.50626
Te	0.19022	1.00000	0.61964	0.61506	0.02750	0.15186	0.15751	-0.07321	0.01461	0.06461	0.20506	0.15602
Cs	0.07113	0.61964	1.00000	0.04642	-0.10366	-0.11392	0.32007	0.05031	0.26319	0.19735	0.12559	0.06791
Ba	0.20513	0.61506	0.04642	1.00000	0.00230	0.18786	0.18644	-0.04226	-0.45019	-0.10385	0.08484	0.09963
Hf	0.05490	0.02750	-0.10366	0.00230	1.00000	0.17608	0.40086	-0.16485	-0.12403	-0.14582	-0.11205	0.00852
Ta	0.18259	0.15186	-0.11392	0.18786	0.17608	1.00000	-0.25915	0.18077	-0.26296	0.48123	0.13904	0.24805
W	0.13369	0.15751	0.32007	0.18644	0.40086	-0.25915	1.00000	-0.09343	0.03701	-0.20297	0.12171	0.16371
Au	-0.08003	-0.07321	0.05031	-0.04226	-0.16485	0.18077	-0.09343	1.00000	0.05193	0.69387	0.56664	0.06921
Hg	0.04491	0.01461	0.26319	-0.45019	-0.12403	-0.26296	0.03701	0.05193	1.00000	0.12575	0.35773	-0.1415
Tl	0.01607	0.06461	0.19735	-0.10385	-0.14582	0.48123	-0.20297	0.69387	0.12575	1.00000	0.43776	0.10289
Pb	0.20997	0.20506	0.12559	0.08484	-0.11205	0.13904	0.12171	0.56664	0.35773	0.43776	1.00000	0.24593
Bi	0.50626	0.15602	0.06791	0.09963	0.00852	0.24805	0.16371	0.06921	-0.14154	0.10289	0.24593	1.00000
Th	0.25122	-0.24917	-0.24069	-0.21140	-0.24959	0.17019	-0.15992	0.38048	0.18233	0.58817	0.41342	0.36897
U	0.14532	-0.17742	-0.34633	-0.09289	-0.25620	0.27770	-0.30942	0.49919	0.02663	0.57419	0.37830	0.36770
Na	0.49501	0.58502	0.01969	0.70820	0.05863	0.26032	0.06543	-0.11951	-0.24477	-0.14483	0.31069	0.36734
Sc	0.26595	-0.21190	-0.23174	-0.15687	-0.17390	0.18633	-0.12651	0.32245	0.15184	0.51561	0.30812	0.25716
Ti	0.31216	-0.21099	-0.28578	-0.15919	0.00991	0.09150	0.09933	0.09827	0.11921	0.17461	0.29766	0.30545
Cr	0.21363	-0.09798	0.07946	-0.40803	0.25788	0.13905	0.25232	0.11186	0.26349	0.24739	0.32443	0.39967
Ga	0.23422	0.44060	-0.02292	0.89693	-0.03696	0.12007	0.33762	-0.06371	-0.39508	-0.02722	0.03858	0.11993
Ge	0.35168	-0.19009	-0.03891	-0.22965	0.11090	0.08962	0.13958	0.19288	0.02454	0.13744	0.27898	0.46178
As	0.31571	-0.22292	-0.00071	-0.41050	-0.07057	-0.00697	-0.07347	0.10186	0.25836	0.23982	0.25838	0.34586
Se	0.19986	-0.18386	0.18895	-0.48240	0.05872	0.12406	0.10319	0.09774	0.24495	0.11493	0.22650	0.46644

	Th	U	Na	Sc	Ti	Cr	Ga	Ge	As	Se
Li	0.12490	0.18806	0.85278	0.32058	0.45661	0.14819	0.53142	0.26619	0.19763	-0.00272
Be	0.46980	0.30521	0.14116	0.31655	0.33385	0.50399	-0.21682	0.67960	0.70955	0.71748
Rb	-0.31085	-0.35704	0.15739	-0.29129	-0.35171	-0.29228	0.37380	-0.12147	-0.43415	-0.23022
Sr	-0.08134	0.12578	0.84912	-0.02414	0.00029	-0.15471	0.51491	-0.06291	-0.08180	-0.12684
Y	0.22101	0.30062	0.15177	0.20668	0.07237	0.06597	0.20282	-0.07888	-0.02086	-0.14102
Zr	-0.22388	-0.27011	0.05534	-0.12200	0.14287	0.44039	-0.15232	0.21198	0.02828	0.22568
Nb	-0.18492	-0.17103	0.44192	0.02507	0.36945	0.33236	0.03934	0.34892	0.06482	0.32541
Pd	-0.09609	-0.20094	-0.12922	-0.14034	-0.01862	0.33345	-0.46492	0.30777	0.32049	0.72406
Ag	0.25254	0.02457	-0.12219	0.08757	-0.03645	0.02693	-0.14212	-0.13294	0.07093	0.00059
Cd	-0.10146	-0.19697	-0.13269	-0.13682	-0.03969	0.11727	-0.32885	0.01124	0.14212	0.46884
In	0.29788	0.13087	-0.01590	0.13906	0.20020	0.49210	-0.31457	0.61633	0.59581	0.72378
Sn	0.29413	0.16128	0.39532	0.29457	0.37177	0.60926	-0.01184	0.32561	0.29938	0.33757
Sb	0.25122	0.14532	0.49501	0.26595	0.31216	0.21363	0.23422	0.35168	0.31571	0.19986
Te	-0.24917	-0.17742	0.58502	-0.21190	-0.21099	-0.09798	0.44060	-0.19009	-0.22292	-0.18386
Cs	-0.24069	-0.34633	0.01969	-0.23174	-0.28578	0.07946	-0.02292	-0.03891	-0.00071	0.18895
Ba	-0.21140	-0.09289	0.70820	-0.15687	-0.15919	-0.40803	0.89693	-0.22965	-0.41050	-0.48240
Hf	-0.24959	-0.25620	0.05863	-0.17390	0.00991	0.25788	-0.03696	0.11090	-0.07057	0.05872
Ta	0.17019	0.27770	0.26032	0.18633	0.09150	0.13905	0.12007	0.08962	-0.00697	0.12406
W	-0.15992	-0.30942	0.06543	-0.12651	0.09933	0.25232	0.33762	0.13958	-0.07347	0.10319
Au	0.38048	0.49919	-0.11951	0.32245	0.09827	0.11186	-0.06371	0.19288	0.10186	0.09774
Hg	0.18233	0.02663	-0.24477	0.15184	0.11921	0.26349	-0.39508	0.02454	0.25836	0.24495
Tl	0.58817	0.57419	-0.14483	0.51561	0.17461	0.24739	-0.02722	0.13744	0.23982	0.11493
Pb	0.41342	0.37830	0.31069	0.30812	0.29766	0.32443	0.03858	0.27898	0.25838	0.22650
Bi	0.36897	0.36770	0.36734	0.25716	0.30545	0.39967	0.11993	0.46178	0.34586	0.46644
Th	1.00000	0.89507	0.04184	0.89249	0.69420	0.48294	0.04624	0.51795	0.59532	0.21187
U	0.89507	1.00000	0.14115	0.86201	0.66854	0.42179	0.06997	0.46806	0.52682	0.19085
Na	0.04184	0.14115	1.00000	0.14436	0.30784	0.06580	0.58155	0.24916	0.07712	0.00326
Sc	0.89249	0.86201	0.14436	1.00000	0.83783	0.58205	0.10577	0.53357	0.60164	0.19289
Ti	0.69420	0.66854	0.30784	0.83783	1.00000	0.70884	0.06617	0.65140	0.54264	0.34576
Cr	0.48294	0.42179	0.06580	0.58205	0.70884	1.00000	-0.29160	0.58249	0.54289	0.63210
Ga	0.04624	0.06997	0.58155	0.10577	0.06617	-0.29160	1.00000	-0.10061	-0.24625	-0.46759
Ge	0.51795	0.46806	0.24916	0.53357	0.65140	0.58249	-0.10061	1.00000	0.63881	0.55271
As	0.59532	0.52682	0.07712	0.60164	0.54264	0.54289	-0.24625	0.63881	1.00000	0.65631
Se	0.21187	0.19085	0.00326	0.19289	0.34576	0.63210	-0.46759	0.55271	0.65631	1.00000

APPENDIX 5

Map showing sample points in the study area

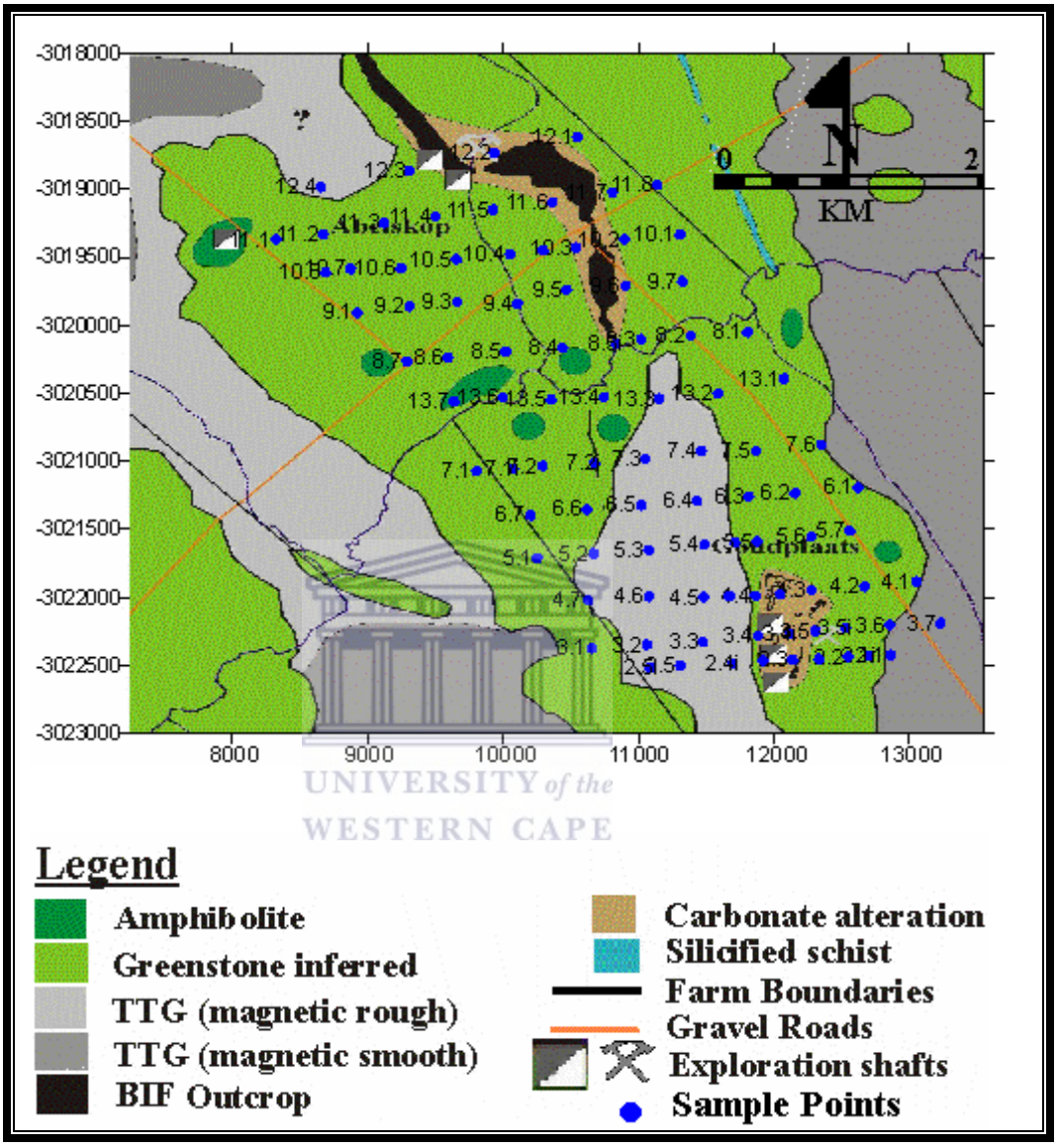
-3018000
-3018500
-3019000
-3019500
-3020000
-3020500
-3021000
-3021500
-3022000
-3022500
-3023000
8000
9000
10000
11000
12000
13000
N
0
2
KM
Abalskop
Grachplants
UNIVERSITY of the
WESTERN CAPE
Legend
Amphibolite
Greenstone inferred
TTG (magnetic rough)
TTG (magnetic smooth)
BIF Outcrop
Carbonate alteration
Silicified schist
Farm Boundaries
Gravel Roads
Exploration shafts
Sample Points